

N O T I C E

THIS DOCUMENT HAS BEEN REPRODUCED FROM
MICROFICHE. ALTHOUGH IT IS RECOGNIZED THAT
CERTAIN PORTIONS ARE ILLEGIBLE, IT IS BEING RELEASED
IN THE INTEREST OF MAKING AVAILABLE AS MUCH
INFORMATION AS POSSIBLE

STABILITY ANALYSIS OF A LIQUID FUEL
ANNULAR COMBUSTION CHAMBER

(NASA-CR-159734) STABILITY ANALYSIS OF A
LIQUID FUEL ANNULAR COMBUSTION CHAMBER M.S.
Thesis (Tennessee Technological Univ.)
151 p HC A08/MF A01

N80-13165

CSCL 21H

Unclas
46335

G3/20

by

G. H. McDonald, J. Peddieson, Jr., and M. Ventrice

Departments of

Engineering Science and Mechanics
and
Mechanical Engineering

Tennessee Technological University
Cookeville, Tennessee 38501

Prepared for

NATIONAL AERONAUTICS AND SPACE ADMINISTRATION

NASA Lewis Research Center
Cleveland, Ohio
Contract NGR 43-003-015
R. J. Priem, Technical Monitor

FOREWORD

This report summarizes a portion of the work done for NASA Grant NGR 43-003-015. It is the masters research of the first author, Gary H. McDonald. John Peddieson was the thesis advisor; M. Ventrice was the principal investigator of the grant.

PRECEDING PAGE BLANK NOT FILMED

TABLE OF CONTENTS

	Page
LIST OF FIGURES	v
LIST OF TABLES	vi
LIST OF SYMBOLS	viii
Chapter	
1. INTRODUCTION AND LITERATURE REVIEW	1
Historic Studies in the Problems of Combustion Instability	4
Statement of the Problem	8
2. DERIVATION OF THE GOVERNING ACOUSTIC WAVE EQUATION	10
Steady State Solution	18
Deviations from Steady State	20
3. DERIVATION OF WAVE EQUATION BASED UPON AN ANNULAR COMBUSTION CHAMBER	25
4. TWO VARIABLE PERTURBATION METHOD APPLIED TO THE ACOUSTIC WAVE EQUATION	36
5. DISCUSSION AND PRESENTATION OF RESULTS	75
6. CONCLUSIONS AND RECOMMENDATIONS	111
REFERENCES	115
APPENDICES	
A. GENERAL TIME DELAY FUNCTION	119
B. RUNGE-KUTTA PROGRAM OF THE MODAL WAVE EQUATIONS	122
C. RUNGE-KUTTA PROGRAM OF THE PERTURBATION EQUATIONS	126
D. PROGRAM FOR EXACT SOLUTIONS FOR STANDING WAVE CASE	131
E. PROGRAM FOR EXACT SOLUTIONS FOR TRAVELING WAVE CASE	135
F. PRESENTATION OF ACOUSTIC PRESSURE CALCULATIONS.	138

LIST OF FIGURES

Figure	Page
1. Schematic of a Liquid Propellant Combustion Chamber	11
2. Dimensional and Dimensionless Form of a Circular Cylindrical Combustion Chamber	25
3. Modal Amplitude F_1 vs time t for Standing Waves - Stable Case .	76
4. Modal Amplitude F_2 vs time t for Standing Waves - Stable Case .	77
5. Modal Amplitude F_1 vs time t for Traveling Waves - Stable Case.	78
6. Modal Amplitude F_2 vs time t for Traveling Waves - Stable Case.	79
7. Modal Amplitude G_1 vs time t for Traveling Waves - Stable Case.	80
8. Modal Amplitude G_2 vs time t for Traveling Waves - Stable Case.	81
9. Modal Amplitude F_1 vs time t for Standing Waves - Unstable Case	83
10. Modal Amplitude F_2 vs time t for Standing Waves - Unstable Case	84
11. Modal Amplitude F_1 vs time t for Traveling Waves - Unstable Case	85
12. Modal Amplitude F_2 vs time t for Traveling Waves - Unstable Case	86
13. Modal Amplitude G_1 vs time t for Traveling Waves - Unstable Case	87
14. Modal Amplitude G_2 vs time t for Traveling Waves - Unstable Case	88
A1. Step Function $J(t)$ vs time t	119
A2. Step Time Delay Function $J(t - \xi)$	120

LIST OF TABLES

Table	Page
<p>1. Comparison of Results for F_1 showing effects of Gas Dynamic Index (i) for ($F_1(0) = 0, F_1'(0) = 1, F_2(0) = 0, F_2'(0) = 0, G_1(0) = 0, G_1'(0) = 0, G_2(0) = 0, G_2'(0) = 0$) - Stable Case (n = 60) - Standing Waves</p>	89
<p>2. Comparison of Results for F_2 showing effects of Gas Dynamic Index (i) for ($F_1(0) = 0, F_1'(0) = 1, F_2(0) = 0, F_2'(0) = 0, G_1(0) = 0, G_1'(0) = 0, G_2(0) = 0, G_2'(0) = 0$) - Stable Case (n = 60) - Standing Waves</p>	90
<p>3. Comparison of Results for F_1 showing effects of Correction Variable (K) for ($F_1(0) = 0, F_1'(0) = 1, F_2(0) = 0, F_2'(0) = 0, G_1(0) = 0, G_1'(0) = 0, G_2(0) = 0, G_2'(0) = 0$) - Stable Case (n = 40) - Standing Waves</p>	92
<p>4. Comparison of Results for F_2 showing effects of correction variable (K) for ($F_1(0) = 0, F_1'(0) = 1, F_2(0) = 0, F_2'(0) = 0, G_1(0) = 0, G_1'(0) = 0, G_2(0) = 0, G_2'(0) = 0$) - Stable Case (n = 40) - Standing Waves</p>	93
<p>5. Comparison of Results for F_1 showing effect of the Gas Dynamic Index (i) for ($F_1(0) = 0, F_1'(0) = 1, F_2(0) = 0, F_2'(0) = 0, G_1(0) = 0, G_1'(0) = 0, G_2(0) = 0, G_2'(0) = 0$) - Unstable Case (n = 75) - Standing Waves</p>	95
<p>6. Comparison of Results for F_2 showing effect of the Gas Dynamic Index (i) for ($F_1(0) = 0, F_1'(0) = 1, F_2(0) = 0, F_2'(0) = 0, G_1(0) = 0, G_1'(0) = 0, G_2(0) = 0, G_2'(0) = 0$) - Unstable Case (n = 75) - Standing Waves</p>	96
<p>7. Comparison of Results for F_1 showing effects of correction variable (K) for ($F_1(0) = 0, F_1'(0) = 1, F_2(0) = 0, F_2'(0) = 0, G_1(0) = 0, G_1'(0) = 0, G_2(0) = 0, G_2'(0) = 0$) - Unstable Case (n = 70) - Standing Waves</p>	97

Table

Page

8. Comparison of Results for F_2 showing effects of correction variable (K) for ($F_1(0) = 0, F_1'(0) = 1, F_2(0) = 0, F_2'(0) = 0, G_1(0) = 0, G_1'(0) = 0, G_2(0) = 0, G_2'(0) = 0$) - Unstable Case ($n = 70$) - Standing Waves 98
9. Comparison of Stability Boundaries based on the Interaction Index (n) - for ($F_1(0) = 0, F_1'(0) = 1, F_2(0) = 0, F_2'(0) = 0, G_1(0) = 0, G_1'(0) = 0, G_2(0) = 0, G_2'(0) = 0$) - Standing Waves - Epsilon = 0.1 99
10. Comparison of Stability Boundaries based on the Interaction Index (n) for ($F_1(0) = 0, F_1'(0) = 1, F_2(0) = 0, F_2'(0) = 0, G_1(0) = 0, G_1'(0) = 0, G_2(0) = 0, G_2'(0) = 0$) - Traveling Waves - Epsilon = 0.1 100
11. Comparison of the Effect of Different Initial Conditions Imposed for Standing and Traveling Waves for $i = 1$ and $K = 1$ Epsilon = 0.1 102
12. Comparison of the Effects of the Order term Epsilon ($F_1(0) = 0, F_1'(0) = 1, F_2(0) = 0, F_2'(0) = 0, G_1(0) = 0, G_1'(0) = 0, G_2(0) = 0, G_2'(0) = 0$) - Standing Waves when $i = 1$ and $K = 1$ 103
13. Comparison of the Effects of the order term Epsilon ($F_1(0) = 0, F_1'(0) = 1, F_2(0) = 0, F_2'(0) = 0, G_1(0) = 0, G_1'(0) = 0, G_2(0) = 0, G_2'(0) = 0$) - Traveling Waves when $i = 1$ and $K = 1$ 104

LIST OF SYMBOLS

Symbol

A_1	perturbation modal amplitude related to f_{10}
A_2	perturbation modal amplitude related to g_{10}
A_3	perturbation modal amplitude related to f_{20}
A_4	perturbation modal amplitude related to g_{20}
$\overset{*}{a}$	dimensional constant (speed of sound)
B_1	perturbation modal amplitude related to f_{10}
B_2	perturbation modal amplitude related to g_{10}
B_3	perturbation modal amplitude related to f_{20}
B_4	perturbation modal amplitude related to g_{20}
B	fuel drop burning rate per unit volume - dimensionless
$\overset{*}{B}$	fuel drop burning rate per unit volume - dimensional
b	thickness of annular combustion chamber's cross-section (dimensionless)
$\overset{*}{b}$	thickness of annular combustion chamber's cross-section (dimensional)
C_1	wave amplitude related to A_1 and B_1
C_2	wave amplitude related to A_2 and B_2
C_3	wave amplitude related to A_3 and B_3
C_4	wave amplitude related to A_4 and B_4
$\frac{D}{Dt}$	total (comoving) derivative with respect to time
$\frac{\partial}{\partial t}$	partial derivative with respect to time
$\overset{+}{e}_\theta$	unit vector in transverse (θ) direction
$\overset{+}{e}_z$	unit vector in axial (z) direction
f	function notation - real time

Symbol

f_{τ}	function notation - time delay
f_1	Fourier series coefficient - functions of time - modal amplitude for standing and traveling waves
f_2	Fourier series coefficient - functions of time - modal amplitude for standing and traveling waves
f_{10}	perturbation variable for f_1 of $O(1)$
f_{20}	perturbation variable for f_2 of $O(1)$
f_{11}	perturbation variable for f_1 of $O(\epsilon)$
f_{21}	perturbation variable for f_2 of $O(\epsilon)$
g_1	Fourier series coefficient - function of time - modal amplitude for traveling waves
g_2	Fourier series coefficient - function of time - modal amplitude for traveling waves
g_{10}	perturbation variable for g_1 of $O(1)$
g_{20}	perturbation variable for g_2 of $O(1)$
g_{11}	perturbation variable for g_1 of $O(\epsilon)$
g_{21}	perturbation variable for g_2 of $O(\epsilon)$
i	gas dynamic index
j	index 0 - no time delay, 1 - time delay
K	correction variable (baffles, wall linings, nozzle, etc) $O(1)$
K_1	correction variable of $O(\epsilon)$
L^*	characteristic length
l	variable index ($l = 1, 2, 3 \dots$)
n	interaction index
0	order notation
\bar{p}	steady-state acoustic pressure
p	pressure of the gas mixture - dimensionless
p^*	pressure of the gas mixture - dimensional

Symbol

r	radius of typical point in annular combustion chamber - dimensionless
r^*	radius of typical point in annular combustion chamber - dimensional
R	inside radius of annular combustion chamber - dimensional
R	dimensionless ratio of $O(1)$
t	time - dimensionless
t^*	time - dimensional
\vec{u}	velocity of the gas - dimensionless
\vec{u}^*	velocity of the gas - dimensional
\vec{u}	steady state velocity vector
\vec{u}'	perturbation velocity vector
u	steady state velocity of the gas - magnitude
u_t'	transverse component of perturbation velocity vector
u_z	perturbation velocity component in axial direction - magnitude
z	axial or longitudinal direction

Greek Symbols

$\vec{\nabla}$	del operator of Cartesian coordinates - dimensionless
$\vec{\nabla}^*$	del operator of Cartesian coordinates - dimensional
$\vec{\nabla}^2$	Laplacian operator
ϵ	order term - epsilon - measure of nonlinearities
η	perturbation variable of time $O(\epsilon)$
θ	transverse (θ) direction
ξ	perturbation variable of time $O(1)$
π	3.14159
ρ	gas density - dimensionless

Greek Symbols

- ρ^* gas density - dimensional
- ρ_0^* initial density of gas - dimensional
- σ burning rate representing small perturbations from steady state of $O(1)$
- $\bar{\sigma}$ steady state burning rate of $O(1)$
- ϕ velocity potential representing small perturbations from steady state
- $\bar{\phi}$ steady state velocity potential
- ϕ_1 phase angle related to A_1 and B_1
- ϕ_2 phase angle related to A_2 and B_2
- ϕ_3 phase angle related to A_3 and B_3
- ϕ_4 phase angle related to A_4 and B_4
- ψ velocity potential
- $\vec{\Omega}$ vorticity vector
- ω burning rate representing small perturbations from steady state of $O(\epsilon)$
- $\bar{\omega}$ steady state burning rate of $O(\epsilon)$

Chapter 1

INTRODUCTION AND LITERATURE REVIEW

During steady operation of a liquid propellant rocket engine the injected propellants are converted by various physical and chemical processes into hot burned gases which are subsequently accelerated to supersonic velocity by passing through a converging-diverging nozzle. The operation of such an engine, however, is seldom perfectly smooth. Instead the quantities which describe the conditions inside the combustor (i.e. pressure, density, temperature, etc.) are time-dependent and oscillatory. Such oscillations can be of either a destructive or nondestructive nature. Nondestructive unsteadiness is characterized by random fluctuations in the flow properties and includes the phenomena of turbulence and combustion noise. Unsteady operation of a destructive nature, on the other hand, is characterized by organized oscillations in which there is a definite correlation between the fluctuations at two different locations in the combustor. Such oscillations have a definite frequency and result in additional thermal and mechanical loads that the system must withstand.

Unsteady operation of the destructive variety, known as combustion instability, was first encountered in 1940. At that time a British group testing a small solid-propellant rocket motor observed sudden increases of pressure to twice the expected level, enough to destroy a motor of flight weight. Since that time every major rocket development program has been plagued by combustion instability of some form. These oscillations in the combustion chamber can have several detrimental effects.

In some cases, particularly in solid-propellant rockets, instability can cause the steady-state pressure to increase to a point at which the rocket motor will explode. In liquid-propellant rocket chambers experiencing unstable combustion, heat transfer rates to the walls considerably exceed the corresponding steady state heat transfer rates, resulting in burn-out of the walls. If the chamber can survive these effects, mechanical vibrations in the rocket system can cause mechanical failure or destroy the effectiveness of the delicate control and guidance systems.

The phenomenon of combustion instability depends heavily upon the unsteady behavior of the combustion process. The organized oscillations of the gas within the chamber must be coupled with the combustion process in such a way as to form a feedback loop. In this manner part of the energy stored in the propellants becomes available to drive large amplitude oscillations. An understanding of this coupling between the combustion process and the wave motion is necessary in order to predict the stability characteristics of rocket engines.

Combustion instability problems in liquid propellant rocket motors usually fall into one of three categories according to the frequency of oscillation. Low frequency combustion instability, also known as chugging, is characterized by frequencies ranging from ten to several hundred hertz, nearly spatially uniform properties, and coupling with the feed system of the rocket. This type of instability is less detrimental than other forms, and the means of preventing it are well understood. Low frequency instability will not be considered.

A second type of combustion instability, which is less frequently observed, has a frequency of several hundred cycles per second. This

type of oscillation is associated with the appearance of entropy waves inside the combustion chamber.

The third and most important form of combustion instability is known as high frequency or acoustic instability. As the name suggests, this type of instability represents the case of forced oscillations of the combustion chamber gases which are driven by the unsteady combustion process and interact with the resonance properties of the combustor geometry. The observed frequencies, which are as high as 10,000 cycles per second, are very close to those of the natural acoustic modes of a closed-ended chamber of the same geometry as the one experiencing unstable combustion. High frequency combustion instability is by far the most destructive and is the type to be considered by the following analysis.

High frequency combustion instability can resemble any of the following acoustic modes: (1) longitudinal, (2) transverse, and (3) combined longitudinal-transverse modes. Longitudinal oscillations are usually observed in chambers whose length to diameter ratio is much greater than one; in this case the velocity fluctuations are parallel to the axis of the chamber and the disturbances depend only on one space dimension. For much shorter chambers the transverse mode of instability is most frequently observed. Transverse oscillations in rocket motors are characterized by a component of the velocity-perturbation which is perpendicular to the axis of the chamber but the disturbances can depend upon three space dimensions. Such oscillations can take either of two forms: (1) the standing form in which the nodal surfaces are stationary and (2) the spinning form in which the nodal surfaces rotate in either the clockwise or counterclockwise direction. Transverse combustion instability, particularly that resembling the first tangential mode, has been

frequently encountered in modern rocket development programs and has been the subject of much current research.

Historic Studies in the Problems of Combustion Instability

Since the early 1950's much experimental and analytical research has been devoted to better understanding the phenomenon of high frequency combustion instability. Most of the theories presented prior to 1966 were restricted to circumstances in which the amplitudes of the pressure oscillations were infinitesimally small in the linear regime. Prominent among these are the pioneering studies of longitudinal instability by Crocco [1] as well as the studies of transverse instability by Scala [2], Reardon [3], and Culick [4]. A complete discussion of these theories is given in the work of Zinn [5] and will not be repeated here.

Although linear theories provide the propulsion engineer with considerable insight into the problem, their applicability and usefulness in design is limited. The linear theories cannot provide answers to such important problems as the limiting value of the pressure amplitude attained by a small disturbance in the case of a linearly unstable engine, or the effect of a finite-amplitude disturbance upon the behavior of a linearly stable engine. In the latter case the result of many tests indicate that under certain conditions the introduction of sufficiently large disturbances into a linearly stable engine can trigger combustion instability. Another shortcoming of linear theories is the fact that their predictions cannot be compared directly with available experimental data; for, in the majority of cases, the experimental data is obtained under conditions in which the combustion instability is fully developed and in a non-linear regime. Therefore, theories accounting for these

nonlinearities associated with combustion instability are needed. A more detailed discussion of the nonlinear aspects of combustion instability can be found in a work by Zinn [5].

In the field of finite amplitude (nonlinear) combustion instability, mathematical difficulties have precluded any exact solutions, and approximate methods and numerical analysis have been used almost exclusively. For this reason publications in this field are scarce. Notable among these is the work of Maslen and Moore [6] who studied the behavior of finite amplitude transverse waves in a circular cylinder. Their major conclusion was that, unlike longitudinal oscillations, transverse waves do not steepen to form shock waves. Maslen and Moore, however, considered only fluid mechanical effects; they did not consider the influences of the combustion process, the steady state flow, and the nozzle which are so important in the analysis of combustion instability problems. Nevertheless, pressure recordings taken from engines experiencing transverse instability reveal the presence of continuous pressure waves similar in form to those predicted by Maslen and Moore.

One of the first nonlinear analyses to include the effects of the combustion process and the resulting steady state flow was performed by Priem and Guentert [7]. In this investigation, the problem was made one-dimensional by considering the behavior of tangential waves traveling in a narrow annular combustor of a liquid propellant rocket motor. They used a computer to solve numerically the resulting nonlinear equations for various values of the parameters involved. Due to the many assumptions involved in the derivation of the one-dimensional equations, the results of this investigation are open to question.

The successful use of the time-lag concept (see Crocco [1]) in the linear theories prompted a number of researchers to apply this model to the analysis of non-linear combustion instability. By considering a chamber with a concentrated combustion zone and a short nozzle, Sirignano [8] demonstrated the existence of continuous, finite-amplitude, longitudinal periodic waves. These solutions were shown to be unstable, however, thus indicating the possibility of triggering longitudinal oscillations. Mitchell [9] extended the work of Sirignano to include the possibility of discontinuous solutions. In this manner he was able to show that the final form of triggered longitudinal instability consisted of shock waves moving back and forth along the combustion chamber. Mitchell also considered the more realistic case of distributed combustion.

In the analyses of Priem, Sirignano, and Mitchell the oscillations were dependent on only one space dimension. One of the first researchers to study finite-amplitude three-dimensional combustion oscillations was Zinn [5] whose work is an extension of the linear transverse theories and the analysis of Maslen and Moore. Using Crocco's time lag model Zinn investigated the nonlinear behavior of transverse waves in a chamber with a concentrated combustion zone at the injector end and an arbitrary converging-diverging nozzle at the other end. In this case, it was necessary to extend Crocco's burning rate expression and transverse nozzle admittance relation to obtain the appropriate boundary conditions for the case when the flow oscillations are of finite size. As a result of this analysis Zinn was able to prove the existence of three dimensional finite-amplitude continuous waves which are periodic in time. In addition, he was able to prove the possibility of triggering combustion oscillations. An analytical criterion for the determination of the

stability of such waves was derived, but because of its complicated form and the limited capacity of available computers no specific numerical results were obtained.

In more recent years other investigators such as Burstein [10] have attempted to solve numerically the equations describing instabilities that depend on two space dimensions. Although the resulting solutions resemble experimentally observed combustion instability, this method requires excessive computer time, and studies of this type for three-dimensional oscillations will have to await the development of a much faster breed of computers.

In a recent publication by Powell [11], the problem of analytically and numerically analyzing multidimensional non-linear combustion instability was investigated. The problem in doing this is that a system of non-linear coupled partial differential equations whose solutions must satisfy a complicated set of boundary conditions governs the phenomena of combustion instability. These boundary conditions may describe the unsteady burning process of the wall of a solid propellant rocket motor; the conditions at an idealized concentrated combustion zone of a liquid-propellant rocket engine; or the unsteady flow of the entrance of a converging-diverging nozzle. Previously, in an effort to obtain analytical solutions to various combustion instability problems, investigators have been forced to simplify the original problem to such an extent that it no longer resembled the real problem that originally was to be solved. Powell proposed a method to perform a nonlinear stability analysis with relative ease. This method, applicable to both linear and non linear problems with complicated boundary conditions, was a modified form of the classical Galerkin method. The Galerkin method [11] is an approximate mathematical

technique which has been successfully employed in the solution of various engineering problems in the field of acoustics. Powell used this method to specifically study the non-linear behavior of combustion driven oscillations in cylindrical combustion chambers in which the liquid propellants are injected uniformly across the injector face and the combustion process is distributed throughout the combustion chamber. Based upon the results of his second and third order theories, the following nonlinear mechanisms were found to be important in determining the non-linear stability characteristics of the system: (1) the transfer of energy between modes, (2) the self-coupling of a mode with itself, and (3) a non-linear combustion mass source. Powell found that the self-coupling mechanism was important in the initiation of triggered instability, while the non-linear driving mechanism was important in the determination of the final amplitude of triggered instability.

Statement of the Problem

In this thesis, the problem of velocity-sensitive instability will be considered. Based upon previous work on this problem, only transverse oscillations will be considered due to mathematical simplicities. Also, the specific geometry of the combustion chamber to be analyzed will be annular or ring-like. The purpose of this thesis is to investigate the mechanisms which cause these instabilities due to the combustion process in a liquid propellant annular combustion chamber and attempt to state which mechanisms or conditions impose the greatest effect upon stability of combustion.

In Chapter 2 of this thesis, the governing equations of fluid motion (i.e., balance of mass and momentum) are stated. From the equations,

the general acoustic wave equation for non-linear combustion is derived. In this derivation, both steady state and deviations from the steady-state conditions are considered and their effects incorporated into the general acoustic wave equation.

In Chapter 3, the Galerkin method is used to obtain, from the general acoustic equation of Chapter 2, equations governing the modal amplitudes associated with the first two modes of transverse oscillation in a thin annular combustion chamber. These equations for the annular combustion chamber are solved numerically by the use of a Runge-Kutta program for various conditions.

In Chapter 4, a set of approximate equations are derived from the modal amplitude equations presented in Chapter 3 by use of the two-variable perturbation technique. These resulting approximate equations are expressed both in the modal amplitude and amplitude-phase angle form. In this chapter, four special cases are presented for which closed-form solutions can be found. These four cases are (1) standing wave--no combustion, (2) standing wave--no gas dynamic nonlinearities, (3) traveling wave--no combustion, and (4) traveling wave--no gas dynamic nonlinearities. For problems not falling within the above categories, a numerical analysis is employed to solve approximate equations.

In Chapter 5, the results contained in the previous two chapters are discussed and compared. Stability limits are obtained and the effect of neglecting various physical effects are discussed. In addition, the accuracy of the perturbation method is evaluated. A summary of the research contained in this thesis is presented in this chapter.

In Chapter 6, a statement of conclusions is made along with recommendations for future research in this area.

Chapter 2

DERIVATION OF THE GOVERNING ACOUSTIC WAVE EQUATION

In order to investigate the non-linear combustion instabilities that occur in liquid propellant rocket engines, one must start with the balance laws of mass and momentum. Also, for this problem, a constitutive equation was formulated relating pressure and density. Mathematically, these principles are respectively

$$\frac{\partial \rho^*}{\partial t^*} + \vec{\nabla} \cdot (\rho^* \vec{u}) = B^* \quad (2.1)$$

$$\rho^* \left(\frac{\partial \vec{u}}{\partial t^*} + \vec{u} \cdot \vec{\nabla} \vec{u} \right) = - \vec{\nabla} p^* \quad (2.2)$$

$$p^* = a^{*2} \rho^*, \quad (2.3)$$

where

ρ^* - gas density

t^* - time

$\vec{\nabla}$ - del operator of the system $\frac{\partial}{\partial x^*} \vec{i} + \frac{\partial}{\partial y^*} \vec{j} + \frac{\partial}{\partial z^*} \vec{k}$

\vec{u} - velocity of the gas

B^* - fuel drop burning rate per unit volume

p^* - pressure of the gas

a^{*2} - constant of proportionality (in this case - speed of sound).

The * representation denotes that the above physical quantities are dimensional. Equations (2.1) - (2.3) are based on the assumption that the fuel drops serve only as a source of mass for the gas phase.

Interphase transfer of momentum and energy are neglected.

Combining equations (2.2) and (2.3), the resulting equation is

$$\rho^* \left(\frac{\partial \mathbf{u}^*}{\partial t^*} + \mathbf{u}^* \cdot \nabla^* \mathbf{u}^* \right) = - a^{*2} \nabla^* \rho^*. \quad (2.4)$$

For the physical situation depicted in Figure 1

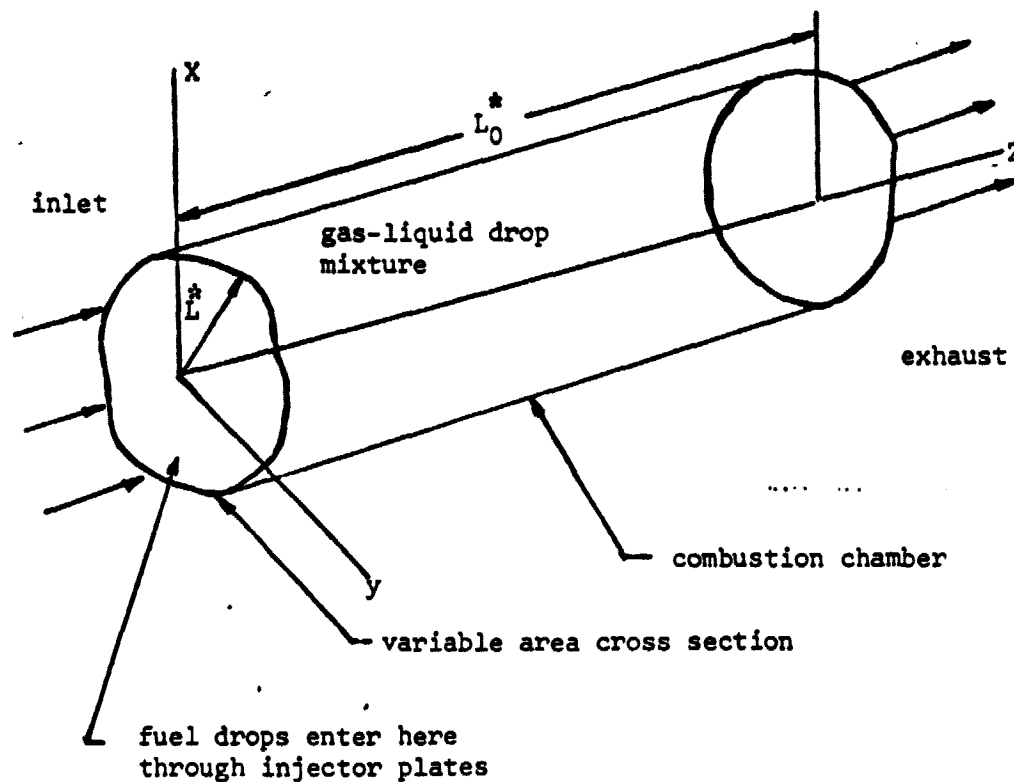


Figure 1. Schematic of a Liquid Propellant Combustion Chamber

A convenient non-dimensionalization of the variables is as follows:

$$\rho^* = \rho_0^* \rho \quad (\rho_0^* - \text{initial density of gas})$$

$$\vec{u}^* = a^* \vec{u}$$

$$\vec{\nabla}^* = \frac{1}{L^*} \vec{\nabla}$$

$$t^* = \frac{L^*}{a^*} t$$

$$p^* = a^{*2} \rho_0^* p$$

$$\frac{\rho_0^* a^*}{L^*} B = B.$$

Substituting these non-dimensional relations into equations (2.1), (2.3), and (2.4), the results are

$$\frac{\partial \rho}{\partial t} + \vec{\nabla} \cdot (\rho \vec{u}) = B \quad (2.5)$$

$$\rho \frac{\partial \vec{u}}{\partial t} + \rho \vec{u} \cdot \vec{\nabla} \vec{u} = - \vec{\nabla} p \quad (2.6)$$

$$p = \rho \quad (2.7)$$

where the unstarred quantities are dimensionless.

Dividing through by density ρ , equation (2.6) becomes

$$\frac{\partial \vec{u}}{\partial t} + \vec{u} \cdot \nabla \vec{u} = - \frac{\nabla \rho}{\rho} \quad (2.8)$$

Since,

$$\frac{\nabla \rho}{\rho} = \nabla \ln \rho,$$

the governing equations can be summarized as

$$\frac{\partial \rho}{\partial t} + \nabla \cdot (\rho \vec{u}) = B \quad (2.9)$$

$$\frac{\partial \vec{u}}{\partial t} + \vec{u} \cdot \nabla \vec{u} = - \nabla \ln \rho \quad (2.10)$$

$$p = \rho. \quad (2.11)$$

It will now be shown that to the order of approximation inherent in these equations, the flow is irrotational, that is $\nabla \times \vec{u} = 0$. To do this, take the curl of equation (2.10) and set it equal to zero. The resulting equation becomes

$$\nabla \times \left(\frac{\partial \vec{u}}{\partial t} + \vec{u} \cdot \nabla \vec{u} \right) = - \nabla \times \nabla \ln \rho = 0. \quad (2.12)$$

Since the curl of any gradient is zero. This may be rewritten as

$$\nabla \times \frac{\partial \vec{u}}{\partial t} + \nabla \times (\vec{u} \cdot \nabla \vec{u}) = 0. \quad (2.13)$$

The vorticity $\vec{\Omega}$ is defined to be

$$\vec{\Omega} = \vec{\nabla} \times \vec{u}. \quad (2.14)$$

Thus,

$$\vec{\nabla} \times \frac{\partial \vec{u}}{\partial t} = \frac{\partial}{\partial t} (\vec{\nabla} \times \vec{u}) = \frac{\partial \vec{\Omega}}{\partial t}. \quad (2.15)$$

From the vector identity

$$\vec{A} \cdot \vec{\nabla} \vec{A} = \vec{\nabla} \left(\frac{1}{2} \vec{A}^2 \right) - \vec{A} \times (\vec{\nabla} \times \vec{A})$$

it follows that

$$\vec{u} \cdot \vec{\nabla} \vec{u} = \vec{\nabla} \left(\frac{1}{2} \vec{u}^2 \right) - \vec{u} \times \vec{\Omega}. \quad (2.16)$$

Therefore,

$$\vec{\nabla} \times (\vec{u} \cdot \vec{\nabla} \vec{u}) = \vec{\nabla} \times \left[\vec{\nabla} \left(\frac{1}{2} \vec{u}^2 \right) - \vec{u} \times \vec{\Omega} \right]. \quad (2.17)$$

Recognizing that the curl of any gradient is zero, equation (2.17)

reduces to

$$\vec{\nabla} \times (\vec{u} \cdot \vec{\nabla} \vec{u}) = - \vec{\nabla} \times (\vec{u} \times \vec{\Omega}). \quad (2.18)$$

Using the vector identity

$$\vec{\nabla} \times (\vec{A} \times \vec{B}) = (\vec{B} \cdot \vec{\nabla}) \vec{A} - \vec{B} (\vec{\nabla} \cdot \vec{A}) - (\vec{A} \cdot \vec{\nabla}) \vec{B} + \vec{A} (\vec{\nabla} \cdot \vec{B})$$

equation (2.18) can be expressed as

$$\vec{\nabla} \times (\vec{u} \cdot \vec{\nabla} \vec{u}) = - [(\vec{\Omega} \cdot \vec{\nabla}) \vec{u} - \vec{\Omega}(\vec{\nabla} \cdot \vec{u}) - (\vec{u} \cdot \vec{\nabla})\vec{\Omega} + \vec{u} (\vec{\nabla} \cdot \vec{\Omega})]. \quad (2.19)$$

Therefore, equation (2.13) becomes

$$\frac{\partial \vec{\Omega}}{\partial t} - (\vec{\Omega} \cdot \vec{\nabla})\vec{u} + \vec{\Omega}(\vec{\nabla} \cdot \vec{u}) + (\vec{u} \cdot \vec{\nabla})\vec{\Omega} - \vec{u}(\vec{\nabla} \cdot \vec{\Omega}) = 0. \quad (2.20)$$

Equation (2.20) can now be modified by using the definition for the total (comoving) derivative which is

$$\frac{D\vec{\Omega}}{Dt} = \frac{\partial \vec{\Omega}}{\partial t} + \vec{u} \cdot (\vec{\nabla} \vec{\Omega}).$$

Substituting this expression into equation (2.20) and simplifying, the resulting equation becomes

$$\frac{D\vec{\Omega}}{Dt} = \vec{\Omega} \cdot (\vec{\nabla} \vec{u}) - (\vec{\Omega} \cdot \vec{\nabla}) \cdot \vec{u} + \vec{u} (\vec{\nabla} \cdot \vec{\Omega}). \quad (2.21)$$

Rewriting $\vec{u} (\vec{\nabla} \cdot \vec{\Omega})$ as $\vec{u} [\vec{\nabla} \cdot (\vec{\nabla} \times \vec{u})]$ which is zero since the divergence of the curl of any vector is zero, equation (2.21) becomes

$$\frac{D\vec{\Omega}}{Dt} = \vec{\Omega} \cdot (\vec{\nabla} \vec{u}) - (\vec{\Omega} \cdot \vec{\nabla}) \cdot \vec{u}. \quad (2.22)$$

The implications of this equation for a fluid starting from rest are as follows. At the initial instant of time ($t = 0$), the vorticity of any

fluid particle will be zero. Thus, the time derivative of the vorticity of the particle will be zero, implying that $\frac{D\vec{\Omega}}{Dt} = 0$ at $t = 0$. Since $\vec{\Omega} = 0$ and $\frac{D\vec{\Omega}}{Dt} = 0$ at $t = 0$, it follows that $\vec{\Omega} = 0$ at the next instant of time. By induction, it can be shown that $\vec{\Omega} = 0$ for all time unless the velocity gradient becomes infinite for any $t = 0$. It is assumed in what follows that this does not occur and the flow is treated as irrotational.

Since irrotationality has been proven, the velocity vector \vec{u} can be expressed as

$$\vec{u} = \vec{\nabla} \psi \quad (2.23)$$

where ψ is the velocity potential. Substituting equation (2.23) into the left hand side of equation (2.10), the result is

$$\begin{aligned} \frac{\partial \vec{u}}{\partial t} + \vec{u} \cdot \vec{\nabla} \vec{u} &= \frac{\partial \vec{u}}{\partial t} + \vec{\nabla} \left(\frac{1}{2} \vec{u}^2 \right) - \vec{u} \times \vec{\Omega} \\ &= \frac{\partial}{\partial t} (\vec{\nabla} \psi) + \vec{\nabla} \left[\frac{1}{2} (\vec{\nabla} \psi)^2 \right] - \vec{\nabla} \psi \times \vec{\Omega}. \end{aligned} \quad (2.24)$$

For irrotational flow ($\vec{\Omega} = 0$), the right hand side of equation (2.24) becomes

$$\vec{\nabla} \left[\frac{\partial \psi}{\partial t} + \frac{1}{2} (\vec{\nabla} \psi \cdot \vec{\nabla} \psi) \right]. \quad (2.25)$$

Therefore, equation (2.10) can be written as

$$\vec{\nabla} \left[\frac{\partial \psi}{\partial t} + \frac{1}{2} (\vec{\nabla} \psi \cdot \vec{\nabla} \psi) + \rho \phi \right] = 0. \quad (2.26)$$

Spatially integrating equation (2.26) produces

$$\frac{\partial \psi}{\partial \tau} + \frac{1}{2} \vec{\nabla} \psi \cdot \vec{\nabla} \psi + \ln \rho = \alpha(\tau) \quad (2.27)$$

where $\alpha(\tau)$ is a function of integration. From equation (2.23), it can be seen that an arbitrary function of time can be added to ψ without affecting the result for \vec{u} . Thus, $\alpha(\tau)$ could be absorbed into ψ . The same thing is accomplished by setting $\alpha = 0$ which results in

$$\ln \rho = -\frac{\partial \psi}{\partial \tau} - \frac{1}{2} \vec{\nabla} \psi \cdot \vec{\nabla} \psi \quad (2.28)$$

or

$$\rho = e^{-\left(\frac{\partial \psi}{\partial \tau} + \frac{1}{2} \vec{\nabla} \psi \cdot \vec{\nabla} \psi\right)} \quad (2.29)$$

Thus, ρ and \vec{u} are both known as functions of ψ . From equation (2.9), the governing equation for ψ can be written symbolically as

$$\frac{\partial \rho}{\partial \tau} + \rho \vec{\nabla}^2 \psi + \vec{\nabla} \psi \cdot \vec{\nabla} \rho = B \quad (2.30.a)$$

$$\rho = \rho = e^{-\left(\frac{\partial \psi}{\partial \tau} + \frac{1}{2} \vec{\nabla} \psi \cdot \vec{\nabla} \psi\right)} \quad (2.30.b)$$

Rather than combining these quantities immediately, it is convenient to first make further simplifications based on the nature of the physical problem that it is desired to analyze.

Steady State Solution

First, the steady state solution of equations (2.30) corresponding to purely axial motion will be found. Define the steady-state velocity potential $\bar{\phi}$ by

$$\psi = \epsilon \bar{\phi}(z) \quad (2.31)$$

where ϵ (assumed small) is the measure of the deviation of the density from its initial value (see equation 2.32 below). The bar notation will represent steady-state conditions. The steady-state burning rate $\bar{\omega}$ is defined from

$$B = \bar{\omega}(z). \quad (2.32)$$

While many other situations are possible, attention will be confined in the present work to the case when $\bar{\omega} = 0(\epsilon)$. To indicate this let

$$\bar{\omega} = \epsilon \bar{\sigma} \quad (\bar{\sigma} = 0(1)). \quad (2.33)$$

Thus, the burning rate B can be expressed as

$$B = \epsilon \bar{\sigma}. \quad (2.34)$$

Equation (2.30.b) can now be written

$$\rho = e^{-\left[\frac{1}{2} \epsilon^2 \left(\frac{d\bar{\phi}}{dz} \right)^2 \right]}. \quad (2.35)$$

Using the Taylor series expansion for the exponential function and retaining only the first two terms, equation (2.35) becomes

$$\rho = 1 - \frac{1}{2}\epsilon^2 \left(\frac{d\bar{\phi}}{dz}\right)^2 + \dots \quad (2.36)$$

Substituting equations (2.31), (2.34), and (2.36) into equation (2.30.a) and dividing the result by ϵ yields

$$\left[1 - \frac{1}{2}\epsilon^2 \left(\frac{d\bar{\phi}}{dz}\right)^2 + \dots\right] \left[\frac{d^2\bar{\phi}}{dz^2}\right] + \frac{d\bar{\phi}}{dz} \left[-\epsilon^2 \left(\frac{d\bar{\phi}}{dz}\right) \left(\frac{d^2\bar{\phi}}{dz^2}\right)\right] = \bar{\sigma} \quad (2.37)$$

or

$$\frac{d^2\bar{\phi}}{dz^2} - \frac{3}{2}\epsilon^2 \left(\frac{d\bar{\phi}}{dz}\right) \left(\frac{d^2\bar{\phi}}{dz^2}\right) + \dots = \bar{\sigma}. \quad (2.38)$$

Retaining only terms of $O(1)$ produces

$$\frac{d^2\bar{\phi}}{dz^2} = \bar{\sigma}. \quad (2.39)$$

For simplicity, only the case of uniformly distributed combustion (i.e. $\bar{\sigma} = \text{constant}$) will be considered. Thus, integrating equation (2.39) one obtains

$$\frac{d\bar{\phi}}{dz} = \bar{\sigma} z + C_1, \quad (2.40)$$

where $\frac{d\bar{\phi}}{dz} = \bar{u}$ is the steady state velocity of the gas.

At the injector ($Z = 0$), $\bar{u} = 0$. Thus, $C_1 = 0$ and

$$\bar{u} = \frac{d\bar{\phi}}{dz} = \bar{\sigma} z. \quad (2.41)$$

Deviations from Steady State

It is now desired to investigate the stability of the steady state solution discussed above. Toward this end, an additional velocity potential related to perturbations from the steady state is defined by the equation

$$\psi = \epsilon [\bar{\phi} + \phi(x, y, z, t)]. \quad (2.42)$$

A perturbation burning rate B is also defined by the equation

$$B = \bar{\omega} + \epsilon\omega. \quad (2.43)$$

It is assumed that $\omega = O(\epsilon)$ and this is indicated by defining a function σ such that $\sigma = O(1)$ and $\omega = \sigma\epsilon$. Then equation (2.43) becomes

$$B = \epsilon(\bar{\sigma} + \sigma). \quad (2.44)$$

Taking the gradient of equation (2.42), one obtains

$$\vec{\nabla}\psi = \epsilon[\vec{\nabla}\bar{\phi} + \vec{\nabla}\phi]. \quad (2.45)$$

or

$$\vec{\nabla}\psi = \epsilon[\bar{u}\vec{e}_z + \vec{\nabla}\phi]. \quad (2.46)$$

From equation (2.42), the time derivative of ψ can be expressed as

$$\frac{\partial\psi}{\partial t} = \epsilon \frac{\partial\phi}{\partial t}. \quad (2.47)$$

Substituting the equations (2.46) and (2.47) into equation (2.30.b) and simplifying, one obtains

$$p = \rho = e - \left[\epsilon \frac{\partial \phi}{\partial t} + \frac{1}{2} \epsilon^2 (\bar{u}^2 + 2\bar{u} \frac{\partial \phi}{\partial z} + \vec{\nabla} \phi \cdot \vec{\nabla} \phi) \right]. \quad (2.48)$$

Expanding (2.48) in a Taylor series and neglecting terms of $O(\epsilon^3)$ and higher produces the expression

$$p = \rho = 1 - \epsilon \frac{\partial \phi}{\partial t} + \epsilon^2 \left[-\frac{1}{2} (\bar{u}^2 + \vec{\nabla} \phi \cdot \vec{\nabla} \phi) - \bar{u} \frac{\partial \phi}{\partial z} + \frac{1}{2} \left(\frac{\partial \phi}{\partial t} \right)^2 \right]. \quad (2.49)$$

Substituting equations (2.42), (2.44), and (2.48) into equation (2.30.a) and dividing the result by ϵ leads to

$$\begin{aligned} & -\frac{\partial^2 \phi}{\partial t^2} + \epsilon \left[-\frac{1}{2} \frac{\partial}{\partial t} (\bar{u}^2 + \vec{\nabla} \phi \cdot \vec{\nabla} \phi) - \bar{u} \frac{\partial^2 \phi}{\partial z \partial t} + \frac{1}{2} \frac{\partial}{\partial t} \left(\frac{\partial \phi}{\partial t} \right)^2 \right] \\ & + \dots + \left[1 - \epsilon \frac{\partial \phi}{\partial t} + \epsilon^2 \left[-\frac{1}{2} (\bar{u}^2 + \vec{\nabla} \phi \cdot \vec{\nabla} \phi) - \bar{u} \frac{\partial \phi}{\partial z} \right. \right. \\ & \left. \left. + \frac{1}{2} \left(\frac{\partial \phi}{\partial t} \right)^2 \right] \right] \cdot \left(\frac{\partial \bar{u}}{\partial z} + \vec{\nabla}^2 \phi \right) + (\bar{u} \vec{e}_z + \vec{\nabla} \phi) \cdot \left(-\epsilon \vec{\sigma} \frac{\partial \phi}{\partial t} \right. \\ & \left. + \epsilon^2 \vec{\nabla} \left(-\frac{1}{2} (\bar{u}^2 + \vec{\nabla} \phi \cdot \vec{\nabla} \phi) \right) - \bar{u} \frac{\partial \phi}{\partial z} + \frac{1}{2} \left(\frac{\partial \phi}{\partial t} \right)^2 \right] = \bar{\sigma} + \epsilon \sigma. \quad (2.50) \end{aligned}$$

Neglecting all terms of $O(\epsilon^2)$ and higher and recalling from the steady-state solution that $\bar{u} = \frac{d\phi}{dz} = \bar{\sigma} z$ and $\frac{d\bar{u}}{dz} = \bar{\sigma}$ yields

$$\begin{aligned} \frac{\partial^2 \phi}{\partial t^2} - \nabla^2 \phi + \epsilon \left[\frac{1}{2} \frac{\partial}{\partial t} (\vec{\nabla} \phi \cdot \vec{\nabla} \phi) + \bar{u} \frac{\partial^2 \phi}{\partial z \partial t} - \frac{\partial \phi}{\partial t} \frac{\partial^2 \phi}{\partial t^2} + \frac{\partial \phi}{\partial t} \vec{\nabla}^2 \phi \right. \\ \left. + \frac{\partial \phi}{\partial t} \bar{\sigma} + \bar{u} \frac{\partial^2 \phi}{\partial z \partial t} + \left(\vec{\nabla} \phi \cdot \vec{\nabla} \frac{\partial \phi}{\partial t} \right) \right] = -\sigma \epsilon. \end{aligned} \quad (2.51)$$

Substituting

$$\frac{1}{2} \frac{\partial}{\partial t} (\vec{\nabla} \phi \cdot \vec{\nabla} \phi) = \vec{\nabla} \phi \cdot \vec{\nabla} \frac{\partial \phi}{\partial t} \quad (2.52)$$

into equation (2.51), results in

$$\begin{aligned} \frac{\partial^2 \phi}{\partial t^2} - \nabla^2 \phi + \epsilon \left[2 \left(\vec{\nabla} \phi \cdot \vec{\nabla} \frac{\partial \phi}{\partial t} \right) + 2 \bar{u} \frac{\partial^2 \phi}{\partial z \partial t} + \frac{\partial \phi}{\partial t} \bar{\sigma} \right. \\ \left. + \frac{\partial \phi}{\partial t} \left(\nabla^2 \phi - \frac{\partial^2 \phi}{\partial t^2} \right) \right] = -\sigma \epsilon \end{aligned} \quad (2.53)$$

where only terms of $O(1)$ and $O(\epsilon)$ have been retained. Equation (2.53) can

be further simplified by observing that $\nabla^2 \phi = \frac{\partial^2 \phi}{\partial t^2} + O(\epsilon)$.

Thus, the last term of equation (2.53) can be written

$$\epsilon \frac{\partial \phi}{\partial t} \left(\nabla^2 \phi - \frac{\partial^2 \phi}{\partial t^2} \right) = \epsilon \frac{\partial \phi}{\partial t} \left(\frac{\partial^2 \phi}{\partial t^2} + O(\epsilon) - \frac{\partial^2 \phi}{\partial t^2} \right) = O(\epsilon^2).$$

Since the other terms of $O(\epsilon^2)$ have already been neglected, consistency requires that this term be deleted and the equation be rewritten as

$$\frac{\partial^2 \phi}{\partial t^2} - \nabla^2 \phi + \epsilon \left[2 \left(\vec{\nabla} \phi \cdot \vec{\nabla} \frac{\partial \phi}{\partial t} \right) + 2 \bar{u} \frac{\partial^2 \phi}{\partial z \partial t} + \frac{\partial \phi}{\partial t} \bar{\sigma} \right] = -\sigma \epsilon. \quad (2.54)$$

In this thesis, attention will be confined to transverse instability.

For this situation

$$\phi = \phi(x, y, t). \quad (2.55)$$

Therefore, equation (2.54) becomes

$$\frac{\partial^2 \phi}{\partial t^2} - \nabla^2 \phi + \epsilon \left[2 \left(\vec{\nabla} \phi \cdot \vec{\nabla} \frac{\partial \phi}{\partial t} \right) + \frac{\partial \phi}{\partial t} \bar{\sigma} \right] = -\sigma \epsilon. \quad (2.56)$$

To account approximately for frequency changes due to baffles, nozzle shapes, etc., a correction term of the form

$$\epsilon K \nabla^2 \left(\frac{\partial^2 \phi}{\partial t^2} \right) \quad (2.57)$$

was introduced into equation (2.56). This form, one of many possible, was chosen so that the linearized form of equation (2.56) would reduce to Love's equation for a one-dimensional problem. This linearized form of (2.56) is

$$\frac{\partial^2 \phi}{\partial t^2} - \frac{\partial^2 \phi}{\partial x^2} - \epsilon K \frac{\partial^4 \phi}{\partial x^2 \partial t^2} = 0. \quad (2.58)$$

Thus, it can be seen that the value K will affect the acoustic frequencies. Physically, this is the purpose of baffles, nozzle shapes, and other physical parts of the combustion chamber. Therefore, inserting the correction term into equation (2.56), the resulting equation becomes

$$\frac{\partial^2 \phi}{\partial t^2} - \nabla^2 \phi + \epsilon \left[\bar{\sigma} \frac{\partial \phi}{\partial t} + 2 \vec{\nabla} \phi \cdot \vec{\nabla} \frac{\partial \phi}{\partial t} - K \nabla^2 \left(\frac{\partial^2 \phi}{\partial t^2} \right) \right] = -\sigma \epsilon. \quad (2.59)$$

where K is the correction factor. This non-linear wave equation will be the basis for numerically and analytically investigating the transverse combustion stability problems occurring in liquid propellant rocket engines.

Chapter 3

DERIVATION OF WAVE EQUATIONS BASED UPON AN ANNULAR COMBUSTION CHAMBER

In Chapter 2, there were no restrictions concerning the geometry of the combustion chamber in the derivation of the acoustic wave equation. In this chapter, however, a set of equations will be developed based upon a narrow annular combustion chamber. A typical cross-section for such a combustion chamber is shown in Figure 2 below in dimensional and dimensionless form.

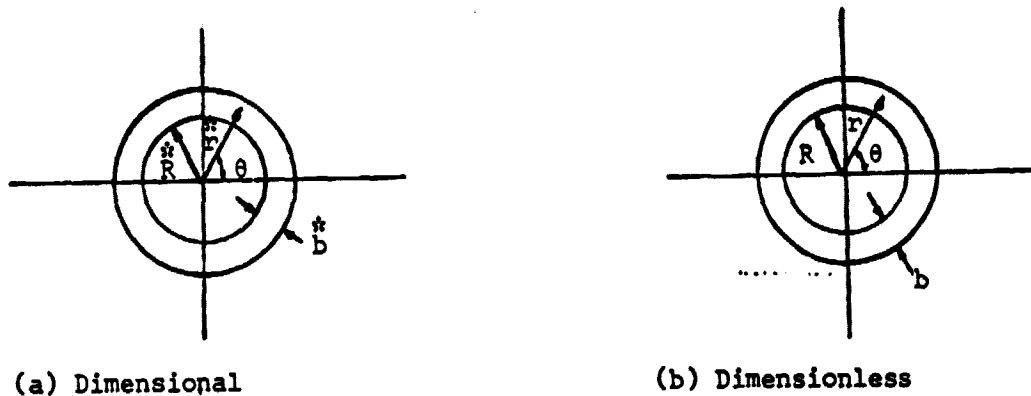


Figure 2. Dimensional and Dimensionless Form of a Circular Cylindrical Combustion Chamber

In Figure 2 (a), the dimensional quantities are

r - radius of a typical point in the combustion chamber

R - inside radius of the combustion chamber

b - thickness of combustion chamber's cross-section.

In Figure 2 (b), the dimensionless quantities are

r - non-dimensional radius of a typical point

$$R = \frac{R^*}{R} = 1$$

$$b = \frac{b^*}{R}$$

The first major assumption to be made in the geometry of the combustion chamber is

$$\frac{b}{R} \ll 1 \quad (3.1)$$

which states that the circular cylinder can be thought of as a thin (ring-like) annulus.

Define the characteristic length L^* by

$$L^* = R^*. \quad (3.2)$$

In restricting the analysis to an annulus, a transformation to polar coordinates is convenient. Recall that the gradient and Laplacian operators in polar coordinates are

$$\vec{\nabla} = \vec{e}_r \frac{\partial}{\partial r} + \frac{\vec{e}_\theta}{r} \frac{\partial}{\partial \theta} + \vec{e}_z \frac{\partial}{\partial z} \quad (3.3)$$

$$\nabla^2 = \frac{\partial^2}{\partial r^2} + \frac{1}{r} \frac{\partial}{\partial r} + \frac{1}{r^2} \frac{\partial^2}{\partial \theta^2} + \frac{\partial^2}{\partial z^2}$$

The second major assumption for the simplification of the velocity potential is restricting

$$\phi = \phi(\theta, t) \quad (3.4)$$

$$r \neq 1 .$$

Therefore, using the operators of equations (3.3) on the function of equation (3.4), the results are

$$\vec{\nabla}\phi = \vec{e}_\theta \frac{\partial\phi}{\partial\theta} \quad (3.5)$$

$$\nabla^2\phi = \frac{\partial^2\phi}{\partial\theta^2}.$$

Substituting the results of equation (3.5) into the general acoustic wave equation (2.58), the modified wave equation becomes

$$\frac{\partial^2\phi}{\partial t^2} - \frac{\partial^2\phi}{\partial\theta^2} + \epsilon \left[\sigma \frac{\partial\phi}{\partial t} + 2 \frac{\partial\phi}{\partial\theta} \cdot \frac{\partial^2\phi}{\partial\theta\partial t} - K \frac{\partial^4\phi}{\partial t^2\partial\theta^2} \right] = -\sigma\epsilon. \quad (3.6)$$

Now, express the velocity vector

$$\vec{u} = \vec{u} + \vec{u}' \quad (3.7)$$

where \vec{u} - steady-state velocity vector

\vec{u}' - perturbation velocity vector.

From the steady state solution in Chapter 2, the velocity vector was defined as

$$\vec{u} = \epsilon \left[\frac{d\bar{\phi}}{dz} \vec{e}_z \right]. \quad (3.8)$$

Define the perturbation velocity vector by

$$\vec{u}' = \epsilon \vec{\nabla} \phi = \epsilon \frac{\partial \phi}{\partial \theta} \vec{e}_\theta. \quad (3.9)$$

Substituting equation (3.8) and (3.9) into equation (3.7) and using equation (2.23) results in

$$\vec{u} = \epsilon \frac{d\phi}{dz} \vec{e}_z + \epsilon \frac{\partial \phi}{\partial \theta} \vec{e}_\theta = \vec{\nabla} \psi. \quad (3.10)$$

To determine only the transverse velocity component of the perturbation velocity vector, subtract the perturbed velocity component along the axial (z) direction of the chamber from the total perturbation velocity vector. Thus,

$$\vec{u}'_t = \vec{u}' - u_z \vec{e}_z. \quad (3.11)$$

In this case, since $u = u(\theta, \tau)$ only, there is no perturbed velocity component in the axial direction; therefore,

$$\vec{u}'_t = \epsilon \frac{\partial \phi}{\partial \theta} \vec{e}_\theta. \quad (3.12)$$

It is now desired to find the burning rate σ in terms of the parameters in the wave equation. To obtain this expression, assume velocity sensitive combustion with no history effects. Mathematically, the burning-rate function for velocity-sensitive combustion will be expressed by the purely phenomenological equation

$$\sigma = \bar{\omega} n f\left(\frac{u_t'^2}{c^2}\right) \quad (3.13)$$

where n is called the interaction index.

Using the derived results for the general time-delay integral (discussed in Appendix A), the burning rate with history effects accounted for by a simple time delay is

$$\sigma = \bar{\omega} n \left\{ f\left(\frac{u_t'^2}{c^2}\right) - f_{\tau}\left(\frac{u_t'^2}{c^2}\right) \right\} \quad (3.14)$$

where the subscript τ represents the time delay. For simplicity, it will be assumed that

$$f\left(\frac{u_t'^2}{c^2}\right) = \frac{u_t'^2}{c^2}.$$

Then, the burning rate can be expressed as

$$\sigma = n\bar{\omega} \left[\left(\frac{\partial \phi}{\partial \theta}\right)^2 - j \left(\frac{\partial \phi}{\partial \theta}\right)_{\tau}^2 \right] \quad (3.16)$$

where $j = 0$ - no time delay

1 - time delay.

Therefore, substituting equation (3.16) into equation (3.6), equation (3.6) can be rewritten

$$\frac{\partial^2 \phi}{\partial t^2} - \frac{\partial^2 \phi}{\partial \theta^2} + c \left[\bar{c} \frac{\partial \phi}{\partial t} + 2 \frac{\partial \phi}{\partial t} \frac{\partial^2 \phi}{\partial \theta \partial t} - k \frac{\partial^4 \phi}{\partial t^2 \partial \theta^2} \right. \\ \left. + n \bar{\omega} \left(\left(\frac{\partial \phi}{\partial \theta} \right)^2 - j \left(\frac{\partial \phi}{\partial \theta} \right)^2 \right) \right] = 0. \quad (3.17)$$

There is no closed form solution of equation (3.17) that appears likely. The main purpose of the present work is to determine the modifications of solutions of the usual acoustic wave equations that are caused by the presence of the nonlinear terms multiplied by c in equation (3.17). Thus, rather than attempt a finite difference numerical solution of equation (3.17), the following procedure was adopted.

The solution is represented by the Fourier series

$$\phi(\theta, t) = f_1(t) \cos \theta + f_2(t) \cos 2\theta + g_1(t) \sin \theta \\ + g_2(t) \sin 2\theta + \dots \quad (3.18)$$

and initial conditions are chosen such that in the absence of the nonlinear terms, the exact solution can be formed using only the first two terms of the Fourier series. Because of the quadratic nature of the non-linearities, the second two terms in equation (3.18) represent a complete first order correction to the acoustic solution due to non-linear gas-dynamic and combustion effects. Only the first four terms in equation (3.18) are, therefore, retained and the approximate solution determined by this method is the simplest one capable of illustrating the influence of the nonlinear

terms. The approximation can, of course, be improved by retaining additional terms in equation (3.10) but this is not investigated.

Substituting equation (3.13) into equation (3.17) and using the multiple angle formulas to simplify terms containing products of trigonometric functions, one obtains

$$\begin{aligned}
 & \left\{ \frac{d^2 f}{dt^2} + f_1 + \bar{\omega} \frac{df}{dt} + 2\epsilon \left[f_2 \frac{df}{dt} + f_1 \frac{df}{dt} + g_2 \frac{dg_1}{dt} + g_1 \frac{dg_2}{dt} \right] \right. \\
 & \quad \left. + K\epsilon \frac{d^2 f}{dt^2} + 2n\epsilon\bar{\omega} \left[f_1 f_2 + g_1 g_2 \right] - 2j\epsilon n\bar{\omega} \left[f_{1\tau} f_{2\tau} + g_{1\tau} g_{2\tau} \right] \right\} \cos \theta \\
 & + \left\{ \frac{d^2 g_1}{dt^2} + g_1 + \bar{\omega} \frac{dg_1}{dt} + 2\epsilon \left[g_2 \frac{df}{dt} + f_1 \frac{dg_2}{dt} - g_1 \frac{df}{dt} - f_2 \frac{dg_1}{dt} \right] \right. \\
 & \quad \left. + K\epsilon \frac{d^2 g_1}{dt^2} + 2n\epsilon\bar{\omega} \left[f_1 g_2 - f_2 g_1 \right] - 2j\epsilon n\bar{\omega} \left[f_{1\tau} g_{2\tau} - f_{2\tau} g_{1\tau} \right] \right\} \sin \theta \\
 & + \left\{ \frac{d^2 f}{dt^2} + 4f_2 + \bar{\omega} \frac{df}{dt} + \epsilon \left[g_1 \frac{dg_1}{dt} - f_1 \frac{df}{dt} \right] + 4K\epsilon \frac{d^2 f}{dt^2} \right. \\
 & \quad \left. + 2j\epsilon n \left[g_1^2 - f_1^2 \right] - 2j\epsilon n \left[g_{1\tau}^2 - f_{1\tau}^2 \right] \right\} \cos 2\theta \\
 & + \left\{ \frac{d^2 g_2}{dt^2} + 4g_2 + \bar{\omega} \frac{dg_2}{dt} - \epsilon \left[g_1 \frac{df}{dt} + f_1 \frac{dg_1}{dt} \right] + 4K\epsilon \frac{d^2 g_2}{dt^2} \right. \\
 & \quad \left. - \omega n \epsilon \left[f_1 g_1 \right] + j\omega n \epsilon \left[f_{1\tau} g_{1\tau} \right] \right\} \sin 2\theta + \dots = 0. \quad (3.19)
 \end{aligned}$$

Equation (3.19) is a summation of terms composed of some function of time t and a term containing θ variation. Since the equation must be valid for all values of θ , each of the time dependent coefficients of the θ -terms must individually be equal to zero. Therefore, four ordinary differential equations governing the time-dependent modal amplitudes f_1 , g_1 , f_2 and g_2 emerge from this analysis as the governing equations to be used for analysis of instability in an annular combustion chamber. These equations are

$$\begin{aligned} \frac{d^2 f}{dt^2} + f_1 + \bar{\omega} \frac{df}{dt} + 2\epsilon \left[f_2 \frac{df_1}{dt} + f_1 \frac{df_2}{dt} + g_2 \frac{dg_1}{dt} + g_1 \frac{dg_2}{dt} \right] \\ + K\epsilon \frac{d^2 f}{dt^2} + 2n\epsilon\bar{\omega} \left[f_1 f_2 + g_1 g_2 \right] - 2j\epsilon n\bar{\omega} \left[f_{1\tau} f_{2\tau} + g_{1\tau} g_{2\tau} \right] = 0 \end{aligned} \quad (3.20.a)$$

$$\begin{aligned} \frac{d^2 g}{dt^2} + g_1 + \bar{\omega} \frac{dg}{dt} + 2\epsilon \left[g_2 \frac{df}{dt} + f_1 \frac{dg_2}{dt} - g_1 \frac{df_2}{dt} - f_2 \frac{dg_1}{dt} \right] \\ + K\epsilon \frac{d^2 g}{dt^2} + 2n\epsilon\bar{\omega} \left[f_1 g_2 - f_2 g_1 \right] - 2j\epsilon n\bar{\omega} \left[f_{1\tau} g_{2\tau} - f_{2\tau} g_{1\tau} \right] = 0 \end{aligned} \quad (3.20.b)$$

$$\begin{aligned} \frac{d^2 f}{dt^2} + 4f_2 + \bar{\omega} \frac{df}{dt} + \epsilon \left[g_1 \frac{dg_1}{dt} - f_1 \frac{df_1}{dt} \right] + 4K\epsilon \frac{d^2 f}{dt^2} \\ + \frac{1}{2}\epsilon n\bar{\omega} \left[g_1^2 - f_1^2 \right] - \frac{1}{2}j\epsilon n\bar{\omega} \left[g_{1\tau}^2 - f_{1\tau}^2 \right] = 0 \end{aligned} \quad (3.20.c)$$

$$\frac{d^2g_2}{dt^2} + 4g_2 + \bar{\omega} \frac{dg_2}{dt} - \epsilon \left[g_1 \frac{df_1}{dt} + f_1 \frac{dg_1}{dt} \right] + 4K\epsilon \frac{d^2g_2}{dt^2} - \bar{\omega}\epsilon \left[f_1g_1 \right] + jn\bar{\omega}\epsilon \left[f_{1\tau}g_{1\tau} \right] = 0. \quad (3.20.d)$$

In the following work only instantaneous combustion will be considered.

Thus, the appropriate equations are equations (3.20) with $j = 0$. These equations are recapitulated below.

$$\frac{d^2f_1}{dt^2} + f_1 + \bar{\omega} \frac{df_1}{dt} + 2\epsilon \left[f_2 \frac{df_1}{dt} + f_1 \frac{df_2}{dt} + g_2 \frac{dg_1}{dt} + g_1 \frac{dg_2}{dt} \right] + K\epsilon \frac{d^2f_1}{dt^2} + 2n\epsilon\bar{\omega} \left[f_1f_2 + g_1g_2 \right] = 0 \quad (3.21.a)$$

$$\frac{d^2g_1}{dt^2} + g_1 + \bar{\omega} \frac{dg_1}{dt} + 2\epsilon \left[g_2 \frac{df_1}{dt} + f_1 \frac{dg_2}{dt} - g_1 \frac{df_2}{dt} - f_2 \frac{dg_1}{dt} \right] + K\epsilon \frac{d^2g_1}{dt^2} + 2n\epsilon\bar{\omega} \left[f_1g_2 - f_2g_1 \right] = 0 \quad (3.21.b)$$

$$\frac{d^2f_2}{dt^2} + 4f_2 + \bar{\omega} \frac{df_2}{dt} + \epsilon \left[g_1 \frac{dg_1}{dt} - f_1 \frac{df_1}{dt} \right] + 4K\epsilon \frac{d^2f_2}{dt^2} + \frac{1}{2}\epsilon\bar{\omega}n \left[g_1^2 - f_1^2 \right] = 0 \quad (3.21.c)$$

$$\frac{d^2g_2}{dt^2} + 4g_2 + \bar{\omega} \frac{dg_2}{dt} - \epsilon \left[c_1 \frac{df}{dt} + f_1 \frac{dg_1}{dt} \right]$$

$$+ 4K\epsilon \frac{d^2g_2}{dt^2} - \bar{\omega}\epsilon \left[g_1 f_1 \right] = 0 \quad (3.21.d)$$

The equations of (3.21) were solved numerically by the use of the quartic (fourth-order) Runge-Kutta method. To use this method, the equations of (3.21) are modified by defining the quantities

$$\frac{df_1}{dt} = a_1$$

$$\frac{df_2}{dt} = a_2$$

$$\frac{dg_1}{dt} = b_1$$

$$\frac{dg_2}{dt} = b_2 \quad (3.22)$$

Substituting these expressions into equations (3.20) and solving these equations for the highest derivative (in this case - second order), we get

$$\frac{da_1}{dt} = \left[-f_1 - \bar{\omega}(a_1) - 2\epsilon i \left(f_2(a_1) + f_1(a_2) + g_2(b_1) \right. \right.$$

$$\left. \left. + g_1(b_2) \right) - 2n\epsilon\bar{\omega}(f_1f_2 + g_1g_2) \right] / (1 + K\epsilon)$$

$$\frac{db_1}{dt} = \left[-g_1 - \bar{\omega}(b_1) - 2\epsilon i \left(g_2(a_1) + f_1(b_2) - g_1(a_2) - f_2(b_1) \right) - 2n\epsilon\bar{\omega}(f_1g_2 - f_2g_1) \right] / (1 + K\epsilon)$$

$$\frac{da_2}{dt} = \left[-4f_2 - \bar{\omega}(a_2) - \epsilon i \left(g_1(b_1) - f_1(a_1) \right) - \frac{1}{2}\epsilon\bar{\omega} \left[g_1^2 - f_1^2 \right] \right] / (1 + 4K\epsilon)$$

$$\frac{db_2}{dt} = \left[-4g_2 - \bar{\omega}(b_2) + \epsilon i \left(g_1(a_1) + f_1(b_1) \right) + \bar{\omega}\epsilon \left(f_1g_1 \right) \right] / (1 + 4K\epsilon) \quad (3.23)$$

where i is the gas-dynamic index.

By the development of a computer program incorporating the Runge-Kutta algorithm which can solve systems of first-order ordinary differential equations, the eight equations (3.22) and (3.23) were numerically solved for the eight variables a_1 , a_2 , b_1 , b_2 , f_1 , f_2 , g_1 , and g_2 . Different cases involving varying the gas-dynamic index, interaction index, the correction variable (K), and the order term (epsilon) will be discussed and compared with the perturbation method of solution in a later chapter. In Appendix B, a sample program listing this calculation appears.

Chapter 4

TWO-VARIABLE PERTURBATION METHOD APPLIED TO THE ACOUSTIC WAVE EQUATIONS

In this chapter, a set of approximate equations will be developed from the governing equations for the modal amplitudes (3.21), by the use of the two-variable perturbation method. The two-variable method is well suited to this type problem since one expects the solution to consist of sinusoidal functions with slowly varying amplitude. Applying this method, define two variables representing time

$$\begin{aligned}\xi &= t \\ \eta &= \epsilon t .\end{aligned}\tag{4.1}$$

Therefore, the four modal amplitudes would now be

$$\begin{aligned}f_1 &= f_1(\xi, \eta) \\ f_2 &= f_2(\xi, \eta) \\ g_1 &= g_1(\xi, \eta) \\ g_2 &= g_2(\xi, \eta) .\end{aligned}\tag{4.2}$$

By applying the chain rule of differentiation, it can be shown that

$$\frac{dZ}{dt} = \frac{\partial Z}{\partial \xi} + \epsilon \frac{\partial Z}{\partial \eta}\tag{4.3}$$

and

$$\frac{d^2 Z}{dt^2} = \frac{\partial^2 Z}{\partial \xi^2} + 2\epsilon \frac{\partial^2 Z}{\partial \xi \partial \eta} + \epsilon^2 \frac{\partial^2 Z}{\partial \eta^2} \quad (4.4)$$

where $Z = f_1, f_2, g_1, g_2$ respectively for each of the above equations. By substituting equations (4.3) and (4.4) for each modal amplitude into equations (3.21) and keeping terms only of $O(1)$ and $O(\epsilon)$, the resulting equations become

$$\frac{\partial^2 f_1}{\partial \xi^2} + f_1 + \epsilon \left[2 \frac{\partial^2 f_1}{\partial \xi \partial \eta} + \bar{\sigma} \frac{\partial f_1}{\partial \xi} + 2f_2 \frac{\partial f_1}{\partial \xi} + 2f_1 \frac{\partial f_2}{\partial \xi} + 2g_2 \frac{\partial g_1}{\partial \xi} \right.$$

$$\left. + 2g_1 \frac{\partial g_2}{\partial \xi} + K \frac{\partial^2 f_1}{\partial \xi^2} + 2n\bar{\omega}(f_1 f_2 + g_1 g_2) \right] = 0$$

$$\frac{\partial^2 g_1}{\partial \xi^2} + g_1 + \epsilon \left[2 \frac{\partial^2 g_1}{\partial \xi \partial \eta} + \bar{\sigma} \frac{\partial g_1}{\partial \xi} + 2g_2 \frac{\partial f_1}{\partial \xi} + 2f_1 \frac{\partial g_2}{\partial \xi} - 2g_1 \frac{\partial f_2}{\partial \xi} \right.$$

$$\left. - 2f_2 \frac{\partial g_1}{\partial \xi} + K \frac{\partial^2 g_1}{\partial \xi^2} + 2n\bar{\omega}(f_1 g_2 - f_2 g_1) \right] = 0$$

$$\frac{\partial^2 f_2}{\partial \xi^2} + 4f_2 + \epsilon \left[2 \frac{\partial^2 f_2}{\partial \xi \partial \eta} + \bar{\sigma} \frac{\partial f_2}{\partial \xi} + g_1 \frac{\partial g_1}{\partial \xi} - f_1 \frac{\partial f_1}{\partial \xi} \right.$$

$$\left. + 4K \frac{\partial^2 f_2}{\partial \xi^2} + \frac{1}{2} \bar{\omega} n (g_1^2 - f_1^2) \right] = 0$$

$$\frac{\partial^2 g_2}{\partial \xi^2} + 4g_2 + \epsilon \left[2 \frac{\partial^2 g_2}{\partial \xi \partial \eta} + \bar{\sigma} \frac{\partial g_2}{\partial \xi} - g_1 \frac{\partial f_1}{\partial \xi} - f_1 \frac{\partial g_1}{\partial \xi} \right.$$

$$\left. + 4K \frac{\partial^2 g_2}{\partial \xi^2} - \bar{\omega} n (f_1 g_1) \right] = 0 \quad (4.5)$$

From the straight-forward perturbation method, define the modal amplitudes by the series expansions

$$\begin{aligned}
 f_1 &= f_{10}(\xi, \eta) + \epsilon f_{11}(\xi, \eta) + \dots \\
 f_2 &= f_{20}(\xi, \eta) + \epsilon f_{21}(\xi, \eta) + \dots \\
 g_1 &= g_{10}(\xi, \eta) + \epsilon g_{11}(\xi, \eta) + \dots \\
 g_2 &= g_{20}(\xi, \eta) + \epsilon g_{21}(\xi, \eta) + \dots \dots \dots
 \end{aligned}
 \tag{4.6}$$

Again by applying the rules of differentiation, it can be shown that

$$\begin{aligned}
 \frac{\partial Z}{\partial \xi} &= \frac{\partial T}{\partial \xi} + \epsilon \frac{\partial K}{\partial \xi} \\
 \frac{\partial^2 Z}{\partial \xi^2} &= \frac{\partial^2 T}{\partial \xi^2} + \epsilon \frac{\partial^2 K}{\partial \xi^2} \\
 \frac{\partial^2 Z}{\partial \xi \partial \eta} &= \frac{\partial^2 T}{\partial \xi \partial \eta} + \epsilon \frac{\partial^2 K}{\partial \xi \partial \eta}
 \end{aligned}
 \tag{4.7}$$

where

$$Z = f_1, f_2, g_1, g_2$$

$$T = f_{10}, f_{20}, g_{10}, g_{20}$$

and

$$K = f_{11}, f_{21}, g_{11}, g_{21}, \text{ respectively.}$$

Substituting the expressions of (4.6) and (4.7) into equations (4.5) and keeping terms only of $O(1)$ and $O(\epsilon)$, the resulting equations become

$$\begin{aligned}
& \frac{\partial^2 f_{10}}{\partial \xi^2} + f_{10} + \epsilon \left[\frac{\partial^2 f_{11}}{\partial \xi^2} + f_{11} + 2 \frac{\partial^2 f_{10}}{\partial \xi \partial \eta} + \bar{\sigma} \frac{\partial f_{10}}{\partial \xi} + 2f_{20} \frac{\partial f_{10}}{\partial \xi} \right. \\
& + 2f_{10} \frac{\partial f_{20}}{\partial \xi} + 2g_{20} \frac{\partial g_{10}}{\partial \xi} + 2g_{10} \frac{\partial g_{20}}{\partial \xi} + K \frac{\partial^2 f_{10}}{\partial \xi^2} \\
& \left. + 2n\bar{\omega}(f_{10}f_{20} + g_{10}g_{20}) \right] = 0 \\
& \frac{\partial^2 g_{10}}{\partial \xi^2} + g_{10} + \epsilon \left[\frac{\partial^2 g_{11}}{\partial \xi^2} + g_{11} + 2 \frac{\partial^2 g_{10}}{\partial \xi \partial \eta} + \bar{\sigma} \frac{\partial g_{10}}{\partial \xi} + 2g_{20} \frac{\partial f_{10}}{\partial \xi} \right. \\
& + 2f_{10} \frac{\partial g_{20}}{\partial \xi} - 2g_{10} \frac{\partial f_{20}}{\partial \xi} - 2f_{20} \frac{\partial g_{10}}{\partial \xi} + K \frac{\partial^2 g_{10}}{\partial \xi^2} \\
& \left. + 2n\bar{\omega}(f_{10}g_{20} - f_{20}g_{10}) \right] = 0 \\
& \frac{\partial^2 f_{20}}{\partial \xi^2} + 4f_{20} + \epsilon \left[\frac{\partial^2 f_{10}}{\partial \xi^2} + 4f_{21} + 2 \frac{\partial^2 f_{20}}{\partial \xi \partial \eta} + \bar{\sigma} \frac{\partial f_{20}}{\partial \xi} \right. \\
& + g_{10} \frac{\partial g_{10}}{\partial \xi} - f_{10} \frac{\partial f_{10}}{\partial \xi} + 4K \frac{\partial^2 f_{20}}{\partial \xi^2} + \frac{1}{2}\bar{\omega}n(g_{10}^2 - f_{10}^2) \left. \right] = 0 \\
& \frac{\partial^2 g_{20}}{\partial \xi^2} + 4g_{20} + \epsilon \left[\frac{\partial^2 g_{21}}{\partial \xi^2} + 4g_{21} + 2 \frac{\partial^2 g_{20}}{\partial \xi \partial \eta} + \bar{\sigma} \frac{\partial g_{20}}{\partial \xi} \right. \\
& \left. - g_{10} \frac{\partial f_{10}}{\partial \xi} - f_{10} \frac{\partial g_{10}}{\partial \xi} + 4K \frac{\partial^2 g_{20}}{\partial \xi^2} - \bar{\omega}n(f_{10}g_{10}) \right] = 0. \tag{4.8}
\end{aligned}$$

By separating the terms of $O(1)$ and $O(\epsilon)$ in the equations of (4.8) and equating both sets of terms equal to zero, the resulting equations become

$$\frac{\partial^2 f_{10}}{\partial \xi^2} + f_{10} = 0$$

$$\frac{\partial^2 g_{10}}{\partial \xi^2} + g_{10} = 0$$

$$\frac{\partial^2 f_{20}}{\partial \xi^2} + 4f_{20} = 0$$

$$\frac{\partial^2 g_{20}}{\partial \xi^2} + 4g_{20} = 0$$

(4.9.a)

$$\frac{\partial^2 f_{11}}{\partial \xi^2} + f_{11} = -2 \frac{\partial^2 f_{10}}{\partial \xi \partial \eta} - \frac{\partial f_{10}}{\partial \xi} - 2f_{20} \frac{\partial f_{10}}{\partial \xi} - 2f_{10} \frac{\partial f_{20}}{\partial \xi}$$

$$-2g_{20} \frac{\partial g_{10}}{\partial \xi} - 2g_{10} \frac{\partial g_{20}}{\partial \xi^2} - K \frac{\partial^2 f_{10}}{\partial \xi^2} - 2n\bar{\omega}(f_{10}f_{20} + g_{10}g_{20})$$

$$\frac{\partial^2 g_{11}}{\partial \xi^2} + g_{11} = -2 \frac{\partial^2 g_{10}}{\partial \xi \partial \eta} - \frac{\partial g_{10}}{\partial \xi} - 2g_{20} \frac{\partial f_{10}}{\partial \xi} - 2f_{10} \frac{\partial g_{20}}{\partial \xi}$$

$$+2g_{10} \frac{\partial f_{20}}{\partial \xi} + 2f_{20} \frac{\partial g_{10}}{\partial \xi} - K \frac{\partial^2 g_{10}}{\partial \xi^2} - 2n\bar{\omega}(f_{10}g_{20} - f_{20}g_{10})$$

$$\frac{\partial^2 f_{21}}{\partial \xi^2} + 4f_{21} = -2 \frac{\partial^2 f_{20}}{\partial \xi \partial \eta} - \frac{\partial f_{20}}{\partial \xi} - g_{10} \frac{\partial g_{10}}{\partial \xi} + f_{10} \frac{\partial f_{10}}{\partial \xi}$$

$$-4K \frac{\partial^2 f_{20}}{\partial \xi^2} - \frac{1}{2}n\bar{\omega}(g_{10}^2 - f_{10}^2)$$

$$\frac{\partial^2 g_{21}}{\partial \xi^2} + 4g_{21} = -2 \frac{\partial^2 g_{20}}{\partial \xi \partial \eta} - \frac{\partial g_{20}}{\partial \xi} + g_{10} \frac{\partial f_{10}}{\partial \xi}$$

$$+ f_{10} \frac{\partial g_{10}}{\partial \xi} - 4K \frac{\partial^2 g_{20}}{\partial \xi^2} + n\bar{\omega}(f_{10}g_{10}) .$$

(4.9.b)

The equations of (4.9.a) are linear second-order differential equations. Therefore, it can be shown that assuming the appropriate form of a solution, the results become

$$\begin{aligned}
 f_{10} &= A_1(\eta) \cos \xi + B_1(\eta) \sin \xi \\
 g_{10} &= A_2(\eta) \cos \xi + B_2(\eta) \sin \xi \\
 f_{20} &= A_3(\eta) \cos 2\xi + B_3(\eta) \sin 2\xi \\
 g_{20} &= A_4(\eta) \cos 2\xi + B_4(\eta) \sin 2\xi.
 \end{aligned} \tag{4.10}$$

Substituting (4.10) into (4.9.b) and using the multiple-angle formulas yields

$$\begin{aligned}
 \frac{\partial^2 f_{11}}{\partial \xi^2} + f_{11} &= -2 \left[-\frac{dA_1}{d\eta} - \frac{1}{2} A_1 \bar{\sigma} + \frac{1}{2} (A_1 A_3 + B_1 B_3) \right. \\
 &\quad - (B_1 B_3 + A_1 A_3) + \frac{1}{2} (A_2 A_4 + B_2 B_4) - (A_2 A_4 + B_2 B_4) \\
 &\quad \left. - \frac{1}{2} K B_1 + n \bar{\omega} \left[\frac{1}{2} (A_1 B_3 - A_3 B_1) + \frac{1}{2} (A_2 B_4 - B_2 A_4) \right] \right] \sin \xi \\
 &\quad - 2 \left[\frac{dB_1}{d\eta} + \frac{1}{2} \bar{\sigma} B_1 + \frac{1}{2} (A_3 B_1 - A_1 B_3) + (A_1 B_3 - A_3 B_1) \right. \\
 &\quad \left. + \frac{1}{2} (A_4 B_2 - A_2 B_4) + (A_2 B_4 - B_2 A_4) - \frac{1}{2} K A_1 \right. \\
 &\quad \left. + n \bar{\omega} \left[\frac{1}{2} (A_1 A_3 + B_1 B_3) + \frac{1}{2} (A_2 A_4 + B_2 B_4) \right] \right] \cos \xi + \dots
 \end{aligned}$$

$$\begin{aligned}
\frac{\partial^2 g_{11}}{\partial \xi^2} + g_{11} &= -2 \left[-\frac{dA_2}{dn} - \frac{1}{2} \bar{\sigma} A_2 + \frac{1}{2} (A_1 A_4 + B_1 B_4) \right. \\
&- (A_1 A_4 + B_1 B_4) + (A_2 A_3 + B_2 B_3) - \frac{1}{2} (A_2 A_3 + B_2 B_3) \\
&- \left. \frac{1}{2} KB_2 + n\bar{\omega} \left[\frac{1}{2} (A_1 B_4 - A_4 B_1) - \frac{1}{2} (A_2 B_3 - A_3 B_2) \right] \right] \sin \xi \\
&- 2 \left[\frac{dB_2}{dn} + \frac{1}{2} \bar{\sigma} B_2 + \frac{1}{2} (A_4 B_1 - B_4 A_1) + (A_1 B_4 - A_4 B_1) \right. \\
&- (A_2 B_3 - B_2 A_3) - \frac{1}{2} (A_3 B_2 - A_2 B_3) - \left. \frac{1}{2} KA_2 \right. \\
&\left. n\bar{\omega} \left[\frac{1}{2} (A_1 A_4 + B_1 B_4) - \frac{1}{2} (A_3 A_2 + B_2 B_3) \right] \right] \cos \xi + \dots
\end{aligned}$$

$$\begin{aligned}
\frac{\partial^2 f_{21}}{\partial \xi^2} + 4f_{21} &= -2 \left[-2 \frac{dA_3}{dn} - \frac{1}{2} \bar{\sigma} (2A_3) \right. \\
&+ \frac{1}{2} \left[\frac{1}{2} (B_2^2 - A_2^2) - \frac{1}{2} (B_1^2 - A_1^2) \right] + 2K(-4B_3) \\
&+ \left. \frac{1}{4} n\bar{\omega} [A_2 B_2 - A_1 B_1] \right] \sin 2\xi - 2 \left[\frac{dB_3}{dn} + \frac{1}{2} \bar{\sigma} (2B_3) + \frac{1}{2} (A_2 B_2 - A_1 B_1) \right. \\
&+ 2K(-4A_3) + \left. \frac{1}{4} n\bar{\omega} \left[\frac{1}{2} (A_2^2 - B_2^2) - \frac{1}{2} (A_1^2 - B_1^2) \right] \right] \cos 2\xi + \dots
\end{aligned}$$

$$\begin{aligned}
\frac{\partial^2 g_{21}}{\partial \xi^2} + 4g_{21} &= -2 \left[-2 \frac{dA_4}{dn} + \frac{1}{2} \bar{\sigma} [-2A_4] - \frac{1}{2} \left[\frac{1}{2} (B_1 B_2 - A_1 A_2) \right. \right. \\
&+ \left. \left. \frac{1}{2} (B_1 B_2 - A_1 A_2) \right] + 2K[-4B_4] - \frac{1}{2} n\bar{\omega} \left[\frac{1}{2} (A_1 B_2 + A_2 B_1) \right] \right] \sin 2\xi \\
&- 2 \left[\frac{dB_4}{dn} + \frac{1}{2} \bar{\sigma} [2B_4] - \frac{1}{2} \left[\frac{1}{2} (B_2 A_1 + A_2 B_1) + \frac{1}{2} (B_2 A_1 + A_2 B_1) \right] \right]
\end{aligned}$$

$$+ 2K[-4A_4] - \frac{1}{2}n\bar{\omega}\left[\frac{1}{2}(A_1A_2 - B_1B_2)\right] \cos 2\xi + \dots \quad (4.11)$$

where \dots indicates terms multiplied by sines and cosines of integral multiples of ξ other than those shown. The particular solutions corresponding to the terms shown on the right-hand sides of (4.11) will contain terms proportional to $\xi \sin n\xi$ or $\xi \cos n\xi$ [$n = 1$ for (4.11.a, b), $n = 2$ for (4.11.c, d)]. Thus, the second approximation would be unbounded for large ξ while the first approximation is bounded for all ξ . These unbounded terms are called singular terms. The terms on the right-hand sides of (4.11) indicated by \dots do not lead to singular terms.

The idea of a perturbation solution is that higher order terms in the series solution represent small corrections to this first term to obtain a uniformly valid expansion. The presence of this singularity causes this fundamental idea to be violated. Therefore, since the expressions of η dependency are independent of the variable causing the singularity, the η -dependent expressions can be set individually equal to zero to avoid this problem. Therefore, from equations (4.11), the resulting equations, which are eight ordinary first-order differential equations having η dependency, become

$$\frac{dA_1}{d\eta} + \frac{1}{2}\bar{\sigma}A_1 + \frac{1}{2}KB_1 + \frac{1}{2}[A_1A_3 + B_1B_3 + A_2A_4 + B_2B_4] \\ + \frac{1}{2}n\bar{\omega}[B_1A_3 - A_1B_3 + B_2A_4 - A_2B_4] = 0$$

$$\frac{dB_1}{d\eta} + \frac{1}{2}\bar{\sigma}B_1 - \frac{1}{2}KA_1 + \frac{1}{2}[A_1B_3 - B_1A_3 - A_4B_2 + A_2B_4]$$

$$+ \frac{1}{2} \bar{\omega} [A_1 A_3 + B_1 B_3 + A_2 A_4 + B_2 B_4] = 0$$

$$\frac{dA_2}{dn} + \frac{1}{2} \bar{\sigma} A_2 + \frac{1}{2} \bar{\kappa} B_2 + \frac{1}{2} [A_1 A_4 + B_1 B_4 - A_2 A_3 - B_2 B_3]$$

$$+ \frac{1}{2} \bar{\omega} [-A_1 B_4 + A_4 B_1 + A_2 B_3 - A_3 B_2] = 0$$

$$\frac{dB_2}{dn} + \frac{1}{2} \bar{\sigma} B_2 - \frac{1}{2} \bar{\kappa} A_2 + \frac{1}{2} [-A_4 B_1 + B_4 A_1 - A_2 A_3 + A_3 B_2]$$

$$+ \frac{1}{2} \bar{\omega} [A_1 A_4 + B_1 B_4 - A_3 A_2 - B_2 B_3] = 0$$

$$\frac{dA_3}{dn} + \frac{1}{2} \bar{\sigma} A_3 + 4 \bar{\kappa} B_3 + \frac{1}{8} [A_2^2 - B_2^2 + B_1^2 - A_1^2]$$

$$+ \frac{1}{8} \bar{\omega} [A_1 B_1 - A_2 B_2] = 0$$

$$\frac{dB_3}{dn} + \frac{1}{2} \bar{\sigma} B_3 - 4 \bar{\kappa} A_3 + \frac{1}{4} [A_2 B_2 - A_1 B_1]$$

$$+ \frac{1}{16} \bar{\omega} [A_2^2 - B_2^2 - A_1^2 + B_1^2] = 0$$

$$\frac{dA_4}{dn} + \frac{1}{2} \bar{\sigma} A_4 + 4 \bar{\kappa} B_4 + \frac{1}{4} [B_1 B_2 - A_1 A_2]$$

$$+ \frac{1}{8} \bar{\omega} [A_1 B_2 + A_2 B_1] = 0$$

$$\frac{dB_4}{dn} + \frac{1}{2} \bar{\sigma} B_4 - 4 \bar{\kappa} A_4 - \frac{1}{4} [B_2 A_1 + A_2 B_1]$$

$$-\frac{1}{8}\bar{\omega}[A_1A_2 - B_1B_2] = 0 \quad (4.12)$$

Since equations (4.12) are first-order nonlinear ordinary differential equations, the fourth-order Runge-Kutta program, previously developed, can be used to solve for the modal amplitude coefficients. By finding these coefficients for various points in time, a relation between the results of equation (3.21) and equation (4.12) can be observed to the approximation of order ϵ .

Solving equations (4.12) for the highest derivative (first order in this case) and substituting $\eta = \epsilon t$, the governing equations for the Runge-Kutta program become

$$\frac{dA_1}{dt} = \epsilon \left[-\frac{1}{2}\bar{\sigma}A_1 - \frac{1}{2}KB_1 - \frac{1}{2}(A_1A_3 + B_1B_3 + A_2A_4 + B_2B_4) \right.$$

$$\left. - \frac{1}{2}\bar{n}\omega(B_1A_3 - A_1B_3 + B_2A_4 - A_2B_4) \right]$$

$$\frac{dB_1}{dt} = \epsilon \left[-\frac{1}{2}\bar{\sigma}B_1 + \frac{1}{2}KA_1 - \frac{1}{2}(A_1B_3 - B_1A_3 - A_4B_2 + A_2B_4) \right.$$

$$\left. - \frac{1}{2}\bar{n}\omega(A_1A_3 + B_1B_3 + A_2A_4 + B_2B_4) \right]$$

$$\frac{dA_2}{dt} = \epsilon \left[-\frac{1}{2}\bar{\sigma}A_2 - \frac{1}{2}KB_2 - \frac{1}{2}(A_1A_4 + B_1B_4 - A_2A_3 - B_2B_3) \right.$$

$$\left. - \frac{1}{2}\bar{n}\omega(A_4B_1 - A_1B_4 + A_2B_3 - A_3B_2) \right]$$

$$\frac{dB_2}{dt} = \epsilon \left[-\frac{1}{2}\bar{\sigma}B_2 + \frac{1}{2}KA_2 - \frac{1}{2}(B_4A_1 - A_4B_1 + A_3B_2 - A_2B_3) \right.$$

$$- \frac{1}{2} \bar{\omega} n (A_1 A_4 + B_1 B_4 - A_3 A_2 - B_2 B_3)]$$

$$\frac{dA_3}{dt} = \epsilon \left[- \frac{1}{2} \bar{\sigma} A_3 - 4KB_3 - \frac{1}{8} (A_2^2 - B_2^2 + B_1^2 - A_1^2) \right.$$

$$\left. - \frac{1}{8} \bar{\omega} n (A_1 B_1 - A_2 B_2) \right]$$

$$\frac{dB_3}{dt} = \epsilon \left[- \frac{1}{2} \bar{\sigma} B_3 + 4KA_3 - \frac{1}{4} (A_2 B_2 - A_1 B_1) \right.$$

$$\left. - \frac{1}{16} \bar{\omega} n (A_2^2 - B_2^2 - A_1^2 + B_1^2) \right]$$

$$\frac{dA_4}{dt} = \epsilon \left[- \frac{1}{2} \bar{\sigma} A_4 - 4KB_4 - \frac{1}{4} (B_1 B_2 - A_1 A_2) \right.$$

$$\left. - \frac{1}{8} \bar{\omega} n (A_1 B_2 + A_2 B_1) \right]$$

$$\frac{dB_4}{dt} = \epsilon \left[- \frac{1}{2} \bar{\sigma} B_4 + 4KA_4 + \frac{1}{4} (B_2 A_1 + A_2 B_1) \right.$$

$$\left. + \frac{1}{8} \bar{\omega} n (A_1 A_2 - B_1 B_2) \right] . \quad (4.13)$$

It is often convenient to express the equations for A_i and B_i in terms of amplitudes, C_i , and phase angles, ϕ_i , which are also functions of the slow time variable η . Mathematically, we can express the relationships between the quantities as

$$A_i = C_i \cos \phi_i \quad (4.14.a)$$

$$B_i = C_i \sin \phi_i \quad (4.14.b)$$

$$\frac{dA_i}{dn} = \frac{dC_i}{dn} \cos \phi_i - C_i \frac{d\phi_i}{dn} \sin \phi_i \quad (4.14.c)$$

$$\frac{dB_i}{dn} = \frac{dC_i}{dn} \sin \phi_i + C_i \frac{d\phi_i}{dn} \cos \phi_i \quad (4.14.d)$$

where $i = 1, 2, 3,$ and 4 for each of the equations above. Substituting the expressions of (4.14) into the first two equations of (4.12), the resulting equations become

$$\begin{aligned} & \frac{dC_1}{dn} \cos \phi_1 - C_1 \frac{d\phi_1}{dn} \sin \phi_1 + \frac{1}{2} \bar{\sigma} C_1 \cos \phi_1 + \frac{1}{2} \kappa C_1 \sin \phi_1 \\ & + \frac{1}{2} [C_1 C_3 \cos \phi_1 \cos \phi_3 + C_1 C_3 \sin \phi_1 \sin \phi_3 \\ & + C_2 C_4 \cos \phi_2 \cos \phi_4 + C_2 C_4 \sin \phi_2 \sin \phi_4] + \frac{1}{2} n \omega [C_1 C_3 \\ & \sin \phi_1 \cos \phi_3 - C_1 C_3 \cos \phi_1 \sin \phi_3 + C_2 C_4 \cos \phi_4 \sin \phi_2 \\ & - C_2 C_4 \cos \phi_2 \sin \phi_4] = 0 \\ & \frac{dC_1}{dn} \sin \phi_1 + C_1 \frac{d\phi_1}{dn} \cos \phi_1 + \frac{1}{2} \bar{\sigma} C_1 \sin \phi_1 - \frac{1}{2} \kappa C_1 \cos \phi_1 \\ & + \frac{1}{2} [C_1 C_3 \cos \phi_1 \sin \phi_3 - C_1 C_3 \cos \phi_3 \sin \phi_1 \\ & - C_2 C_4 \cos \phi_4 \sin \phi_2 + C_2 C_4 \cos \phi_2 \sin \phi_4] + \frac{1}{2} n \omega [C_1 C_3 \\ & \cos \phi_1 \cos \phi_3 + C_1 C_3 \sin \phi_1 \sin \phi_3 + C_2 C_4 \cos \phi_2 \cos \phi_4 \end{aligned}$$

$$+ C_2 C_4 \sin \phi_2 \sin \phi_4] = 0 . \quad (4.15)$$

Multiplying the first equation by $\cos \phi_1$ and the second equation by $\sin \phi_1$, adding the two expressions together, and using appropriate multiple-angle identities from trigonometry, the resulting equation for C_1 becomes

$$\begin{aligned} \frac{dC_1}{dn} + \frac{1}{2} \bar{\sigma} C_1 + \frac{1}{2} [C_1 C_3 [\cos(2\phi_1 - \phi_3)] \\ + C_2 C_4 [\cos(\phi_2 - \phi_4 + \phi_1)]] + \frac{1}{2} n \bar{\omega} [C_1 C_3 \\ \sin(2\phi_1 - \phi_3) + C_2 C_4 \sin(\phi_2 - \phi_4 + \phi_1)] = 0 . \end{aligned} \quad (4.16)$$

Similarly, multiplying the first equation of (4.15) by $-\sin \phi_1$ and the second equation by $\cos \phi_1$, adding the two expressions together, and using appropriate multiple-angle identities for trigonometry, the resulting equation for ϕ_1 becomes

$$\begin{aligned} \frac{d\phi_1}{dn} - \frac{1}{2} K - \frac{1}{2} [C_3 \sin(2\phi_1 - \phi_3) + \frac{C_2 C_4}{C_1} \sin(\phi_2 - \phi_4 + \phi_1)] \\ + \frac{1}{2} n \bar{\omega} [C_3 \cos(2\phi_1 - \phi_3) + \frac{C_2 C_4}{C_1} \cos(\phi_1 + \phi_2 - \phi_4)] = 0 . \end{aligned} \quad (4.17)$$

Using these procedures discussed above, equations for C_2 , ϕ_2 , C_3 , ϕ_3 , C_4 , and ϕ_4 can be derived. Thus, these transformed equations are

$$\begin{aligned} \frac{dC_2}{dn} + \frac{1}{2} \bar{\sigma} C_2 + \frac{1}{2} [C_1 C_4 \cos(\phi_1 - \phi_4 + \phi_2) - C_2 C_3 \cos(2\phi_2 - \phi_3)] \\ + \frac{1}{2} n \bar{\omega} [C_1 C_4 \sin(\phi_1 - \phi_4 + \phi_2) - C_2 C_3 \sin(2\phi_2 - \phi_3)] = 0 \end{aligned}$$

$$\frac{d\phi_2}{dn} - \frac{1}{2}K - \frac{1}{2}\left[\frac{C_1 C_4}{C_2} \sin(\phi_1 - \phi_4 + \phi_2) - C_3 \sin(2\phi_2 - \phi_3)\right]$$

$$+ \frac{1}{2}n\bar{\omega}\left[\frac{C_1 C_4}{C_2} \cos(\phi_1 - \phi_4 + \phi_2) + C_3 \cos(2\phi_2 - \phi_3)\right] = 0$$

$$\frac{dC_3}{dn} + \frac{1}{2}\bar{\sigma}C_3 + \frac{1}{8}[C_2^2 \cos(2\phi_2 - \phi_3) - C_1^2 \cos(2\phi_1 - \phi_3)]$$

$$- \frac{1}{16}n\bar{\omega}[C_2^2 \sin(2\phi_2 - \phi_3) - C_1^2 \sin(2\phi_1 - \phi_3)] = 0$$

$$\frac{d\phi_3}{dn} - 4K + \frac{1}{8}\left[\frac{C_2^2}{C_3} \sin(2\phi_2 - \phi_3) - \frac{C_1^2}{C_3} \sin(2\phi_1 - \phi_3)\right]$$

$$+ \frac{1}{16}n\bar{\omega}\left[\frac{C_2^2}{C_3} \cos(2\phi_2 - \phi_3) - \frac{C_1^2}{C_3} \cos(2\phi_1 - \phi_3)\right] = 0$$

$$\frac{dC_4}{dn} + \frac{1}{2}\bar{\sigma}C_4 - \frac{1}{4}[C_1 C_2 \cos(\phi_1 + \phi_2 - \phi_4)] + \frac{1}{8}n\bar{\omega}[C_1 C_2$$

$$\sin(\phi_1 + \phi_2 - \phi_4)] = 0$$

$$\frac{d\phi_4}{dn} - 4K + \frac{1}{4}\left[\frac{C_1 C_2}{C_4} \sin(\phi_1 + \phi_2 - \phi_4)\right] - \frac{1}{8}n\bar{\omega}\left[\frac{C_1 C_2}{C_4}$$

$$\cos(\phi_1 + \phi_2 - \phi_4)\right] = 0. \quad (4.18)$$

Equations (4.16), (4.17), and (4.18) are the general combustion equations in terms of amplitudes and phase angles. From this point, special cases can be investigated isolating certain conditions and closed-

form solutions can be obtained for these cases. It is convenient to do this in order to check the closed-form results of the special cases with the results from the general equations (4.16), (4.17), and (4.18) when the same conditions are imposed.

The first case to be evaluated is the case for standing waves with no combustion effects. To simulate standing wave effect, set the amplitudes C_2 and C_4 and phase angles ϕ_2 and ϕ_4 equal to zero. This automatically satisfies four of the eight equations (4.18). To achieve the no-combustion effect, set the interaction index, n , equal to zero. Also, set the correction variable, K , equal to zero since the effect of K will be investigated separately at a later time. Imposing these conditions, the governing equations reduce to

$$\frac{dC_1}{d\eta} + \frac{1}{2} \bar{\sigma} C_1 + \frac{1}{2} C_1 C_3 \cos(2\phi_1 - \phi_3) = 0 \quad (4.19.a)$$

$$\frac{d\phi_1}{d\eta} - \frac{1}{2} [C_3 \sin(2\phi_1 - \phi_3)] = 0 \quad (4.19.b)$$

$$\frac{dC_3}{d\eta} + \frac{1}{2} \bar{\sigma} C_3 - \frac{1}{8} C_1^2 \cos(2\phi_1 - \phi_3) = 0 \quad (4.19.c)$$

$$\frac{d\phi_3}{d\eta} - \frac{1}{8} \frac{C_1^2}{C_3} \sin(2\phi_1 - \phi_3) = 0. \quad (4.19.d)$$

The initial conditions imposed for this case are

$$C_1(0) = 1$$

$$C_3(0) = 0$$

$$\phi_1(0) = \phi_{10}$$

$$\phi_3(0) = \phi_{30} \quad (4.20)$$

To attempt a closed-form solution, let

$$C_1 = e^{-\frac{1}{2}\bar{\sigma}\eta} F_1 \quad (4.21.a)$$

$$C_3 = e^{-\frac{1}{2}\bar{\sigma}\eta} F_3 \quad (4.21.b)$$

$$\frac{dC_1}{d\eta} = e^{-\frac{1}{2}\bar{\sigma}\eta} (-\bar{\sigma}) F_1 + e^{-\frac{1}{2}\bar{\sigma}\eta} \left(\frac{dF_1}{d\eta} \right) \quad (4.21.c)$$

$$\frac{dC_3}{d\eta} = e^{-\frac{1}{2}\bar{\sigma}\eta} (-\bar{\sigma}) F_3 + e^{-\frac{1}{2}\bar{\sigma}\eta} \left(\frac{dF_3}{d\eta} \right) \quad (4.21.d)$$

Substituting these expressions into equations (4.19.a) and (4.19.c) and dividing through by $e^{-\frac{1}{2}\bar{\sigma}\eta}$, the resulting equations become

$$\frac{dF_1}{d\eta} + \frac{1}{2} \cos(2\phi_1 - \phi_3) e^{-\frac{1}{2}\bar{\sigma}\eta} F_1 F_3 = 0 \quad (4.22.a)$$

$$\frac{dF_3}{d\eta} - \frac{1}{8} \cos(2\phi_1 - \phi_3) e^{-\frac{1}{2}\bar{\sigma}\eta} F_1^2 = 0 \quad (4.22.b)$$

Multiplying equation (4.22.a) by $1/4$ and equation (4.22.b) by F_3/F_1 and adding the two equations, terms containing the $\cos(2\phi_1 - \phi_3) e^{-\frac{1}{2}\bar{\sigma}\eta}$ are eliminated. In doing so, the result becomes

$$\frac{dF_1}{dn} + 4 \frac{F_3}{F_1} \frac{dF_3}{dn} = 0 . \quad (4.23)$$

Multiplying through equation (4.23) by F_1 gives

$$\frac{1}{2} \frac{d}{dn} [F_1^2 + 4F_3^2] = 0 . \quad (4.24)$$

Integrating with respect to n then dividing by $1/2$, the resulting equation becomes

$$F_1^2 + 4F_3^2 = D_1 \quad (4.25)$$

where D_1 is a constant of integration. This constant depends upon the initial conditions imposed on the problem. From the initial conditions given in (4.20) and using the transformation (4.21.a) and (4.21.b), it can be shown that $F_1(0) = 1$ and $F_3(0) = 0$. Therefore, D_1 equals to 1. Thus, equation (4.25) becomes

$$F_1^2 = 1 - 4F_3^2 . \quad (4.26)$$

Taking equation (4.26) and substituting into equation (4.22.b), then separating variables, the resulting equation becomes

$$\frac{dF_3}{[1-4F_3^2]} = \frac{1}{8} e^{-\frac{1}{2}\bar{\sigma}n} \cos(2\phi_1 - \phi_3) dn . \quad (4.27)$$

Letting $2\phi_1 - \phi_3 = \ell\pi$, which satisfies equations (4.19.b, d), yields $\cos(2\phi_1 - \phi_3) = (-1)^\ell$ where $\ell = 0, 1, 2, 3, \dots$. Substituting this expression and integrating the above equation, the resulting equation becomes

$$\frac{1}{2} \tanh^{-1} 2F_3 = \frac{1}{8} \left[-\frac{2}{\bar{\sigma}} e^{-\frac{1}{2}\bar{\sigma}\eta + D_2} \right] (-1)^\ell \quad (4.28)$$

where D_2 is a constant of integration. Using the initial condition $F_3(0) = 0$, then, it can be shown that $D_2 = 2/\bar{\sigma}$. Substituting and taking the hyperbolic tangent of both sides of equation (4.28), the result becomes

$$F_3 = \frac{1}{2} \tanh \left[\frac{1}{2\bar{\sigma}} (-1)^\ell (1 - e^{-\frac{1}{2}\bar{\sigma}\eta}) \right] . \quad (4.29)$$

Substituting this expression into equation (4.26) and simplifying, the resulting equation becomes

$$F_1 = \operatorname{sech} \left[\frac{(-1)^\ell}{2\bar{\sigma}} (1 - e^{-\frac{1}{2}\bar{\sigma}\eta}) \right] . \quad (4.30)$$

Substituting equations (4.29) and (4.30) into equations (4.21.a) and (4.21.b), and substituting $\eta = \epsilon t$ and $\bar{\omega} = \bar{\sigma}\epsilon$, the resulting closed-form solution for wave amplitudes C_1 and C_3 are

$$C_1 = e^{-\frac{1}{2}\bar{\omega}t} \left\{ \operatorname{sech} \left[\frac{\epsilon(-1)^\ell}{2\bar{\omega}} (1 - e^{-\frac{1}{2}\bar{\omega}t}) \right] \right\} \quad (4.31.a)$$

$$C_3 = \frac{e^{-\frac{1}{2}\bar{\omega}t}}{2} \left\{ \tanh \left[\frac{\epsilon(-1)^\ell}{2\bar{\omega}} (1 - e^{-\frac{1}{2}\bar{\omega}t}) \right] \right\} . \quad (4.31.b)$$

To find expressions for ϕ_1 and ϕ_3 , substitute the relation that $2\phi_1 - \phi_3 = \ell\pi$ into equations (4.19.b) and (4.19.d) and integrate and evaluate the constants of integration with the initial conditions; the results are

$$\phi_1 = \phi_{10}$$

$$\phi_3 = \phi_{30} = 2\phi_{10} - \ell\pi \quad (4.32)$$

where ϕ_{10} is a constant and ϕ_3 is $\ell\pi$ radians out of phase with $2\phi_1$. It can be seen that a special set of initial conditions is necessary to be consistent with this solution. A representative set is $\phi_{10} = \phi_{30} = 0$ which corresponds to $\ell = 0$.

Inspection of equations (4.31) reveals that the magnitude of C_1 continually decreases with time while the magnitude of C_3 first increases and then decreases. An interesting special case of equations (4.31) occurs in the absence of steady-state combustion ($\bar{u} = 0$). The results of this case are

$$C_1 = \operatorname{sech}\left[\frac{(-1)\ell\epsilon t}{4}\right]$$

$$C_3 = \frac{1}{2} \tanh\left[\frac{(-1)\ell\epsilon t}{4}\right] \quad (4.33)$$

These results show that a disturbance in the form of the first mode is transferred to the second mode as time increases. It is thought that this indicates the beginning of the steepening that leads to the formation of a shock wave. It can be seen that the presence of damping, in the form of steady-state combustion, inhibits this process.

The second case to be investigated is that of standing waves with gas-dynamic nonlinearities neglected. To simulate the standing wave effect, let the amplitudes C_2 and C_4 and the phase angles ϕ_2 and ϕ_4 equal zero. Again, this automatically satisfies four of the eight equations of (4.18). To achieve omission of gas-dynamic nonlinearities, let $i = 0$. Also, let the correction variable, K , be equal to zero for simplicity.

In doing so, the resulting equations, based upon equation (4.18), become

$$\frac{dC_1}{d\eta} + \frac{1}{2} \bar{\omega} C_1 + \frac{1}{2} n \bar{\omega} [C_1 C_3 \sin(2\phi_1 - \phi_3)] = 0$$

$$\frac{d\phi_1}{d\eta} + \frac{1}{2} n \bar{\omega} [C_3 \cos(2\phi_1 - \phi_3)] = 0$$

$$\frac{dC_3}{d\eta} + \frac{1}{2} \bar{\omega} C_3 - \frac{1}{16} n \bar{\omega} [-C_1^2 \sin(2\phi_1 - \phi_3)] = 0$$

$$\frac{d\phi_3}{d\eta} + \frac{1}{16} n \bar{\omega} \left[-\frac{C_1^2}{C_3} \cos(2\phi_1 - \phi_3) \right] = 0 \quad (4.34)$$

The initial conditions imposed for this case are

$$C_1(0) = 1$$

$$C_3(0) = 0$$

$$\phi_1(0) = \phi_{10}$$

$$\phi_3(0) = \phi_{30} \quad (4.35)$$

Let $2\phi_1 - \phi_3 = (2\ell + 1)\pi/2$, $\ell = 0, 1, 2, \dots$. This implies that $\sin(2\phi_1 - \phi_3) = (-1)^\ell$ and $\cos(2\phi_1 - \phi_3) = 0$. Substituting into (4.34) and solving in the manner indicated previously one obtains expressions for the amplitudes for C_1 and C_3 which are

$$C_1 = e^{-\frac{1}{2}\bar{\omega}t} \left\{ \sec\left[\frac{\sqrt{2}}{4} n \bar{\omega} (-1)^\ell (1 - e^{-\frac{1}{2}\bar{\omega}t})\right] \right\} \quad (4.36.a)$$

$$C_3 = \frac{e^{-\frac{1}{2}\bar{\omega}t}}{2^{1/2}} \left\{ \tan\left[\frac{\sqrt{2}}{4} n\epsilon(-1)^\ell (1 - e^{-\frac{1}{2}\bar{\omega}t})\right] \right\} \quad (4.36.b)$$

$$\phi_1 = \phi_{10} \quad (4.36.c)$$

$$\phi_3 = 2\phi_{10} - \left(\frac{2\ell+1}{2}\right)\pi \quad (4.36.d)$$

where ϕ_{10} is constant and ϕ_3 is $(2\ell+1)\pi/2$ radians out of phase with $2\phi_1$. As in the previous solution, special initial conditions are required to produce this solution. A representative set is $\phi_{10} = 0$, $\phi_{30} = -\pi/2$, which corresponds to $\ell = 0$.

The secant and tangent both become infinite when their arguments take on the value $\pm\pi/2$. In (4.36.a, b), the arguments of these functions start at zero at $t = 0$ and have a maximum absolute value at $n\epsilon/2^{3/2}$. Thus, if $n\epsilon/2^{3/2} < \pi/2$, the tangent and secant never become infinite and C_1 and C_3 eventually decay to zero due to the influence of the exponential function. This is a stable situation. If, on the other hand, $n\epsilon/2^{3/2} > \pi/2$, the tangent and secant become infinite at $t_{\infty} = (2/\bar{\omega}) \left| \ell n \left[1 - 2^{3/2} \pi / (n\epsilon) \right] \right|$ causing C_1 and C_3 to become infinite. This is an unstable situation. Thus, the boundary between stable and unstable behavior is indicated by the equation

$$n\epsilon/2^{3/2} = \pi/2 \quad (4.37)$$

The stability equation in the n - ϵ plane has the form

$$n = 2^{3/2} \pi / \epsilon = 4.442 / \epsilon \quad (4.38)$$

This has the form of a rectangular hyperbola and is independent of $\bar{\omega}$.

For the case of traveling waves, it is more convenient to work with the general perturbation equations expressed in modal amplitudes in terms of the real time variables, equation (4.13). To simulate the effect of spinning or traveling waves, let the following modal amplitudes be equal. These relations are .

$$B_2 = A_1$$

$$B_4 = A_3$$

$$B_1 = -A_2$$

$$B_3 = -A_4 \quad . \quad (4.39)$$

It can be shown that substituting the relations (4.39) into equation (4.10), expressing the results in terms of the real time variables, substituting these expressions into equation (3.18), and using appropriate multiple-angle formulas leads to

$$\begin{aligned} \phi(\theta, t) = & A_1 \cos(t-\theta) - A_2 \sin(t-\theta) + A_3 \cos 2(t-\theta) \\ & - A_4 \sin 2(t-\theta) + \dots \quad (4.40) \end{aligned}$$

which has the form of a sum of traveling waves. Substituting the expressions in (4.39) into equations (4.13), these eight equations reduce to four pairs of identical equations. The four independent equations listed below are

$$\frac{dA_1}{dt} = \epsilon \left[-\frac{1}{2} \bar{\sigma} A_1 + \frac{1}{2} K A_2 - i(A_1 A_3 + A_2 A_4) - n \bar{\omega} (A_1 A_4 - A_2 A_3) \right]$$

$$\frac{dA_2}{dt} = \epsilon \left[-\frac{1}{2} \bar{\sigma} A_2 - \frac{1}{2} K A_1 - i(A_1 A_4 - A_2 A_3) + n\bar{\omega}(A_2 A_4 + A_1 A_3) \right]$$

$$\frac{dA_3}{dt} = \epsilon \left[-\frac{1}{2} \bar{\sigma} A_3 + 4K A_4 + \frac{1}{4} i(A_1^2 - A_2^2) + \frac{1}{4} n\bar{\omega}(A_1 A_2) \right]$$

$$\frac{dA_4}{dt} = \epsilon \left[-\frac{1}{2} \bar{\sigma} A_4 - 4K A_3 + \frac{1}{2} i(A_1 A_2) - \frac{1}{8} n\bar{\omega}(A_1^2 - A_2^2) \right]. \quad (4.41)$$

By making the substitution, we have reduced to a system of four equations and four unknowns. By solving for the modal amplitudes A_j , the modal amplitudes B_j are readily computed by using the relations of (4.39) to determine the entire nature of the wave form.

For the case of traveling waves omitting gas-dynamic nonlinearities, let the amplitudes A_1 and A_3 equal zero. Then set i , the gas-dynamic index, equal to zero. Again, for simplicity, let the correction variable, K , controlling physical chamber configurations, be zero. In doing so, in terms of the transformation variable, η , the resulting equations become

$$\frac{dA_2}{d\eta} + \frac{1}{2} \bar{\sigma} A_2 - n\bar{\omega}[A_2 A_4] = 0$$

$$\frac{dA_4}{d\eta} + \frac{1}{2} \bar{\sigma} A_4 - \frac{1}{8} n\bar{\omega} A_2 = 0 \quad (4.42)$$

which is a system of two equations and two unknown modal amplitudes. To find an exact closed-form solution to these equations, let

$$A_2 = e^{-\frac{1}{2}\bar{\sigma}\eta} F_1$$

$$A_4 = e^{-\frac{1}{2}\bar{\sigma}\eta} F_2$$

$$\frac{dA_2}{d\eta} = e^{-\frac{1}{2}\bar{\sigma}\eta} \left(-\frac{1}{2}\bar{\sigma}\right) F_1 + e^{-\frac{1}{2}\bar{\sigma}\eta} \frac{dF_1}{d\eta}$$

$$\frac{dA_4}{d\eta} = e^{-\frac{1}{2}\bar{\sigma}\eta} \left(-\frac{1}{2}\bar{\sigma}\right) F_2 + e^{-\frac{1}{2}\bar{\sigma}\eta} \frac{dF_2}{d\eta} \quad (4.43)$$

Using these transformations, the procedure for solution is exactly the same as for the standing wave case for both no combustion and no gas dynamics. The initial conditions for this case are

$$A_2(0) = 1$$

$$A_4(0) = 0 \quad (4.44)$$

Substituting the expressions of (4.42) into (4.41), the resulting equations are

$$\frac{dF_1}{d\eta} - n\bar{\omega}F_1F_2 e^{-\frac{1}{2}\bar{\sigma}\eta} = 0$$

$$\frac{dF_2}{d\eta} - \frac{1}{8}n\bar{\omega}F_1^2 e^{-\frac{1}{2}\bar{\sigma}\eta} = 0 \quad (4.45)$$

with initial conditions

$$F_1(0) = 1$$

$$F_2(0) = 0 \quad .$$

Solving these equations in the manner outlined in the standing wave solutions, the results are

$$F_1 = \sec\left[\frac{\sqrt{2}}{2} \frac{n\bar{\omega}}{\bar{\sigma}} (1 - e^{-\frac{1}{2}\bar{\sigma}n})\right]$$

$$F_2 = \frac{\tan\left[\frac{\sqrt{2}}{2} \frac{n\bar{\omega}}{\bar{\sigma}} (1 - e^{-\frac{1}{2}\bar{\sigma}n})\right]}{2\sqrt{2}} \quad (4.46)$$

Expressing the results of (4.45) in terms of modal amplitudes by substituting into (4.42), the resulting equations become

$$A_2 = e^{-\frac{1}{2}\bar{\sigma}n} \sec\left[\frac{\sqrt{2}}{2} \frac{n\bar{\omega}}{\bar{\sigma}} (1 - e^{-\frac{1}{2}\bar{\sigma}n})\right]$$

$$A_4 = \frac{e^{-\frac{1}{2}\bar{\sigma}n}}{2\sqrt{2}} \tan\left[\frac{\sqrt{2}}{2} \frac{n\bar{\omega}}{\bar{\sigma}} (1 - e^{-\frac{1}{2}\bar{\sigma}n})\right] \quad (4.47)$$

The results for traveling waves (4.47) are quite similar to the results for standing waves (4.36) for the case of no gas-dynamic nonlinearities. The same behavior can be expected as was discussed in the standing wave case about the nature of oscillation of the modal amplitudes. The only significant difference is the value to determine the boundary of stability for the interaction index governing the combustion terms. The stability condition for traveling waves is

$$\frac{\sqrt{2}}{2} n\epsilon = \frac{\pi}{2} \quad (4.48)$$

Thus, the equation of the stability boundary in the n - ϵ plane is

$$n = \frac{\pi}{2\frac{\sqrt{2}}{2}\epsilon} = \frac{2.22}{\epsilon} \quad (4.49)$$

Comparing equation (4.49) to (4.38) shows that the stability boundary for the interaction index is half as great for the traveling wave case as for

the standing wave case for any ϵ . This will be verified in a later presentation of results of various numerical cases.

For the case of traveling waves with no combustion, let the amplitudes A_2 and A_4 equal to zero. Then set n , the interaction index, equal to zero, and, again, let the correction variable K equal to zero. Substituting into equations (4.40) and transforming into variable η , the results are

$$\begin{aligned}\frac{dA_1}{d\eta} + \frac{1}{2} \bar{\sigma} A_1 + A_1 A_3 &= 0 \\ \frac{dA_3}{d\eta} + \frac{1}{2} \bar{\sigma} A_3 - \frac{1}{4} A_1^2 &= 0\end{aligned}\tag{4.50}$$

with initial conditions

$$A_1(0) = 1$$

$$A_3(0) = 0$$

which again is a system of two equations and two unknown modal amplitudes. To find an exact closed-form solution to these equations, use similar transformations as shown in (4.42). In doing so, and simplifying, the results are

$$\begin{aligned}\frac{dF_1}{d\eta} + e^{-\frac{1}{2}\bar{\sigma}\eta} F_1 F_2 &= 0 \\ \frac{dF_2}{d\eta} - \frac{1}{4} e^{-\frac{1}{2}\bar{\sigma}\eta} F_1^2 &= 0\end{aligned}\tag{4.51}$$

with initial conditions

$$F_1(0) = 1$$

$$F_2(0) = 0$$

Solving these equations in the same manner as before, the results are

$$\begin{aligned} F_1 &= \operatorname{sech}[1/\bar{\sigma}(1-e^{-\frac{1}{2}\bar{\sigma}\eta})] \\ F_2 &= \frac{1}{2} \tanh[1/\bar{\sigma}(1-e^{-\frac{1}{2}\bar{\sigma}\eta})] \end{aligned} \quad (4.52)$$

Again, expressing the results of (4.51) in terms of the modal amplitudes of the form of equation (4.43), the resulting equations become

$$\begin{aligned} A_1 &= e^{-\frac{1}{2}\bar{\sigma}\eta} \operatorname{sech}[1/\bar{\sigma}(1-e^{-\frac{1}{2}\bar{\sigma}\eta})] \\ A_3 &= \frac{e^{-\frac{1}{2}\bar{\sigma}\eta}}{2} \tanh[1/\bar{\sigma}(1-e^{-\frac{1}{2}\bar{\sigma}\eta})] \end{aligned} \quad (4.53)$$

The results for the traveling waves (4.52) are similar to the results for standing waves (4.31) for the case of no combustion. A disturbance initially having the form of the first mode eventually is transformed into one having the form of the second mode. To compare these results for standing waves and traveling waves to the general perturbation equations, two computer programs were written (Appendices D and E) which numerically evaluate the modal amplitudes of various conditions for standing and traveling waves.

One last special case is an investigation of the effect of the correction variable K . In the special cases previously discussed, the correction variable K was set equal to zero. But, in this discussion, the correction variable K will be of primary importance in the equations. To start this analysis, refer to equations (3.21). Based upon these equations, impose the following conditions. First, neglect combustion effects (i.e., $n = 0$). Then, let us consider only the case of standing waves (i.e., $g_1 = g_2 = 0$). Finally, let us neglect the steady state burning rate (i.e., $\bar{\sigma} = 0$) and assume that the terms multiplied by ϵK are larger than those multiplied by ϵ above. This can be accomplished by writing

$$K_1 = \epsilon K \quad (4.54)$$

and treating K_1 as a quantity of $O(1)$. Imposing the above conditions and substituting equation (4.54) into the equations (3.21), the resulting equations become

$$[1+K_1] \frac{d^2 f_1}{dt^2} + f_1 + 2\epsilon [f_2 \frac{df_1}{dt} + f_1 \frac{df_2}{dt}] = 0 \quad (4.55.a)$$

$$[1+4K_1] \frac{d^2 f_2}{dt^2} + 4f_2 - \epsilon f_1 \frac{df_1}{dt} = 0 \quad (4.55.b)$$

with initial conditions

$$f_1(0) = 1$$

$$\frac{df_1}{dt}(0) = 0$$

$$f_2(0) = 0$$

$$\frac{df_2}{dt}(0) = 0$$

First, assume a straightforward perturbation solution similar to the equations (4.6) except the functions are dependent upon the real time t . Substituting these assumed solutions into the equations and initial conditions of (4.55) and keeping terms of $O(1)$ and $O(\epsilon)$, the separated equations become

$$\frac{d^2f_{10}}{dt^2} + \frac{1}{(1+K_1)} f_{10} = 0 \quad (4.56.a)$$

$$\frac{d^2f_{20}}{dt^2} + \frac{4}{(1+4K_1)} f_{20} = 0 \quad (4.56.b)$$

$$\frac{d^2f_{11}}{dt^2} + \left(\frac{1}{1+K_1}\right) f_{11} = \frac{2}{(1+K_1)} \left[-f_{20} \frac{df_{10}}{dt} - f_{10} \frac{df_{20}}{dt} \right] \quad (4.56.c)$$

$$\frac{d^2f_{21}}{dt^2} + \left(\frac{4}{1+4K_1}\right) f_{21} = \frac{1}{(1+4K_1)} \left[f_{10} \frac{df_{10}}{dt} \right] \quad (4.56.d)$$

with initial conditions

$$f_{10}(0) = 1$$

$$f_{11}(0) = 0$$

$$\frac{df_{10}}{dt}(0) = 0 \qquad \frac{df_{11}}{dt}(0) = 0$$

$$f_{20}(0) = 0 \qquad f_{21}(0) = 0$$

$$\frac{df_{20}}{dt}(0) = 0 \qquad \frac{df_{21}}{dt}(0) = 0$$

The first-order equations (4.56.a and b) can be solved by assuming the usual assumed solution for linear differential equations. Doing this and applying the appropriate initial conditions, the results for the first-order terms are

$$f_{10} = \cos \sqrt{\frac{1}{1+K_1}} t$$

$$f_{20} = 0 \quad . \qquad (4.57)$$

Substituting (4.57) into the right-hand side of (4.56.c) the equation becomes a homogeneous linear differential equation. Solving in the usual manner and applying the appropriate initial conditions

$$f_{11} = 0 \quad . \qquad (4.58)$$

Substituting (4.57) into the right-hand side of equation (4.56.d), the resulting equation becomes a linear differential equation with a particular solution. By assuming an appropriate homogeneous and particular solution and evaluating the constants using the appropriate initial conditions, the result becomes

$$f_{21} = \frac{-\sqrt{1+4K_1}}{24K_1} \sin \frac{2}{\sqrt{1+4K_1}} t + \frac{1}{24K_1} \sqrt{1+K_1} \sin \frac{2}{\sqrt{1+K_1}} t. \quad (4.59)$$

Therefore, substituting equations (4.57), (4.58), and (4.59) into the assumed perturbation solution and letting $K_1 = \epsilon K$, the resulting equations become

$$f_1 = \cos \frac{1}{\sqrt{1+K\epsilon}} t \quad (4.60.a)$$

$$f_2 = \frac{-\sqrt{1+K\epsilon}}{24K} \left[\sqrt{\frac{1+4K\epsilon}{1+K\epsilon}} \sin \frac{2}{\sqrt{1+4\epsilon K}} t - \sin \frac{2}{\sqrt{1+K\epsilon}} t \right]. \quad (4.60.b)$$

Recall that in the two-variable perturbation method, f_1 and f_2 expressed in terms of the perturbation variables were

$$f_1 = A_1(\eta) \cos \xi + B_1(\eta) \sin \xi \quad (4.61.a)$$

$$f_2 = A_3(\eta) \cos 2\xi + B_3(\eta) \sin 2\xi. \quad (4.61.b)$$

By transforming equation (4.60.a) into perturbation variables and expanding the argument of the cosine function by the Taylor series and using appropriate sum and difference trigonometric identities f_1 can be expressed as

$$f_1 = \cos \frac{1}{2} K\eta \cos \xi + \sin \frac{1}{2} K\eta \sin \xi. \quad (4.62)$$

Therefore, comparing this to equation (4.61.a), the functions A_1 and B_1 must be

$$A_1(\eta) = \cos \frac{1}{2} K\eta$$

$$B_1(\eta) = \sin \frac{1}{2} K\eta \quad . \quad (4.63)$$

By similar procedure, it can be shown that evaluating equation (4.60.b) and comparing it to equation (4.61.b), the results are

$$A_3(\eta) = \frac{1}{24K} [\sin 4K\eta - \sin K\eta]$$

$$B_3(\eta) = \frac{1}{24K} [\cos K\eta - \cos 4K\eta] \quad . \quad (4.64)$$

To show the validity of equations (4.63) and (4.64), the problem is now solved using equations (4.12) which are derived from equations (3.21) by the use of the two-variable perturbation method. To reproduce the conditions imposed on the problem just discussed, let there be no combustion (i.e., $n = 0$), let there be no steady-state burning rate (i.e., $\bar{\sigma} = 0$), and let there be only standing waves existing (i.e., $A_2 = A_4 = B_2 = B_4 = 0$). Imposing these conditions on equations (4.12), the resulting equations become

$$\frac{dA_1}{d\eta} + \frac{1}{2} KB_1 + \frac{1}{2} [A_1 A_3 + B_1 B_3] = 0$$

$$\frac{dB_1}{d\eta} - \frac{1}{2} KA_1 + \frac{1}{2} [A_1 B_3 - B_1 A_3] = 0$$

$$\frac{dA_3}{d\eta} + 4KB_3 + \frac{1}{8} [B_1^2 - A_1^2] = 0$$

$$\frac{dB_3}{d\eta} - 4KA_3 - \frac{1}{4} A_1 B_1 = 0 . \quad (4.65)$$

In the previous solution it was assumed that the frequency correction terms were larger than the gas-dynamic nonlinearities. To be consistent with this assumption the following procedure is used. By a change of variable $\eta = \zeta/K$, equation (4.65) can be rewritten as

$$\frac{dA_1}{d\zeta} + \frac{1}{2} B_1 + \frac{1}{2K} [A_1 A_3 + B_1 B_3] = 0$$

$$\frac{dB_1}{d\zeta} - \frac{1}{2} A_1 + \frac{1}{2K} [A_1 B_3 - B_1 A_3] = 0$$

$$\frac{dA_3}{d\zeta} + 4B_3 + \frac{1}{8K} [B_1^2 - A_1^2] = 0$$

$$\frac{dB_3}{d\zeta} - 4A_3 - \frac{1}{4K} A_1 B_1 = 0 . \quad (4.66)$$

Assuming a straightforward expansion of the form

$$A_1 = A_{10} + \frac{1}{K} A_{11} + \dots$$

$$B_1 = B_{10} + \frac{1}{K} B_{11} + \dots$$

$$A_3 = A_{30} + \frac{1}{K} A_{31} + \dots$$

$$B_3 = B_{30} + \frac{1}{K} B_{31} + \dots \quad (4.67)$$

then substituting these expressions into the equations (4.66) and keeping terms of $O(1)$ and $O(1/K)$, the resulting separated equations become

$$\frac{dA_{10}}{d\zeta} + \frac{1}{2} B_{10} = 0 \quad (4.68.a)$$

$$\frac{dB_{10}}{d\zeta} - \frac{1}{2} A_{10} = 0 \quad (4.68.b)$$

$$\frac{dA_{30}}{d\zeta} + 4B_{30} = 0 \quad (4.68.c)$$

$$\frac{dB_{30}}{d\zeta} - 4A_{30} = 0 \quad (4.68.d)$$

$$\frac{dA_{11}}{d\zeta} + \frac{1}{2} B_{11} = -\frac{1}{2}[A_{10}A_{30} + B_{10}B_{30}] \quad (4.68.e)$$

$$\frac{dB_{11}}{d\zeta} - \frac{1}{2} A_{11} = -\frac{1}{2}[A_{10}B_{30} - B_{10}A_{30}] \quad (4.68.f)$$

$$\frac{dA_{31}}{d\zeta} + 4B_{31} = -\frac{1}{8}[B_{10}^2 - A_{10}^2] \quad (4.68.g)$$

$$\frac{dB_{31}}{d\zeta} - 4A_{31} = \frac{1}{4}[A_{10}B_{10}] \quad (4.68.h)$$

with the initial conditions

$$A_{10}(0) = 1 \quad B_{10}(0) = 0$$

$$A_{11}(0) = 0 \quad B_{11}(0) = 0$$

$$A_{30}(0) = 0 \quad B_{30}(0) = 0$$

$$A_{31}(0) = 0 \quad B_{31}(0) = 0 .$$

Since the first-order equations are coupled, differentiate equations (4.68.a and c) once with respect to ζ then substitute equations (4.68.b and d) into these equations resulting in

$$\begin{aligned} \frac{d^2 A_{10}}{d\zeta^2} + \frac{1}{4} A_{10} &= 0 \\ \frac{d^2 A_{30}}{d\zeta^2} + 16 A_{30} &= 0 \end{aligned} \quad (4.69)$$

As can be seen, equations (4.69) are linear differential equations which can be evaluated by the usual manner. In doing so and applying the appropriate initial conditions, the resulting first-order modal amplitudes are

$$\begin{aligned} A_{10} &= \cos \frac{1}{2}\zeta = \cos \frac{1}{2}K\eta \\ A_{30} &= 0 . \end{aligned} \quad (4.70)$$

Knowing values for A_{10} and A_{30} , substitute these values into equations (4.68.b and d) and apply appropriate initial conditions. The results become

$$\begin{aligned} B_{10} &= \sin \frac{1}{2}\zeta = \sin \frac{1}{2}K\eta \\ B_{30} &= 0 . \end{aligned} \quad (4.71)$$

Substituting the results of (4.70) and (4.71) into the right-hand side of equations (4.68.e-h), the resulting equations become

$$\frac{dA_{11}}{d\zeta} = -\frac{1}{2} B_{11} \quad (4.72.a)$$

$$\frac{dB_{11}}{d\zeta} = \frac{1}{2} A_{11} \quad (4.72.b)$$

$$\frac{dA_{31}}{d\zeta} + 4B_{31} = \frac{1}{8} \cos \zeta \quad (4.72.c)$$

$$\frac{dB_{31}}{d\zeta} - 4A_{31} = \frac{1}{8} \sin \zeta \quad (4.72.d)$$

Since equations (4.72.c and d) are coupled, differentiate both equations once with respect to ζ and substituting equations (4.72.c and d) into the appropriate terms of the new set of equations, the resulting equations are

$$\frac{d^2A_{31}}{d\zeta^2} + 16A_{31} = -\frac{5}{8} \sin \zeta$$

$$\frac{d^2B_{31}}{d\zeta^2} + 16B_{31} = \frac{5}{8} \cos \zeta \quad (4.73)$$

Equations (4.73) are a set of linear differential equations with homogeneous and particular solutions. Solving these equations in the usual manner and using the appropriate initial conditions, the resulting modal amplitudes are

$$A_{31} = \frac{1}{24} (\sin 4\zeta - \sin \zeta) = \frac{1}{24} (\sin 4K\eta - \sin K\eta)$$

$$B_{31} = \frac{1}{24}(\cos \zeta - \cos 4\zeta) = \frac{1}{24}(\cos K\eta - \cos 4K\eta). \quad (4.74)$$

In a similar manner, the results for the modal amplitudes A_{11} and B_{11} can be determined to be

$$A_{11} = 0$$

$$B_{11} = 0 \quad (4.75)$$

evaluated with the appropriate initial conditions. Therefore, substituting the results of (4.70), (4.71), (4.73), and (4.74) into the assumed perturbation solution of (4.67), the resulting modal amplitudes become

$$A_1 = \cos \frac{1}{2} K\eta + \dots$$

$$B_1 = \sin \frac{1}{2} K\eta + \dots$$

$$A_3 = \frac{1}{24K}(\sin 4K\eta - \sin K\eta) + \dots$$

$$B_3 = \frac{1}{24K}(\sin 4K\eta - \sin K\eta) + \dots \quad (4.76)$$

It can be seen that equations (4.76) are identical to equations (4.63) and (4.64). This indicates that the two-variable method produces the correct solution. Equations (4.60) indicate that the presence of K changes the frequency of each of the first two acoustic modes and further renders the ratio of the second frequency to the first a non-integer number in general.

Equations (4.76) show how this effect manifests itself in the two-variable perturbation solution.

These results can be used in another way. If the nonlinear terms are neglected in (4.55.a), the results are

$$(1+K_1) \frac{d^2 f_1}{dt^2} + f_1 = 0$$

$$(1+4K_1) \frac{d^2 f_2}{dt^2} + 4f_2 - \epsilon f_1 \frac{df_1}{dt} = 0$$

$$f_1(0) = 1, \quad \frac{df_1(0)}{dt} = 0, \quad f_2(0) = 0, \quad \frac{df_2(0)}{dt} = 0. \quad (4.77)$$

It can be easily shown that equations (4.60) constitute the exact solution of equation (4.77). If the corresponding terms are neglected in equations (4.65), the results are

$$\frac{dA_1}{d\eta} + \frac{1}{2} KB_1 = 0$$

$$\frac{dB_1}{d\eta} - \frac{1}{2} KA_1 = 0$$

$$\frac{dA_3}{d\eta} + 4KB_3 + \frac{1}{8}(B_1^2 - A_1^2) = 0$$

$$\frac{dB_3}{d\eta} - 4KA_3 - \frac{1}{4} A_1 B_1 = 0 \quad (4.78)$$

where

$$A_1(0) = 1$$

$$B_1(0) = 0$$

$$A_3(0) = 0$$

$$B_3(0) = 0 .$$

It can be shown that equations (4.76) are the exact solution of equation (4.78). These facts were used to check the accuracy of the computer programs to be discussed later.

In the remainder of this thesis, a comparison of the magnitudes of the modal amplitudes will be represented in graphical and tabular form. Under a given set of conditions, the acoustic modal amplitude program, the general perturbation program, and the analytical cases that were programmed will be used and results compared. Varying certain conditions will show their effect on the changes in magnitude of the modal amplitudes through a set range of time which is related to maintaining stability. From these various cases, it will be determined which parameters and conditions have the greatest effect in changing modal amplitudes and which in turn affect the stability criteria for combustion by the methods discussed above.

Chapter 5

DISCUSSION AND PRESENTATION OF RESULTS

In this chapter, results are presented both in graphical and tabular form which are representative of the results generated by the programs listed in the Appendices B through E. From these representative sets of results, basic observations will be made to observe which parameters or conditions have the greatest effects on the problems of stability.

In Figures 3 and 4, modal amplitudes F_1 and F_2 are graphically represented versus time for a stable standing wave case. For these figures, $F_1(0) = 0$, $F_1'(0) = 1$, $F_2(0) = 0$, $F_2'(0) = 0$, $G_1(0) = 0$, $G_1'(0) = 0$, $G_2(0) = 0$, $G_2'(0) = 0$, $n = 35$, $i = 1$, $K = 0$, $\epsilon = 0.1$ and $\bar{\omega} = 0.1$. The step size used was 0.1. Experimentation showed that this was a small enough step size to produce accurate results and was used throughout. From these figures, one notices that both the first and second order modal amplitudes decrease in amplitude with increasing time. Also, F_2 , the second order modal amplitude, tends to oscillate at twice the frequency of F_1 . These figures are based upon one set of parametric values; however, these figures represent qualitatively the results obtained using a wide variety of initial conditions and parametric values. In Figures 5 through 8, modal amplitudes F_1 , F_2 , G_1 , and G_2 are graphically represented versus time for a stable traveling wave case. For these figures, $F_1(0) = 0$, $F_1'(0) = -1$, $F_2(0) = 0$, $G_1(0) = 1$, $G_1'(0) = 0$, $G_2(0) = 0$, $G_2'(0) = 0$, $n = 15$, $i = 1$, $K = 0$, $\bar{\omega} = 0.1$ and $\epsilon = 0.1$. The general shape of the

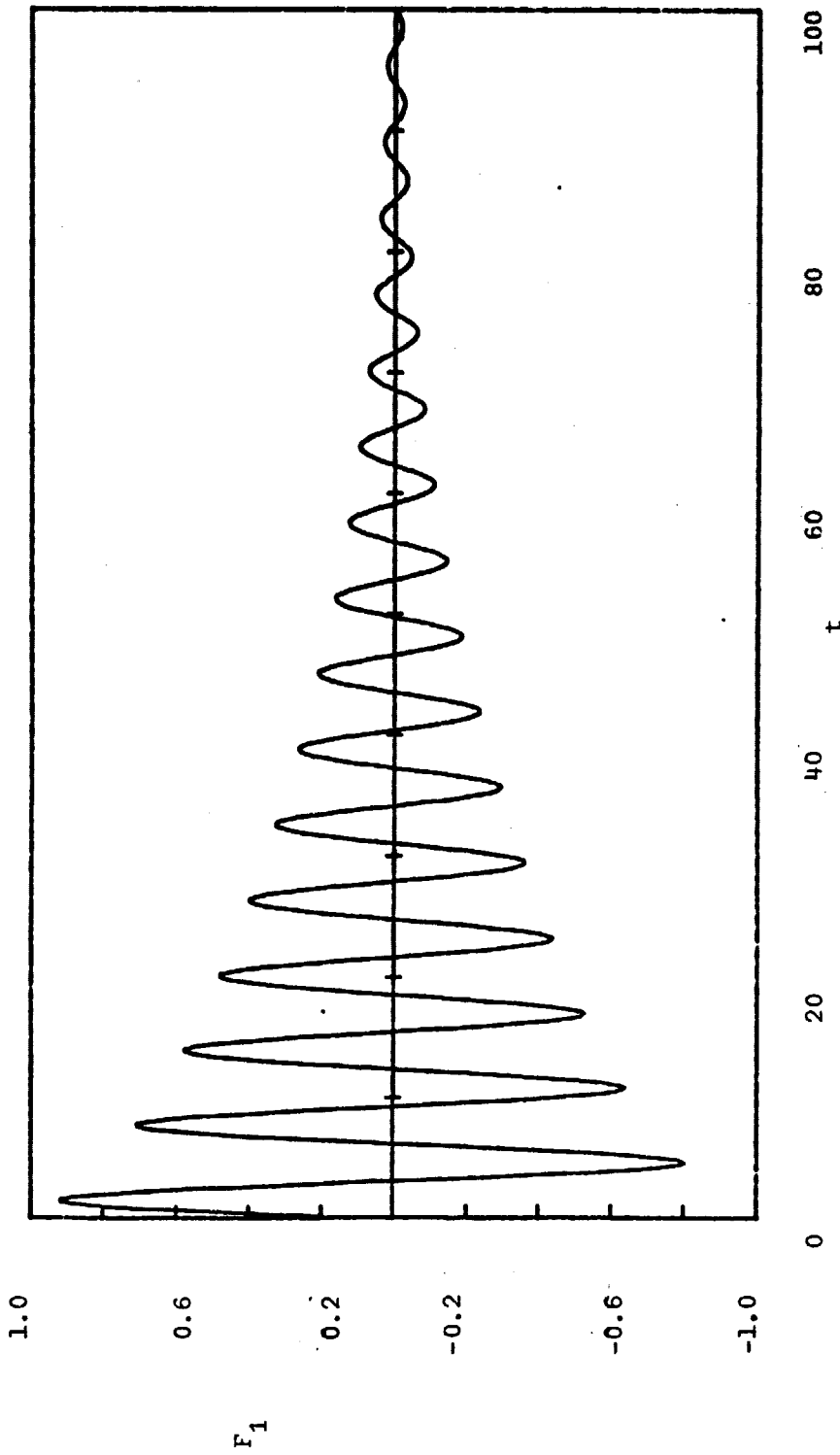


Figure 3. Modal Amplitude F_1 vs. time t for Standing Waves - Stable Case

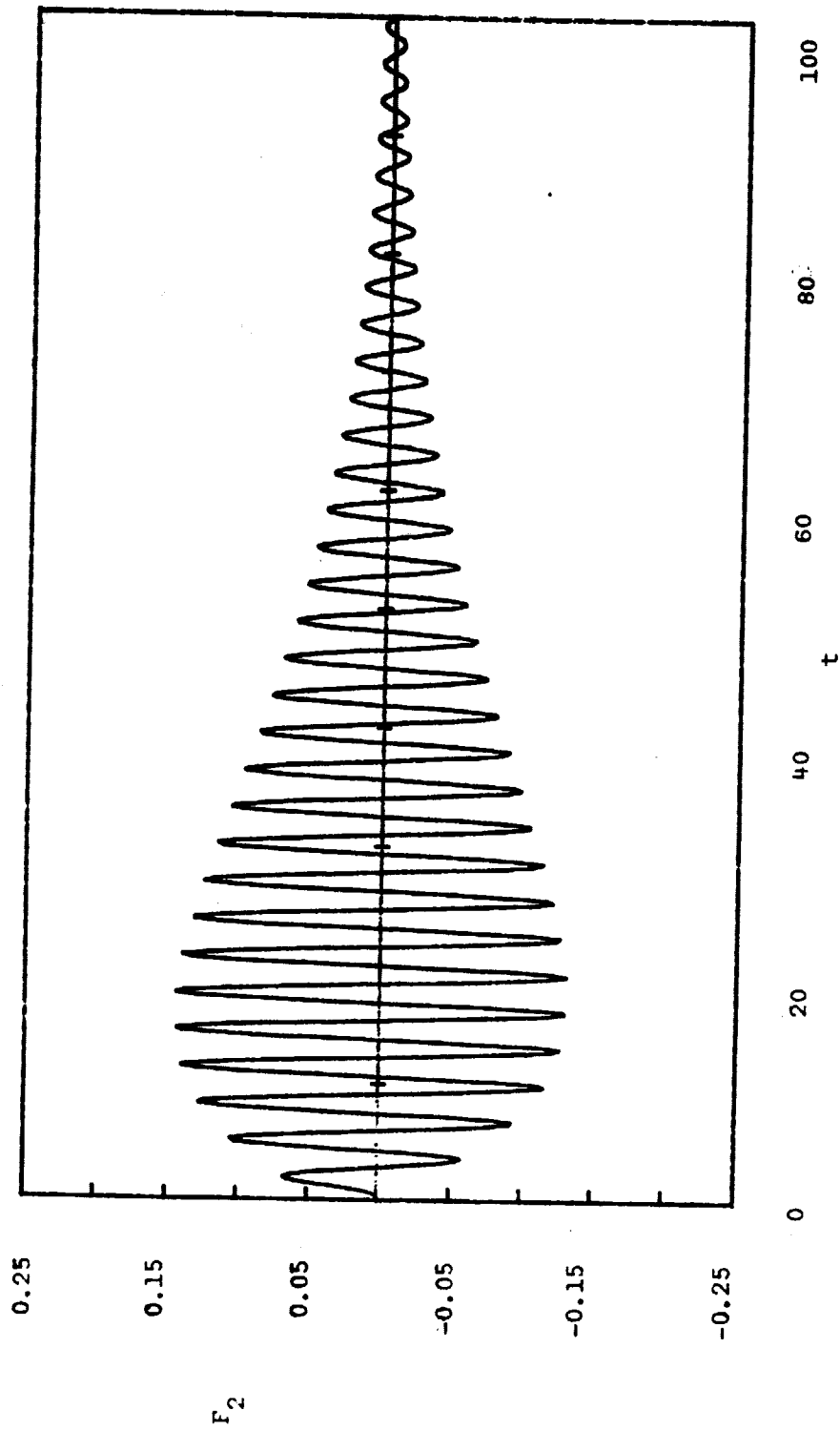


Figure 4. Modal Amplitude F_2 vs. time t for Standing Waves - Stable Case

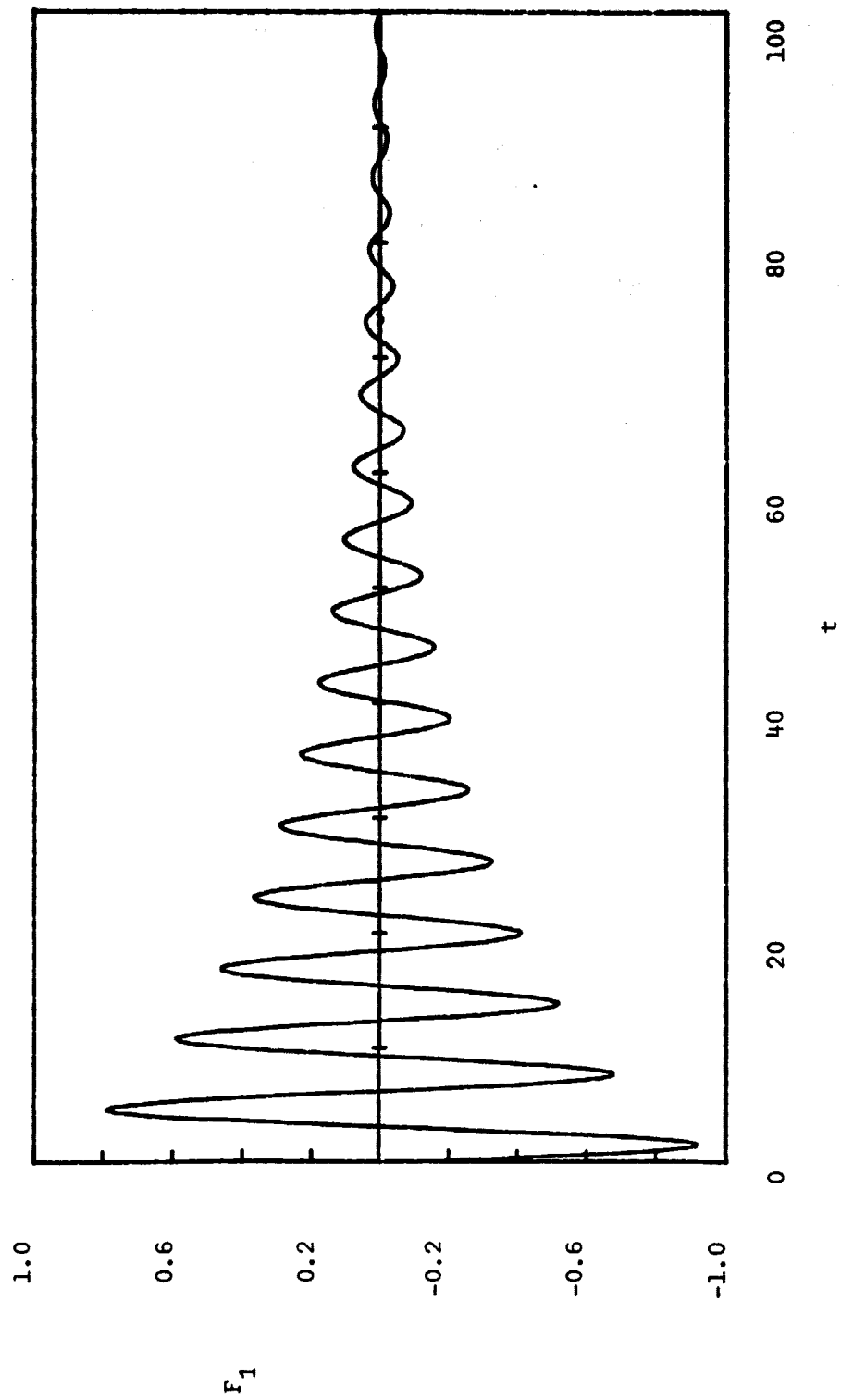


Figure 5. Modal Amplitude F_1 vs time t for Traveling Waves - Stable Case

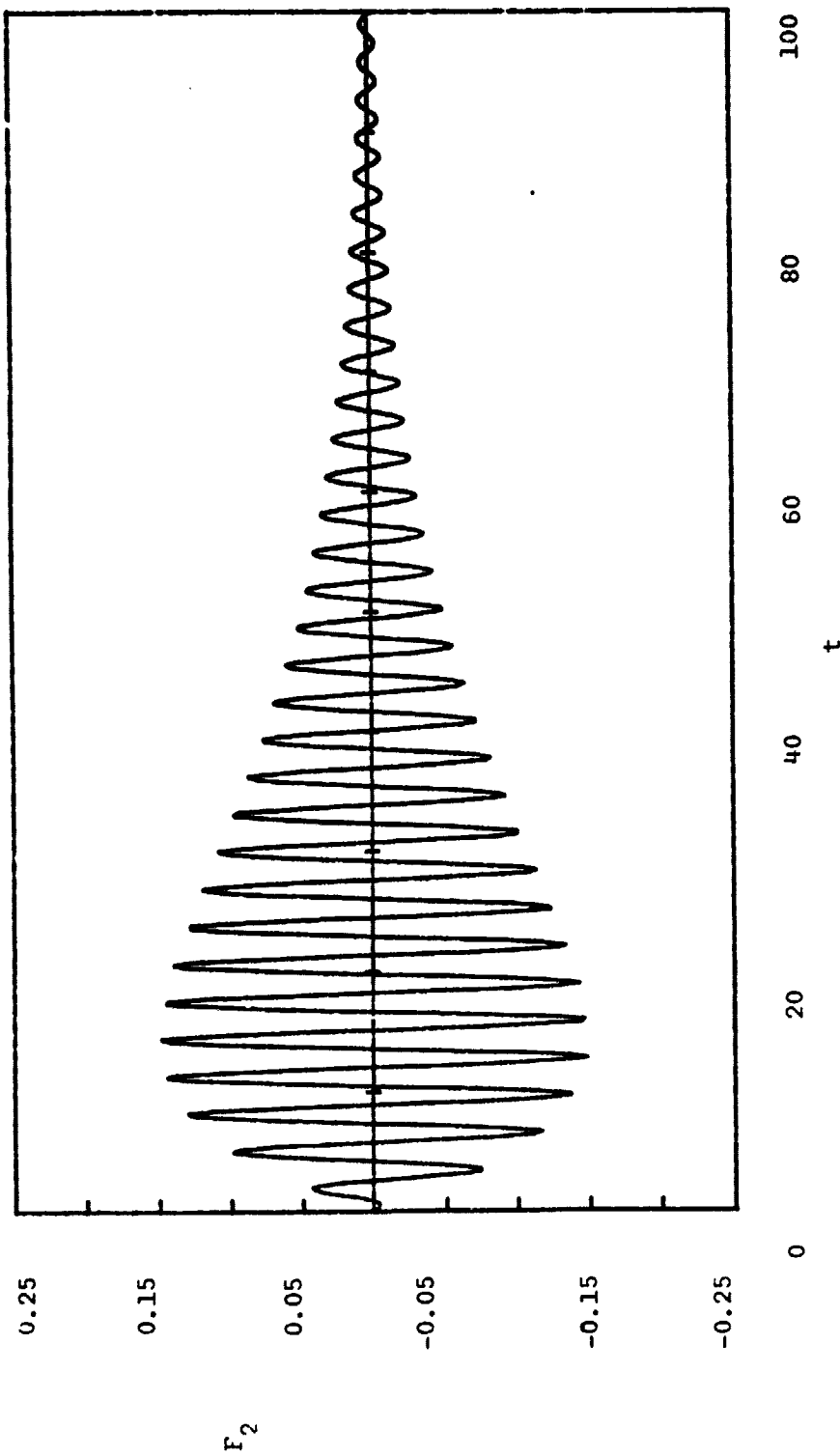


Figure 6. Modal Amplitude F_2 vs time t for Traveling Waves - Stable Case

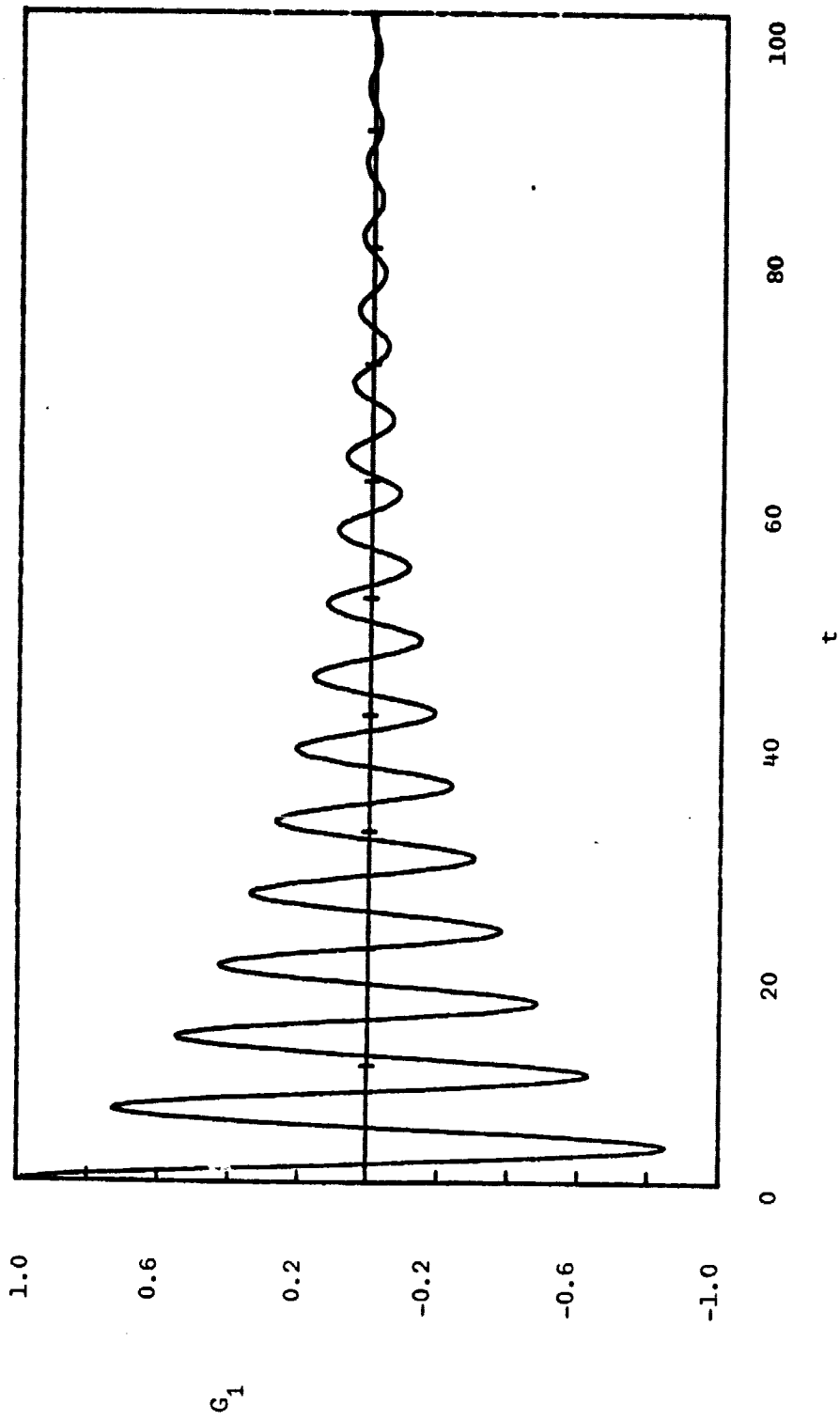


Figure 7. Modal Amplitude G_1 vs time t for Traveling Waves - Stable Case

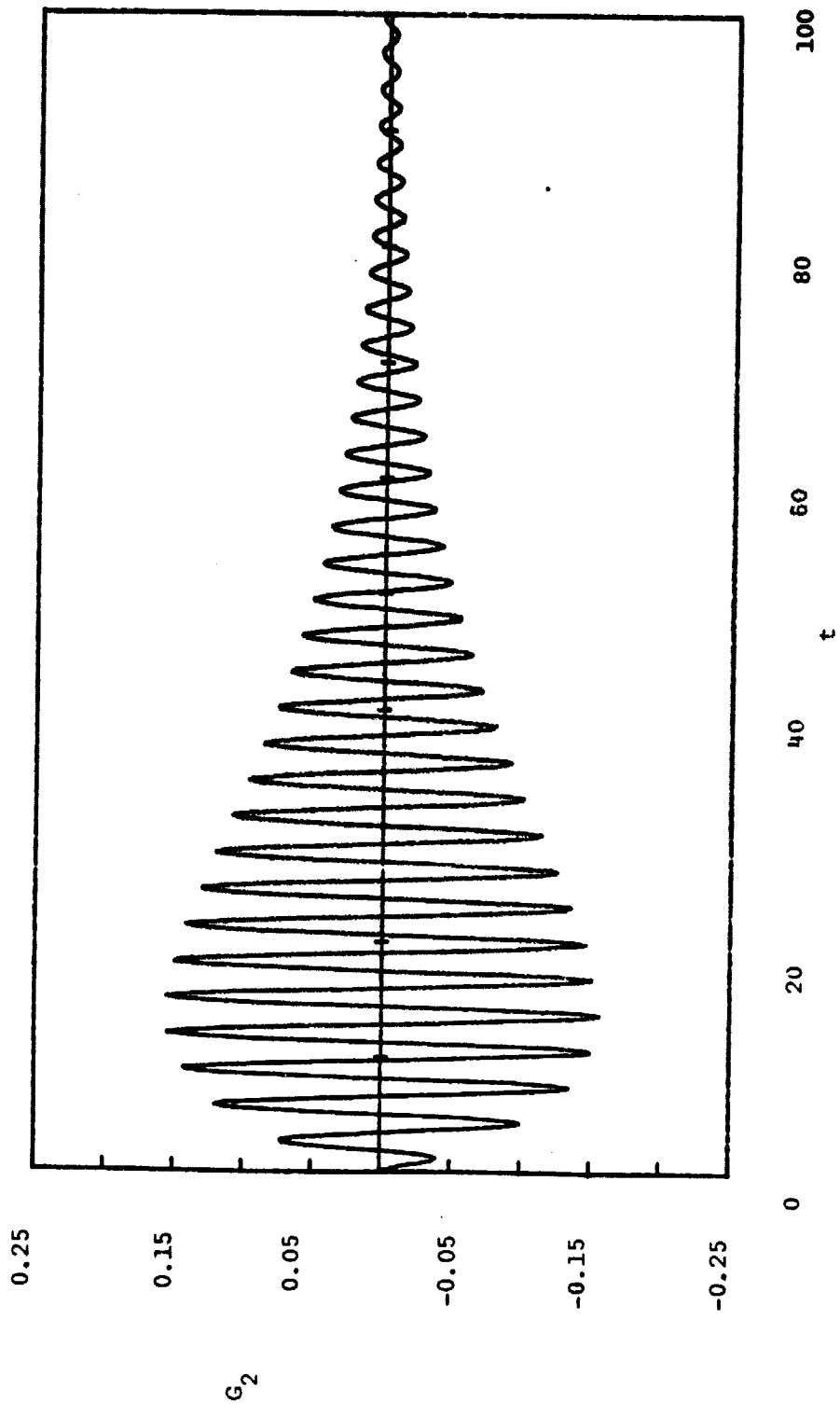


Figure 8. Modal Amplitude G_2 vs time t for Traveling Waves - Stable Case

curves and the relative frequencies of oscillation are qualitatively similar to the stable standing wave case.

In Figures 9 and 10, modal amplitudes F_1 and F_2 are graphically represented versus time for an unstable standing wave case with the same conditions as the stable case except that $n = 50$. As can be seen, the maximum amplitude of F_1 starts to decrease then increase dramatically for increasing time. The maximum amplitude of F_2 increases continuously. In Figures 11 through 14, modal amplitudes F_1 , F_2 , G_1 , and G_2 are represented versus time for an unstable traveling wave case. Again, the conditions are the same as for the stable traveling wave case except that $n = 30$. Drastic increases in amplitudes are observed for all the modal amplitudes shown as time increases. The behavior is similar to the unstable standing wave case. The period of time for traveling waves to become unstable is about one-half the period of time for standing waves to become unstable. Thus, it seems that traveling waves are less stable than are standing waves.

In Tables 1 and 2, a comparison of results is presented for modal amplitudes F_1 and F_2 for a stable standing wave case. For these cases, $F_1(0) = 0$, $F_1'(0) = 1$, $F_2(0) = 0$, $F_2'(0) = 0$, $G_1(0) = 0$, $G_1'(0) = 0$, $G_2(0) = 0$, $G_2'(0) = 0$, $n = 60$, $\epsilon = 0.1$, and $\bar{\omega} = 0.1$. These tables quantitatively show the effect of neglecting gas dynamic non-linearities on the accuracy of the computations. Also, a comparison can be made between the exact solution method (Appendix B program) and the perturbation solution method (Appendix C program). From Table 1, one can observe that the effect of neglecting gas-dynamic nonlinearities is small where quantitatively comparing values of the modal amplitude F_1 . Even though, quantitatively, the values for the exact solutions and perturbation

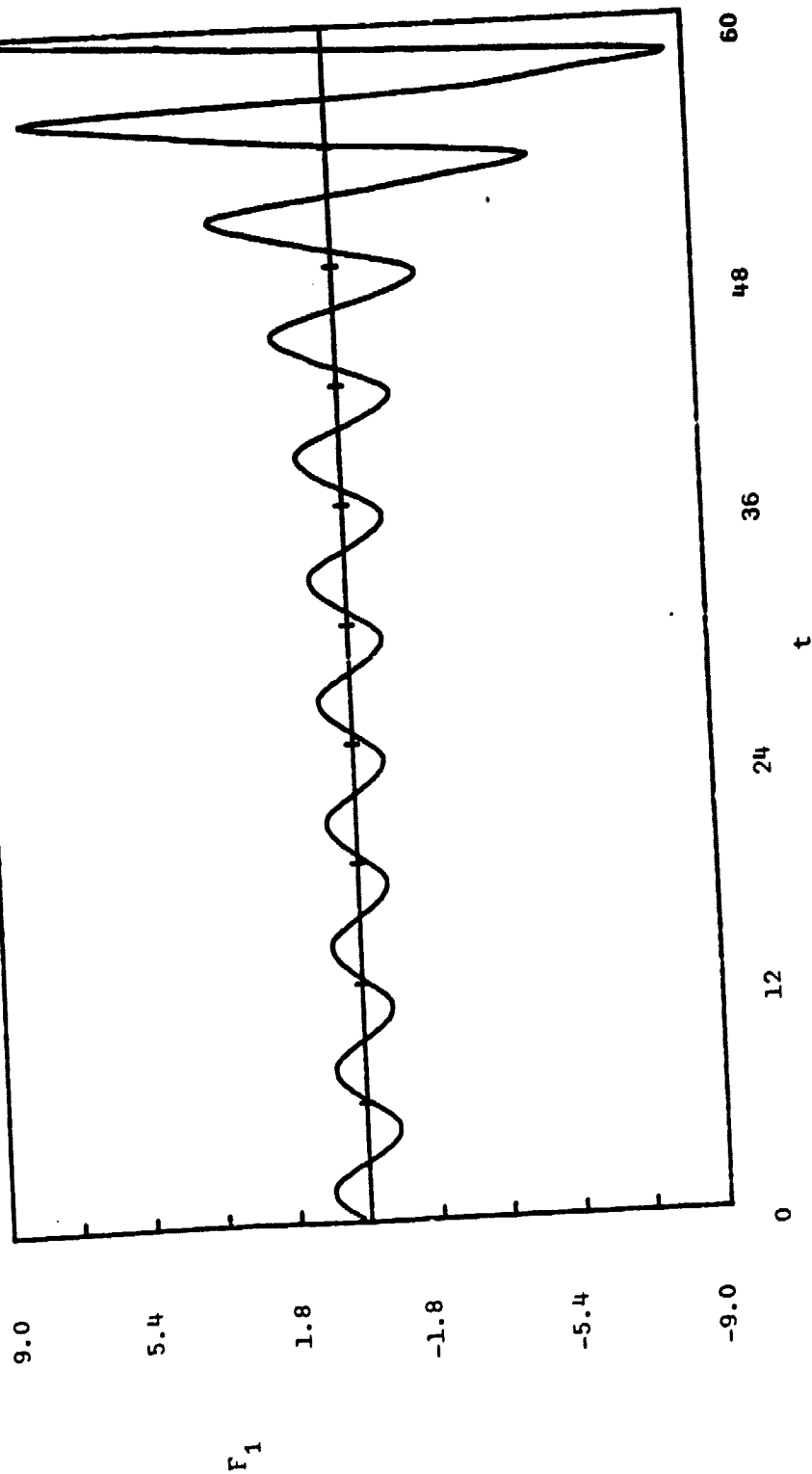


Figure 9. Modal Amplitude F_1 vs time t for Standing Waves - Unstable Case

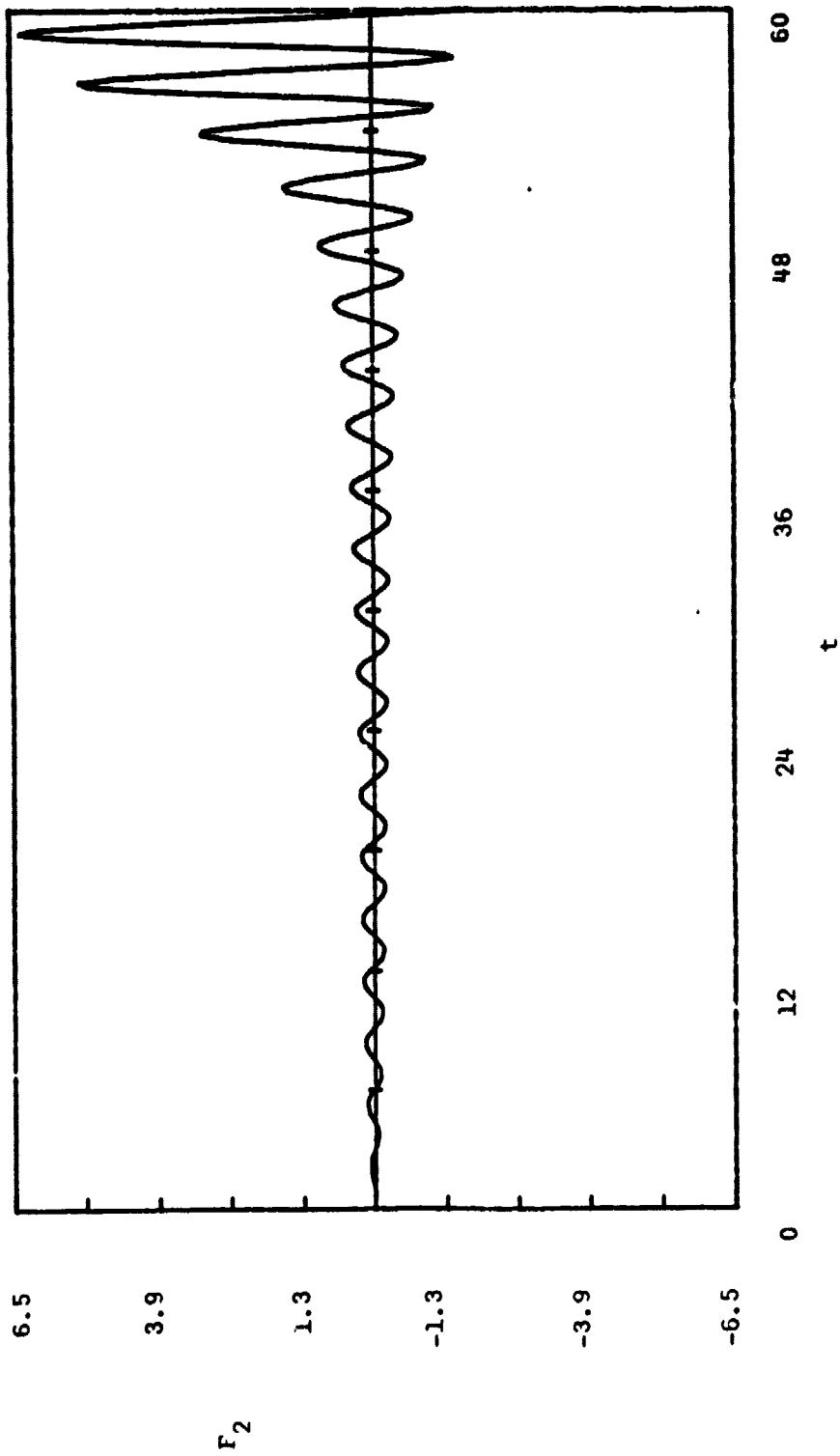


Figure 10. Modal Amplitude F_2 vs time t for Standing Waves - Unstable Case

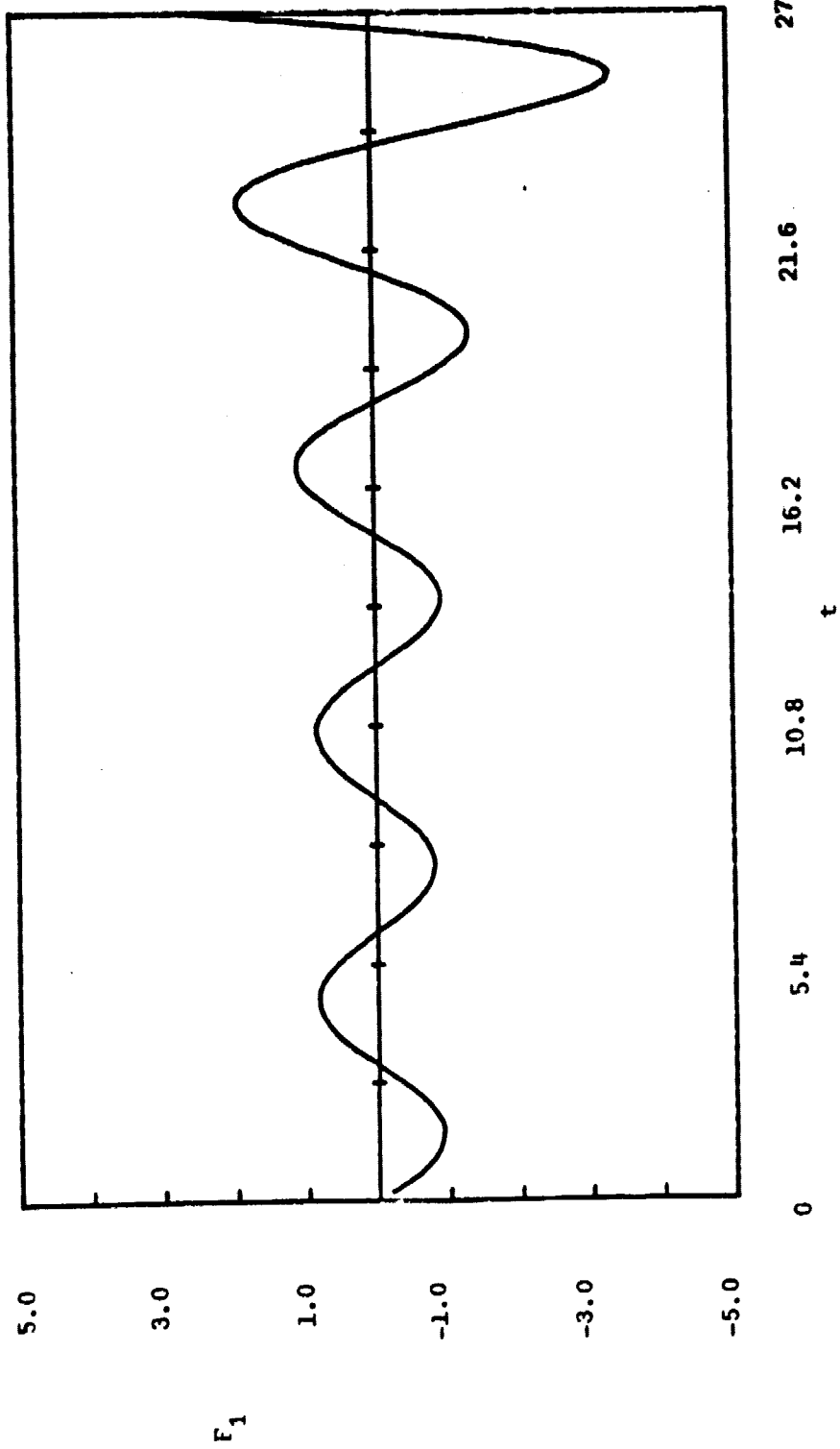


Figure 11. Modal Amplitude F_1 vs time t for Traveling Waves - Unstable Case

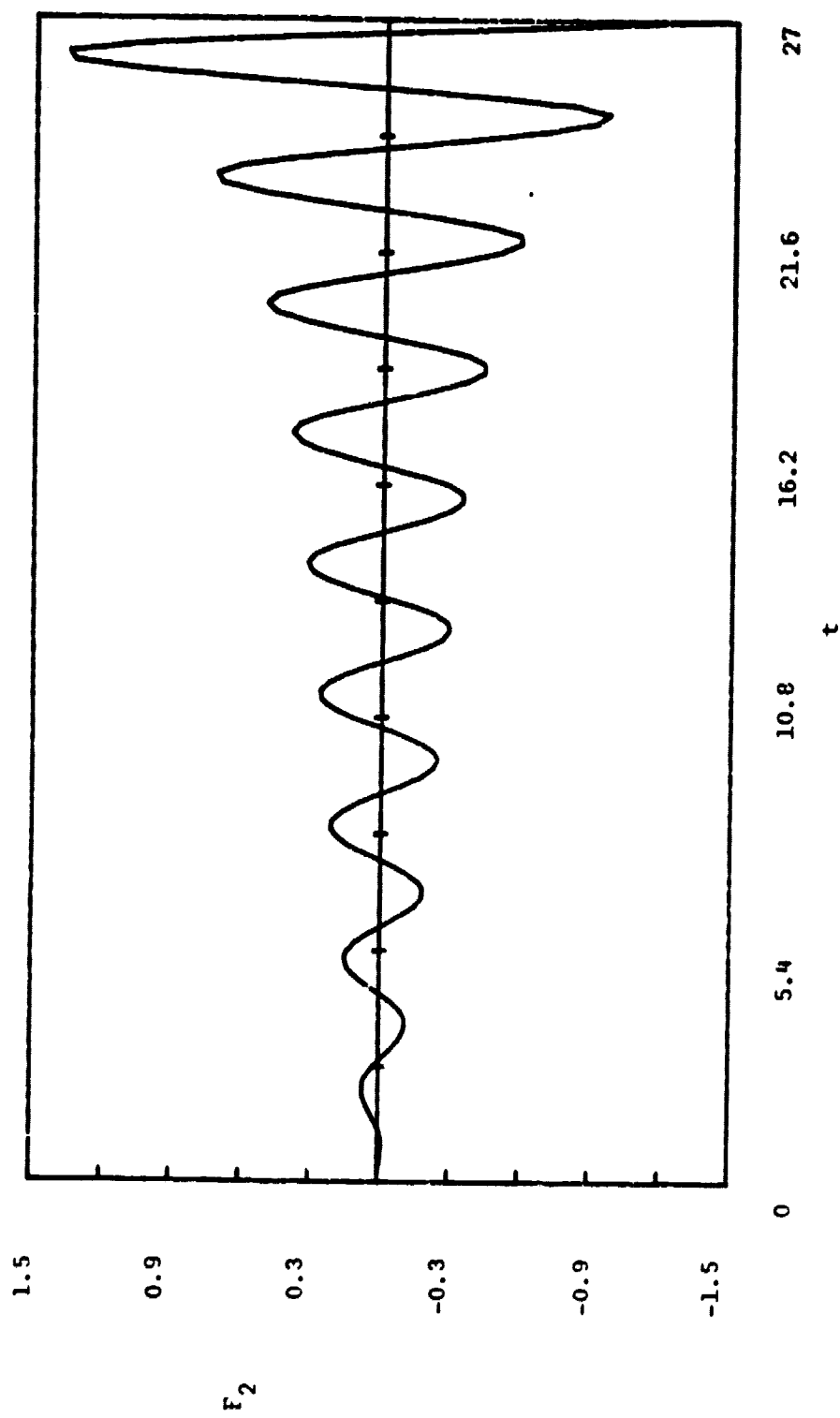


Figure 12. Modal Amplitude F_2 vs time t for Traveling Waves - Unstable Case

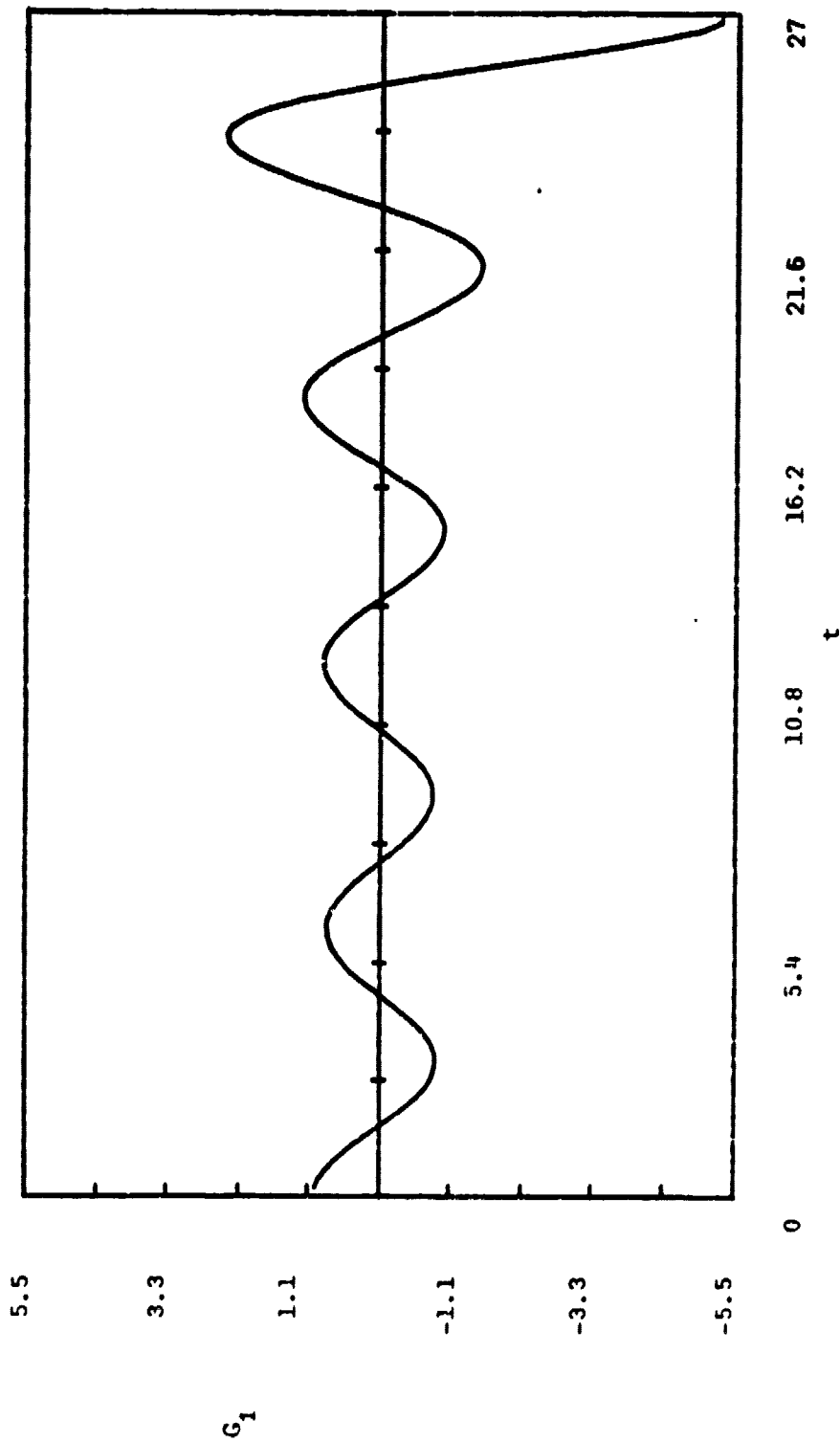


Figure 13. Modal Amplitude G_1 vs time t for Traveling Waves - Unstable Case

C2

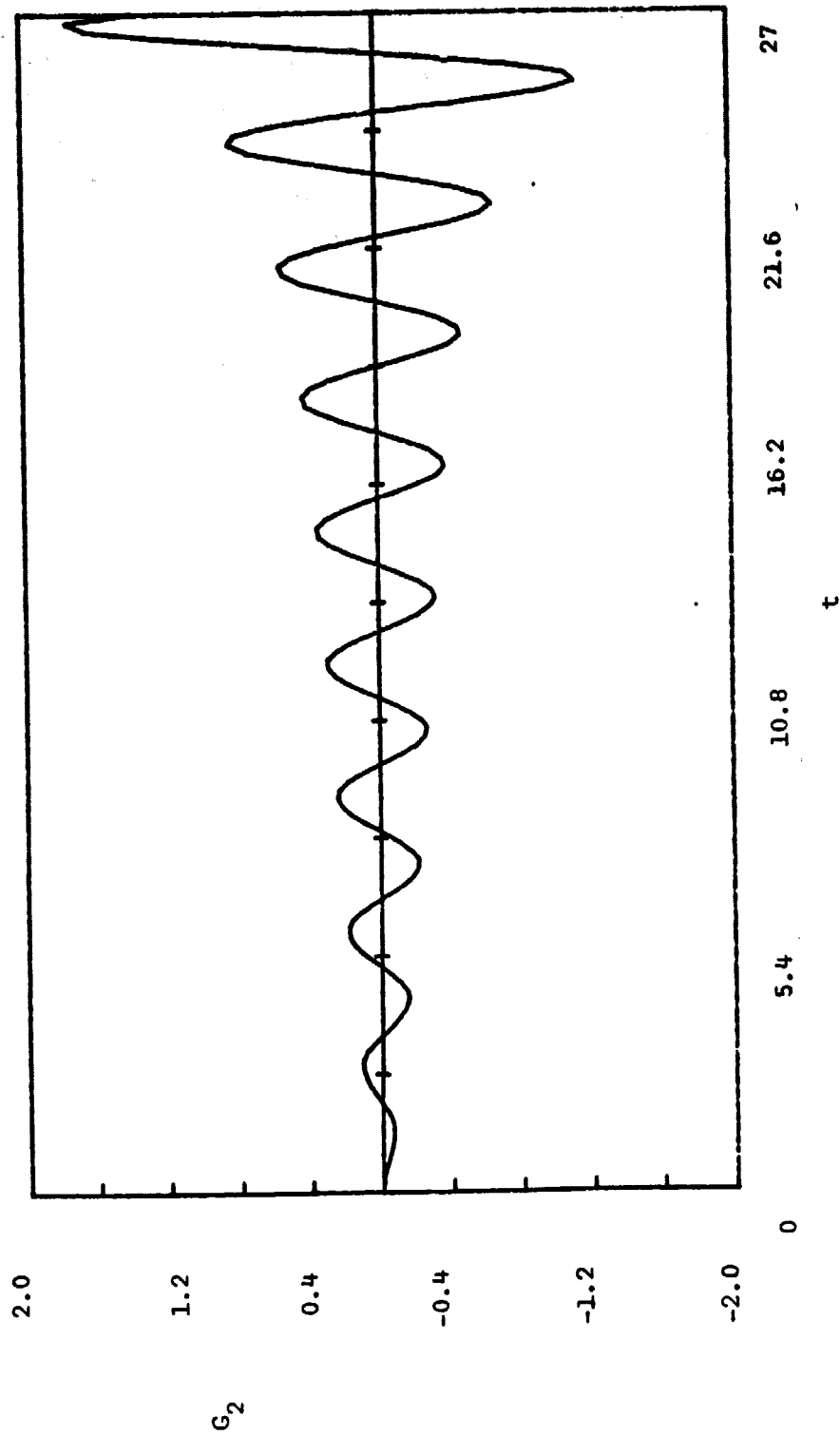


Figure 14. Modal Amplitude G_2 vs time t for Traveling Waves - Unstable Case

Table 1. Comparison of Results for F_1 Showing Effects of Gas Dynamic Index (i) - ($F_1 = 0, F_1' = 1, F_2 = 0, F_2' = 0, G_1 = 0, G_1' = 0, G_2 = 0, G_2' = 0$) - Stable Cases ($n = 60$) - Standing Waves

t	i = 1 K = 1		i = 0 K = 1	
	Exact Solution	Perturbation Solution	Exact Solution	Perturbation Solution
0.2	0.19699	0.18712	0.19699	0.18702
0.4	0.38335	0.36426	0.38336	0.36386
0.6	0.55252	0.52540	0.55259	0.52462
0.8	0.69856	0.66518	0.69885	0.66400
1.0	0.81627	0.77905	0.81719	0.77758
1.2	0.90132	0.86340	0.90354	0.86186
1.4	0.95043	0.91572	0.95489	0.91443
1.6	0.96159	0.93461	0.96936	0.93399
1.8	0.93432	0.91986	0.94632	0.92040
2.0	0.86985	0.87244	0.88656	0.87466
2.2	0.77125	0.79443	0.79242	0.79884
2.4	0.64330	0.68895	0.66783	0.69602
2.6	0.49211	0.56003	0.51822	0.57016
2.8	0.32469	0.41247	0.35021	0.42593
3.0	0.14827	0.25167	0.17115	0.26856
3.2	-0.03017	0.08340	-0.01142	0.10366
3.4	-0.20430	-0.08633	-0.19032	-0.06300
3.6	-0.36859	-0.25158	-0.35912	-0.22566
3.8	-0.51829	-0.40659	-0.51242	-0.37879
4.0	-0.64917	-0.54604	-0.64583	-0.51727
4.2	-0.75738	-0.66519	-0.75583	-0.63655
4.4	-0.83921	-0.76006	-0.83953	-0.73278
4.6	-0.89118	-0.82756	-0.89450	-0.80297
4.8	-0.91029	-0.86556	-0.91868	-0.84504
5.0	-0.89444	-0.87297	-0.91049	-0.85789
5.2	-0.84300	-0.84979	-0.86909	-0.84143
5.4	-0.75726	-0.79704	-0.79483	-0.79656
5.6	-0.64071	-0.71679	-0.68959	-0.72514
5.8	-0.49885	-0.61200	-0.55708	-0.62988
6.0	-0.33868	-0.48646	-0.40279	-0.51427
6.2	-0.16794	-0.34466	-0.23365	-0.38244
6.4	0.00574	-0.19159	-0.05742	-0.23901
6.6	0.17554	-0.03259	0.11809	-0.08892
6.8	0.33582	0.12685	0.28578	0.06271
7.0	0.48221	0.28126	0.43974	0.21080
7.2	0.61134	0.42538	0.57552	0.35042
7.4	0.72042	0.55435	0.68999	0.47703
7.6	0.80682	0.66387	0.78099	0.58653
7.8	0.86778	0.75032	0.84693	0.67550
8.0	0.90042	0.81090	0.88644	0.74121

Table 2. Comparison of Results for F_2 Showing Effects of Gas Dynamic Index (i) - ($F_1 = 0, F_1' = 1, F_2 = 0, F_2' = 0, G_1 = 0, G_1' = 0, G_2 = 0, G_2' = 0$) - Stable Cases ($n = 60$) - Standing Waves

t	i = 1 K = 1		i = 0 K = 1	
	Exact Solution	Perturbation Solution	Exact Solution	Perturbation Solution
0.2	0.00012	-0.00485	0.00003	-0.00253
0.4	0.00113	-0.01309	0.00043	-0.00938
0.6	0.00422	-0.02223	0.00205	-0.01865
0.8	0.01060	-0.02944	0.00602	-0.02784
1.0	0.02110	-0.03215	0.01336	-0.03424
1.2	0.03582	-0.02854	0.02471	-0.03553
1.4	0.05397	-0.01795	0.03497	-0.03023
1.6	0.07375	-0.00104	0.05816	-0.01798
1.8	0.09260	0.02022	0.07742	0.00026
2.0	0.10749	0.04283	0.09521	0.02232
2.2	0.11543	0.06317	0.10863	0.04514
2.4	0.11407	0.07764	0.11493	0.06516
2.6	0.10215	0.08319	0.11198	0.07891
2.8	0.07988	0.07788	0.09878	0.08357
3.0	0.04909	0.06128	0.07573	0.07745
3.2	0.01309	0.03461	0.04478	0.06031
3.4	-0.02375	0.00071	0.00929	0.03352
3.6	-0.05653	-0.03632	-0.02639	-0.00006
3.8	-0.08051	-0.07164	-0.05749	-0.03640
4.0	-0.09180	-0.10031	-0.07945	-0.07083
4.2	-0.08798	-0.11801	-0.08865	-0.09863
4.4	-0.06850	-0.12165	-0.08296	-0.11571
4.6	-0.03490	-0.10993	-0.06211	-0.11921
4.8	0.00924	-0.08353	-0.02786	-0.10793
5.0	0.05868	-0.04515	0.01610	-0.08257
5.2	0.10711	0.00077	0.06458	-0.04571
5.4	0.14796	0.04864	0.11144	-0.00152
5.6	0.17534	0.09236	0.15041	0.04468
5.8	0.18493	0.12615	0.17593	0.08715
6.0	0.17466	0.14534	0.18393	0.12042
6.2	0.14513	0.14699	0.17255	0.14004
6.4	0.09957	0.13035	0.14243	0.14314
6.6	0.04352	0.09700	0.09680	0.12888
6.8	-0.01592	0.05073	0.0411	0.09857
7.0	-0.07104	-0.00295	-0.01771	0.05557
7.2	-0.11448	-0.05745	-0.07205	0.00488
7.4	-0.14027	-0.10594	-0.11471	-0.04743
7.6	-0.14458	-0.14223	-0.13988	-0.09498
7.8	-0.12628	-0.16158	-0.14384	-0.13189
8.0	-0.08716	-0.16128	-0.12556	-0.15352

solutions are not exactly the same, the order of magnitude and behavior of results is similar. From Table 2, the same observations can be made for the behavior of F_2 . There is, however, more error, quantitatively, between the results for exact and perturbation methods and a region of qualitative inaccuracy between the exact and perturbation solutions exists near $t = 0$. This takes the form of a difference in sign of F_2 between results from the exact solution as compared to the perturbations solution. This discrepancy occurred also in the other calculations performed (not shown) and will be discussed in more detail later in this chapter.

In Tables 3 and 4, a comparison of results is presented for modal amplitudes F_1 and F_2 for a stable standing wave case. The initial conditions for the results in these tables are $F_1(0) = 0$, $F_1'(0) = 1$, $F_2(0) = 0$, $F_2'(0) = 0$, $G_1(0) = 0$, $G_1'(0) = 0$, $G_2(0) = 0$, $G_2'(0) = 0$, $n = 40$, $\epsilon = 0.1$, and $\bar{\omega} = 0.1$. However, these tables quantitatively present the effect of deviations of the ratio of the second acoustic frequency to the first from the integer value of 2 (this is controlled by the parameter K). These results show that solutions for finite values of K are qualitatively similar to those for $K = 0$. This indicates that the ratio of the second acoustic frequency to the first does not have to be an integer in order to produce the type of behavior observed here. A ratio near an integer value will lead to similar results. Tables 3 and 4 also allow a comparison to the results generated by the program in Appendix D for the approximate analytical solution (4.31). These results presented in the last column of Tables 3 and 4 can be compared to the fourth column in each of these tables to determine the accuracy of (4.31). These comparisons present further evidence that the neglect of gas dynamic nonlinearities does not have an important qualitative effect.

Table 3. Comparison of Results for F_1 Showing Effects of the Correction Variable (K) - ($F_1 = 0, F_1' = 1, F_2 = 0, F_2' = 0, G_1 = 0, G_1' = 0, G_2 = 0, G_2' = 0$) - Stable Case ($n = 40$) - Standing Waves

	$i = 1$ $K = 1$		$i = 1$ $K = 0$		$i = 0$ $K = 0$
t	Exact Solution	Perturbation Solution	Exact Solution	Perturbation Solution	Analytic Solution
0.2	0.19699	0.18707	0.19670	0.19678	0.19671
0.4	0.38335	0.36396	0.38172	0.38210	0.38186
0.6	0.55254	0.52460	0.54795	0.54890	0.54843
0.8	0.69867	0.66358	0.68903	0.69093	0.69029
1.0	0.81667	0.77635	0.79957	0.60302	0.80234
1.2	0.90247	0.85935	0.87537	0.88124	0.88075
1.4	0.95312	0.91014	0.91361	0.92306	0.92304
1.6	0.96699	0.92744	0.91310	0.92740	0.92820
1.8	0.94390	0.91120	0.87443	0.89468	0.89666
2.0	0.88523	0.86255	0.80001	0.82676	0.83027
2.2	0.79388	0.78374	0.69393	0.72690	0.73221
2.4	0.67411	0.67805	0.56163	0.59954	0.60682
2.6	0.53129	0.54969	0.40948	0.45016	0.45947
2.8	0.37154	0.40358	0.24432	0.28905	0.29627
3.0	0.20133	0.24520	0.07300	0.11102	0.12386
3.2	0.02712	0.08039	-0.09782	-0.06484	-0.05085
3.4	-0.14491	-0.08439	-0.26190	-0.23547	-0.22097
3.6	-0.30901	-0.24474	-0.41335	-0.39410	-0.37989
3.8	-0.45992	-0.39354	-0.54662	-0.53453	-0.52152
4.0	-0.59287	-0.52617	-0.65660	-0.65139	-0.64055
4.2	-0.70357	-0.63813	-0.73872	-0.74028	-0.73261
4.4	-0.78821	-0.72574	-0.78928	-0.79800	-0.79446
4.6	-0.84362	-0.78623	-0.80583	-0.82264	-0.82407
4.8	-0.86746	-0.81785	-0.78760	-0.81364	-0.82069
5.0	-0.85849	-0.81988	-0.73571	-0.77179	-0.78490
5.2	-0.81682	-0.79266	-0.65317	-0.69920	-0.71852
5.4	-0.74409	-0.73757	-0.54464	-0.59917	-0.62456
5.6	-0.64352	-0.65697	-0.41585	-0.47611	-0.50704
5.8	-0.51967	-0.55405	-0.27311	-0.33525	-0.37090
6.0	-0.37816	-0.43279	-0.12272	-0.18253	-0.22172
6.2	-0.22516	-0.29772	0.02937	-0.02427	-0.06554
6.4	-0.06694	-0.15382	0.17767	0.13305	0.09140
6.6	0.09056	-0.0063	0.31714	0.28307	0.24291
6.8	0.24192	0.13957	0.44298	0.41977	0.38308
7.0	0.38242	0.27867	0.55061	0.53776	0.50650
7.2	0.50795	0.40617	0.63563	0.63247	0.60850
7.4	0.61493	0.51774	0.69408	0.70029	0.68527
7.6	0.70017	0.60967	0.72786	0.73878	0.73407
7.8	0.76090	0.67898	0.72020	0.74667	0.75327
8.0	0.79476	0.72355	0.68609	0.72400	0.74234

Table 4. Comparison of Results for F_2 Showing Effects of the Correction Variable (K) - ($F_1 = 0, F_1' = 1, F_2 = 0, F_2' = 0, G_1 = 0, G_1' = 0, G_2 = 0, G_2' = 0$) - Stable Case ($n = 40$) - Standing Waves

	$i = 1$ K = 1		$i = 1$ K = 0		$i = 0$ K = 0
t	Exact Solution	Perturbation Solution	Exact Solution	Perturbation Solution	Analytic Solution
0.2	0.00011	-0.00400	0.00015	-0.00419	-0.00192
0.4	0.00099	-0.00996	0.00136	-0.01035	-0.00696
0.6	0.00354	-0.01599	0.00479	-0.01597	-0.01337
0.8	0.00860	-0.02013	0.01141	-0.01856	-0.01885
1.0	0.01665	-0.02071	0.02149	-0.01626	-0.02113
1.2	0.02761	-0.01669	0.03443	-0.00838	-0.01856
1.4	0.04072	-0.00793	0.04866	0.00438	-0.01059
1.6	0.05458	0.00479	0.06180	0.01995	0.00208
1.8	0.06726	0.01983	0.07113	0.03529	0.01749
2.0	0.07663	0.03491	0.07416	0.04696	0.03278
2.2	0.08072	0.04750	0.06910	0.05185	0.04472
2.4	0.07803	0.05521	0.05549	0.04793	0.05038
2.6	0.06793	0.05622	0.03439	0.03468	0.04776
2.8	0.05081	0.04957	0.00841	0.01343	0.03626
3.0	0.02816	0.03542	-0.01867	-0.01282	0.01697
3.2	0.00244	0.01507	-0.04246	-0.03978	-0.00745
3.4	-0.02323	-0.00917	-0.05871	-0.06265	-0.03313
3.6	-0.04544	-0.03425	-0.06410	-0.07695	-0.05561
3.8	-0.06099	-0.05679	-0.05687	-0.07938	-0.07067
4.0	-0.06735	-0.07356	-0.03727	-0.06854	-0.07507
4.2	-0.06307	-0.08196	-0.00764	-0.04530	-0.06722
4.4	-0.04802	-0.08040	0.02778	-0.01278	-0.04759
4.6	-0.02355	-0.06854	0.06351	0.02408	-0.01872
4.8	0.00767	-0.04745	0.09363	0.05926	0.01509
5.0	0.04187	-0.01945	0.11279	0.08668	0.04845
5.2	0.07470	0.01210	0.11719	0.10127	0.07573
5.4	0.10173	0.04330	0.10529	0.09987	0.09206
5.6	0.11915	0.07013	0.07824	0.08191	0.09414
5.8	0.12425	0.08905	0.03976	0.04959	0.08095
6.0	0.11586	0.09745	-0.00434	0.00764	0.05395
6.2	0.09462	0.09402	-0.04711	-0.03736	0.01700
6.4	0.06286	0.07894	-0.08154	-0.07807	-0.02424
6.6	0.02438	0.05389	-0.10178	-0.10757	-0.06318
6.8	-0.01630	0.02182	-0.10409	-0.12058	-0.09336
7.0	-0.05322	-0.01335	-0.08754	-0.11433	-0.10952
7.2	-0.08237	-0.04728	-0.05423	-0.08921	-0.10854
7.4	-0.09956	-0.07576	-0.00908	-0.04879	-0.09001
7.6	-0.10237	-0.09523	0.04092	0.00093	-0.05639
7.8	-0.09018	-0.10322	0.08777	0.05190	-0.01267
8.0	-0.06428	-0.09872	0.12375	0.09586	0.03434

In Tables 5 and 6, a comparison of results are presented for modal amplitudes F_1 and F_2 for an unstable standing wave showing the effect of neglecting gas-dynamic nonlinearities. It can be seen that the gas dynamic nonlinearities have little qualitative effect on the results.

In Tables 7 and 8, a comparison of results are presented for modal amplitudes F_1 and F_2 for an unstable standing wave case showing the effects of K . The results for zero and non-zero are qualitatively similar.

These tables are representative of the cases that were investigated in the course of this research. Only cases involving standing waves were presented. The same behavior, however, can be observed for the cases involving traveling waves.

In Table 9, a comparison of stability boundaries is presented based upon the interaction index (n) which is a measure of the strength of the combustion process. For standing waves and the given conditions shown, the stability limit for a process with gas dynamic nonlinearities considered and $K = 0$ is between 45-50. When both gas dynamic nonlinearities and the correction variable are considered, the stability limit is increased to 67.5-69. Finally, when considering only the correction variable with no gas-dynamic non-linearity effect, the stability limit is 72-72.5. The results show that the neglect of gas dynamic nonlinearities slightly underestimates the stability boundary and that the increasing K increases the stability limit.

In Table 10, a comparison of stability boundaries is presented based upon the interaction index for traveling waves. These results provide additional confirmation of the conclusions discussed in the previous paragraph and also illustrate the fact that standing waves are roughly twice as stable as traveling waves. This is consistent with the

Table 5. Comparison of Results for F_1 Showing Effect of the Gas Dynamic Index (i) - ($F_1 = 0, F_1' = 1, F_2 = 0, F_2' = 0, G_1 = 0, G_1' = 0, G_2 = 0, G_2' = 0$) - Unstable Case ($n = 75$) - Standing Waves

t	i = 1 K = 1		i = 0 K = 1	
	Exact Solution	Perturbation Solution	Exact Solution	Perturbation Solution
0.2	0.19699	0.18717	0.19699	0.18703
0.4	0.38335	0.38215	0.38336	0.36402
0.6	0.55250	0.52613	0.55258	0.52513
0.8	0.69847	0.69244	0.69881	0.66518
1.0	0.81592	0.80625	0.81700	0.77974
1.2	0.90030	0.86736	0.90294	0.86535
1.4	0.94803	0.92126	0.95337	0.91952
1.6	0.95671	0.94184	0.96695	0.94089
1.8	0.92557	0.92873	0.94003	0.92921
2.0	0.85572	0.88276	0.87584	0.88529
2.2	0.75039	0.80579	0.77580	0.81106
2.4	0.61484	0.70079	0.64411	0.70941
2.6	0.45593	0.57161	0.48677	0.58410
2.8	0.28147	0.42287	0.31118	0.43963
3.0	0.09945	0.25987	0.12554	0.28107
3.2	-0.08272	0.08829	-0.06194	0.11388
3.4	-0.25864	-0.08588	-0.24371	-0.05620
3.6	-0.42307	-0.25669	-0.41342	-0.22350
3.8	-0.57177	-0.41827	-0.56608	-0.38241
4.0	-0.70107	-0.56512	-0.69790	-0.52773
4.2	-0.80745	-0.69228	-0.80594	-0.63473
4.4	-0.88721	-0.79547	-0.88767	-0.75934
4.6	-0.93641	-0.87123	-0.94056	-0.83825
4.8	-0.95124	-0.91703	-0.96203	-0.88902
5.0	-0.92862	-0.93138	-0.94961	-0.91020
5.2	-0.86710	-0.91381	-0.90146	-0.90121
5.4	-0.76771	-0.86492	-0.81711	-0.86255
5.6	-0.63434	-0.78635	-0.69815	-0.79563
5.8	-0.47368	-0.68071	-0.54872	-0.70274
6.0	-0.29439	-0.55149	-0.37551	-0.58703
6.2	-0.10598	-0.40299	-0.18717	-0.45231
6.4	0.08258	-0.22558	0.00672	-0.30299
6.6	0.26374	-0.06815	0.19691	-0.14391
6.8	0.43198	0.10715	0.37555	0.01979
7.0	0.58355	0.28009	0.53682	0.18290
7.2	0.71613	0.44478	0.67707	0.34025
7.4	0.82779	0.59627	0.79428	0.48686
7.6	0.91635	0.72909	0.88737	0.61813
7.8	0.97878	0.83897	0.95535	0.72996
8.0	1.01111	0.92224	0.99664	0.81891

Table 6. Comparison of Results for F_2 Showing Effect of the Gas Dynamic Index (i) - ($F_1 = 0, F_1' = 1, F_2 = 0, F_2' = 0, G_1 = 0, G_1' = 0, G_2 = 0, G_2' = 0$) - Unstable Case - ($n = 75$) - Standing Waves

t	i = 1 K = 1		i = 0 K = 1	
	Exact Solution	Perturbation Solution	Exact Solution	Perturbation Solution
0.2	0.00013	-0.00548	0.00003	-0.00316
0.4	0.00124	-0.01544	0.00054	-0.01172
0.6	0.00473	-0.02691	0.00257	-0.02333
0.8	0.01210	-0.03643	0.00752	-0.03484
1.0	0.02443	-0.04077	0.01670	-0.04288
1.2	0.04197	-0.03749	0.03089	-0.04728
1.4	0.06387	-0.025518	0.04994	-0.03793
1.6	0.08806	-0.005425	0.07263	-0.02258
1.8	0.11143	0.02061	0.0966	0.00033
2.0	0.13027	0.049007	0.1186	0.02813
2.2	0.14082	0.07537	0.13504	0.05696
2.4	0.14005	0.09513	0.14236	0.08237
2.6	0.12628	0.10426	0.13796	0.09995
2.8	0.09967	0.10004	0.12064	0.10606
3.0	0.06242	0.08152	0.09109	0.09851
3.2	0.01860	0.04984	0.05192	0.07688
3.4	-0.02636	0.008166	0.0076	0.04283
3.6	-0.06636	-0.03858	-0.03628	-0.00096
3.8	-0.09548	-0.08436	-0.07362	-0.046816
4.0	-0.10889	-0.12285	-0.09877	-0.09134
4.2	-0.10354	-0.14826	-0.10733	-0.12758
4.4	-0.07873	-0.15626	-0.09688	-0.15016
4.6	-0.03636	-0.14461	-0.06742	-0.15524
4.8	0.01909	-0.11361	-0.02153	-0.14104
5.0	0.08104	-0.06617	0.03583	-0.10827
5.2	0.14148	-0.00758	0.09778	-0.06010
5.4	0.19206	0.055118	0.15638	-0.00186
5.6	0.22528	0.11399	0.20358	0.05954
5.8	0.23565	0.16121	0.23235	0.11651
6.0	0.22067	0.19016	0.23779	0.16168
6.2	0.18130	0.19633	0.21796	0.18888
6.4	0.12201	0.17793	0.17434	0.19397
6.6	0.05019	0.13633	0.11182	0.17547
6.8	-0.02482	0.07595	0.03808	0.13477
7.0	-0.09302	-0.02526	-0.03737	0.07614
7.2	-0.14503	-0.07144	-0.10448	0.006209
7.4	-0.17338	-0.140235	-0.15407	-0.06680
7.6	-0.17347	-0.19368	-0.17900	-0.13401
7.8	-0.14428	-0.22450	-0.17519	-0.18700
8.0	-0.08859	-0.22808	-0.14216	-0.21888

Table 7. Comparison of Results for F_1 Showing the Effects of the Correction Variable (K) - ($F_1 = 0, F_1' = 1, F_2 = 0, F_2' = 0, G_1 = 0, G_1' = 0, G_2 = 0, G_2' = 0$) - Unstable Cases ($n = 70$) - Standing Waves

τ	$i = 1$ $K = 1$		$i = 1$ $K = 0$		$i = 0$ $K = 0$
	Exact Solution	Perturbation Solution	Exact Solution	Perturbation Solution	Analytic Solution
0.2	0.19699	0.187155	0.19670	0.19687	0.19675
0.4	0.38335	0.36462	0.38172	0.38261	0.38217
0.6	0.55251	0.52587	0.54791	0.55028	0.54942
0.8	0.69850	0.66615	0.68878	0.69371	0.69249
1.0	0.81604	0.78072	0.79865	0.80767	0.80630
1.2	0.90066	0.86596	0.87280	0.88811	0.88696
1.4	0.94887	0.91928	0.90775	0.93226	0.93184
1.6	0.95842	0.93925	0.90166	0.93878	0.93468
1.8	0.92863	0.92554	0.85477	0.90772	0.91061
2.0	0.86067	0.87904	0.76962	0.84061	0.84612
2.2	0.75771	0.80166	0.65109	0.74802	0.74903
2.4	0.62481	0.69648	0.50590	0.61107	0.62333
2.6	0.46860	0.56735	0.34194	0.45807	0.47407
2.8	0.29658	0.41903	0.16733	0.26849	0.30714
3.0	0.11649	0.25679	-0.01027	0.10616	0.12906
3.2	-0.06441	0.08639	-0.18416	-0.05313	-0.05327
3.4	-0.23973	-0.08618	-0.34860	-0.25962	-0.23280
3.6	-0.40414	-0.25437	-0.49854	-0.42949	-0.40262
3.8	-0.55318	-0.41415	-0.62912	-0.58151	-0.55621
4.0	-0.68301	-0.55829	-0.73533	-0.70960	-0.68766
4.2	-0.78998	-0.68250	-0.81197	-0.80859	-0.79192
4.4	-0.87041	-0.78258	-0.85399	-0.87449	-0.86494
4.6	-0.92055	-0.85525	-0.85736	-0.90458	-0.90388
4.8	-0.93689	-0.89811	-0.82008	-0.89755	-0.90718
5.0	-0.91671	-0.90981	-0.74306	-0.85356	-0.87463
5.2	-0.85886	-0.89005	-0.63045	-0.80213	-0.80736
5.4	-0.76447	-0.83962	-0.48925	-0.66264	-0.70785
5.6	-0.63724	-0.76029	-0.32818	-0.52309	-0.57982
5.8	-0.48340	-0.65486	-0.15634	-0.36111	-0.42807
6.0	-0.31100	-0.52691	0.01809	-0.18308	-0.25635
6.2	-0.12888	-0.38083	0.18852	-0.07645	-0.07712
6.4	0.05445	-0.22156	0.34995	0.10764	0.10864
6.6	0.23170	-0.05445	0.49844	0.37422	0.29176
6.8	0.39723	0.11485	0.63023	0.46032	0.46509
7.0	0.54707	0.28072	0.74089	0.69003	0.62177
7.2	0.67846	0.43759	0.82500	0.81052	0.75551
7.4	0.78917	0.58027	0.87632	0.89873	0.86085
7.6	0.87687	0.70394	0.88888	0.95061	0.93330
7.8	0.93868	0.80457	0.85847	0.96357	0.96962
8.0	0.97109	0.87877	0.78419	0.93647	0.96786

Table 8. Comparison of Results for F_2 Showing the Effects of the Correction Variable (K) - ($F_1 = 0, F_1' = 1, F_2 = 0, F_2' = 0, G_1 = 0, G_1' = 0, G_2 = 0, G_2' = 0$) - Unstable Cases ($n = 70$) - Standing Waves

	$i = 1$ $K = 1$		$i = 1$ $K = 0$		$i = 0$ $K = 0$
t	Exact Solution	Perturbation Solution	Exact Solution	Perturbation Solution	Analytic Solution
0.2	0.00013	-0.00527	0.00017	-0.00562	-0.00336
0.4	0.00120	-0.01466	0.00165	-0.01557	-0.01219
0.6	0.00456	-0.02534	0.00619	-0.02603	-0.02343
0.8	0.01160	-0.03411	0.01544	-0.03276	-0.03305
1.0	0.02332	-0.03789	0.03024	-0.03218	-0.03709
1.2	0.03992	-0.03451	0.05013	-0.02232	-0.03264
1.4	0.06057	-0.02299	0.07306	-0.01862	-0.01865
1.6	0.08330	-0.00396	0.09555	0.021911	0.00367
1.8	0.10517	0.02047	0.11324	0.04915	0.03093
2.0	0.12271	0.04692	0.12170	0.07264	0.05810
2.2	0.13242	0.07126	0.11751	0.08675	0.07947
2.4	0.13150	0.08922	0.09917	-0.087046	0.08978
2.6	0.11839	0.097153	0.06770	0.071414	0.08535
2.8	0.09328	0.11651	0.02679	0.04063	0.06502
3.0	0.05822	0.07467	-0.01761	-0.001408	0.03053
3.2	0.01701	0.04468	-0.05827	-0.04828	-0.01346
3.4	-0.02528	0.00567	-0.08789	-0.09196	-0.06005
3.6	-0.06295	-0.03775	-0.10041	-0.12426	-0.10122
3.8	-0.09049	-0.07994	-0.09221	-0.13827	-0.12919
4.0	-0.10337	-0.11504	-0.06290	-0.12986	-0.13785
4.2	-0.09872	-0.13779	-0.01566	-0.09854	-0.12403
4.4	-0.07590	-0.1442	0.04299	-0.04785	-0.08825
4.6	-0.03665	-0.13261	0.10404	0.01493	-0.03490
4.8	0.01487	-0.1032	0.15731	0.07988	-0.02828
5.0	0.07254	-0.05894	0.19315	0.13602	0.09131
5.2	0.12595	-0.00478	0.20424	0.17311	0.14357
5.4	0.17637	0.05266	0.18706	0.183575	0.17558
5.6	0.20783	0.10617	0.14284	0.163922	0.18070
5.8	0.21824	0.14862	0.07764	0.11562	0.15640
6.0	0.20519	0.17409	0.00147	0.04509	0.10495
6.2	0.16949	0.17865	-0.0733	-0.03703	0.03331
6.4	0.11514	0.16089	-0.13397	-0.11757	-0.04784
6.6	0.04883	0.12229	-0.16972	-0.182899	-0.12564
6.8	-0.02090	0.06705	-0.17346	-0.22122	-0.18709
7.0	-0.08483	0.00165	-0.14308	-0.22468	-0.22125
7.2	-0.13429	-0.06594	-0.08205	-0.19089	-0.22111
7.4	-0.16228	-0.12723	0.00095	-0.12367	-0.18495
7.6	-0.16442	-0.17433	0.09312	-0.03255	-0.11630
7.8	-0.13960	-0.20087	0.17949	0.06839	-0.02652
8.0	-0.09020	-0.21857	0.24522	0.16275	0.07753

Table 9. Comparison of Stability Boundaries Based on the Interaction Index (n) - ($F_1 = 0, F_1' = 1, F_2 = 0, F_2' = 0, G_1 = 0, G_1' = 0, G_2 = 0, G_2' = 0$) - Standing Waves - Epsilon - 0.1

Gas Dynamic Index Correction Variable	Stability Boundaries	
	Exact Solution n - Stable - Unstable	Perturbation Solution n - Stable - Unstable
i = 1 K = 1	67.5 - 69	67.5 - 69
i = 0 K = 1	72 - 72.5	72.5 - 73
i = 1 K = 0	45 - 50	45 - 50

Table 10. Comparison of Stability Boundaries Based on the Interaction Index (n) - ($F_1 = 0, F_1' = -1, F_2 = 0, F_2' = 0, G_1 = 1, G_1' = 0, G_2 = 0, G_2' = 0$) - Traveling Waves - Epsilon - 0.1

Gas Dynamic Index Correction Variable	Stability Boundaries	
	Exact Solution n - Stable - Unstable	Perturbation Solution n - Stable - Unstable
i = 1 K = 1	27.5 - 28	31.5 - 32
i = 0 K = 1	30 - 31	36.35 - 36.5
i = 1 K = 0	25 - 30	25-30

approximate analytical stability equations (4.31) and (4.52). The perturbation method tends to predict slightly higher stability limits than the exact solution method for both standing and traveling waves. Within the accuracy of the tabulated values, this is apparent only in the first two rows of Table 10.

In Table 11, a comparison of the effect of different initial conditions imposed on the stability boundaries for both standing and traveling waves is presented. From the results of two sets of initial conditions for each case, it can be seen that the varying of initial conditions has no significant effect on the stability boundaries for both standing waves or traveling waves.

In Table 12, the variation of the stability limit with ϵ is presented for standing waves. From Table 12, the results show that the smaller the term epsilon the greater the stability limit. Therefore, the order term has a significant effect on the interaction index. In Chapter 4, a relation was proposed for the case of $i = 0$ and $K = 0$ which was $n = C/\epsilon$ where C is a constant. Assuming the validity of the relation, the values for this constant are given for each given epsilon and interaction index. This shows that, in general, C is a weak function of ϵ .

In Table 13, a comparison of the effect of ϵ is presented for traveling waves when both gas dynamic nonlinearities and correction variables are considered. Again, the results show that the smaller the term epsilon, the greater the stability limit. The perturbation method again predicts slightly greater stability limits than does the exact solution method. Therefore, again, the order term has a strong effect concerning the stability of combustion.

Table 11. Comparison of the Effect of Different Initial Conditions Imposed for Standing and Traveling Waves for $i = 1$ and $K = 1$
Epsilon = 0.1

- (a) Standing Waves - 1. $F_1 = 0, F_1' = 1, F_2 = 0, F_2' = 0$
 $G_1 = 0, G_1' = 0, G_2 = 0, G_2' = 0$
2. $F_1 = 1, F_1' = 0, F_2 = 0, F_2' = 0$
 $G_1 = 0, G_1' = 0, G_2 = 0, G_2' = 0$

Initial Condition Sets	Stability Boundaries	
	Exact Solution n - Stable - Unstable	Perturbation Solution n - Stable - Unstable
1.	67.5 - 69	67.5 - 69
2.	65 - 70	65 - 70

- (b) Traveling Waves - 1. $F_1 = 0, F_1' = -1, F_2 = 0, F_2' = 0$
 $G_1 = 1, G_1' = 0, G_2 = 0, G_2' = 0$
2. $F_1 = 1, F_1' = 0, F_2 = 0, F_2' = 0$
 $G_1 = 0, G_1' = -1, G_2 = 0, G_2' = 0$

Initial Condition Sets	Stability Boundaries	
	Exact Solution n - Stable - Unstable	Perturbation Solution n - Stable - Unstable
1.	27.5 - 28	31.5 - 32
2.	27.5 - 28.5	31 - 31.5

Table 12. Comparison of the Effects of the Order Term Epsilon -
 ($F_1 = 0, F_1' = 1, F_2 = 0, F_2' = 0, G_1 = 0, G_1' = 0, G_2 = 0,$
 $G_2' = 0$) - Standing Waves - when $i = 1, K = 1$

Epsilon	Stability Boundaries		Constant $C = n\epsilon$
	Exact Solution n - Stable - Unstable	Perturbation Solution n - Stable - Unstable	
0.05	107.5 - 110	107.5 - 110	5.5
0.1	67.5 - 69	67.5 - 69	6.9
0.2	48.5 - 49.5	48.5 - 49.5	9.8

Table 13. Comparison of the Effects of the Order Term Epsilon ($F_1 = 0, F_1' = -1, F_2 = 0, F_2' = 0, G_1 = 1, G_1' = 0, G_2 = 0, G_2' = 0$) Traveling Waves - when $i = 1, K = 1$

Epsilon	Stability Boundaries			
	Exact Solution n - Stable - Unstable	Perturbation Solution n - Stable - Unstable	Constant C = nε (Exact Solution)	Constant C = nε (Perturbation Sol)
0.05	51 - 52	52 - 53	2.575	2.625
0.1	27.5 - 28	31.5 - 32	2.775	3.175
0.2	15.5 - 16	18.5 - 19.5	3.15	3.75

Thus, from these representative tables of results, it is observed that the correction variable is important in the stability of standing waves, but does not play a major role in the stability of traveling waves. It is observed that the gas dynamic nonlinearities seem to have little influence on the stability of either standing or traveling waves. It is observed that initial conditions of the modal amplitudes have little or no influence in the stability of either standing or traveling waves. And finally, it is observed that the order term epsilon and the interaction index governing the strength of combustion in the process are strongly coupled thus affecting the limits of stability.

Before completing this chapter, it is desired to investigate the sign discrepancy mentioned previously between the exact and perturbation solutions for f which occur near $t = 0$. For simplicity, it will be assumed that $i = K = 0$ and that for $t \ll 1$ the first modal amplitude can be represented with sufficient accuracy by $f_1 = \sin t$. Then, the equation for f_2 will be solved and the result simplified for $t \ll 1$. This will be done first for $\bar{\omega} = 0$ and then for $\bar{\omega} \neq 0$. For $\bar{\omega} = 0$, (3.21) leads to

$$\frac{d^2 f_2}{dt^2} + 4f_2 = \frac{1}{4} \epsilon \bar{\omega} n [1 - \cos 2t] \quad (5.1)$$

with initial conditions

$$f_2(0) = 0$$

$$f_2'(0) = 0.$$

Evaluating the homogeneous and particular solutions by the usual manner and evaluating the constants, the results become

$$f_2 = \frac{1}{16} \epsilon \bar{\omega} \bar{\eta} \left[1 - \cos 2t - t \sin 2t \right]. \quad (5.2)$$

In terms of the perturbation parameters (4.1), equation (5.2) can be written as

$$f_2 = \frac{1}{16} \bar{\omega} \bar{\eta} \left[\epsilon (1 - \cos 2\xi) - \eta \sin 2\xi \right]. \quad (5.3)$$

To the order of approximation ϵ which the perturbation solution should model, equation (5.3) becomes

$$f_2 = -\frac{1}{16} \bar{\omega} \bar{\eta} \eta \sin 2\xi + O(\epsilon). \quad (5.4)$$

By expanding equation (5.2) into a Taylor series expansion of three terms, equation (5.2) becomes

$$f_2 = \frac{1}{24} \epsilon \bar{\omega} \bar{\eta} t^4 + \dots \quad (5.5)$$

which is always positive.

Therefore, the exact method for small time will yield f_2 modal amplitude always as a positive quantity.

By imposing identical conditions to the perturbation equations (4.12), the result becomes

$$\frac{dB_2}{d\eta} = -\frac{1}{16} \bar{\omega} n \quad (5.6)$$

with the condition

$$B_2(0) = 0.$$

Solving equation (5.6),

$$B_2 = -\frac{1}{16} \bar{\omega} n \eta. \quad (5.7)$$

Recalling that $f_2 = B_2 \sin 2\xi$, the result becomes

$$f_2 = -\frac{1}{16} \bar{\omega} n \eta \sin 2\xi + O(\epsilon) \quad (5.8)$$

which is identical to the result of equation (5.4) for the wave equation solution. Thus, the perturbation method gives the correct result. It can be seen that for $t \ll 1$ the exact solution predicts a positive f_2 and by inspection of equation (5.8), the perturbation method predicts a negative f_2 . This is precisely the behavior observed in the numerical solutions.

For $\bar{\omega} \neq 0$, a similar analysis can be performed. The appropriate equation for f_2 is now

$$\frac{d^2 f_2}{dt^2} + \bar{\omega} \frac{df_2}{dt} + 4f_2 = \frac{1}{4} \epsilon \bar{\omega} n [1 - \cos 2t] \quad (5.9)$$

with conditions

$$f_2(0) = 0$$

$$f_2'(0) = 0.$$

Solving the homogeneous and particular solution by the usual manner and evaluating the appropriate constants the result becomes

$$f_2 = e^{-\bar{\omega}/2t} \left[-\frac{1}{16} \epsilon \bar{\omega} n \cos \left(\frac{\sqrt{16 - \bar{\omega}^2}}{2} t \right) + \frac{\epsilon n}{16} \left[\frac{8 - \bar{\omega}^2}{\sqrt{16 - \bar{\omega}^2}} \right] \sin \frac{\sqrt{16 - \bar{\omega}^2}}{2} t + \frac{1}{16} \epsilon \bar{\omega} n - \frac{1}{8} \epsilon n \sin 2t \right]. \quad (5.10)$$

Expanding (5.10) for small $\bar{\omega}$ into the appropriate Taylor series, expanding and neglecting terms of $O(\bar{\omega})$ leads to

$$f_2 = \frac{1}{16} \epsilon \bar{\omega} n \left[1 - \cos 2t - t \sin 2t \right] \quad (5.11)$$

which is identical to (5.2).

By imposing the identical conditions on the perturbation equation (4.12), the resulting equation become

$$\frac{dB}{d\eta} + \frac{1}{2} \bar{\sigma} B_2 = -\frac{1}{16} \bar{\omega} n \quad (5.12)$$

with the condition

$$B_2(0) = 0.$$

Solving equation (5.12) by the usual manner, evaluating the constants, and transforming the perturbation variables to real time variables

$$f_2 = -\frac{n\epsilon}{8} \left[1 - e^{-\frac{1}{2}\bar{\omega}t} \right] \sin 2t. \quad (5.13)$$

This is always negative for $t \ll 1$. Expanding the exponential function by the Taylor series expansion and neglect terms of $o(\bar{\omega})$ leads to

$$f_2 = -\frac{n\bar{\omega}}{16} \eta \sin 2\xi + o(\epsilon) \quad (5.14)$$

which is identical to (5.8).

To observe the behavior of equation (5.10) for small time, expand this equation into a Taylor series of $o(t^4)$. Expanding and grouping terms according to their order of magnitude, the terms of $o(1)$, $o(t)$, $o(t^2)$, $o(t^3)$ vanish. Therefore, f_2 is comprised of terms from $o(t^4)$ which is

$$f_2 = \frac{\epsilon n \bar{\omega} t^4}{24} \left[1 + \frac{3\bar{\omega}^2}{8} + \frac{\bar{\omega}^4}{64} \right]. \quad (5.15)$$

Again, for any small time t , f_2 is always positive since t^4 is always positive. Neglecting higher powers of $\bar{\omega}$, the resulting equation becomes equation (5.5) for the undamped case. Again it can be seen that the exact and perturbation methods predict opposite signs for f_2 when $t \ll 1$. These results are based on approximations and cannot be considered

definitive. They do, however, lend plausibility to the numerical results discussed earlier. It is believed that this sign discrepancy is due to the inability of the perturbation solution to accurately represent the exact solution for $t \ll 1$ and not due to any error in the computer program used to compute the perturbation solution.

Chapter 6

CONCLUSION AND RECOMMENDATIONS

The primary objective of this presentation has been the development of analytical techniques to solve the problem of combustion instabilities occurring in an annular combustion chamber. The analytical techniques used were the modified Galerkin method applied to the acoustic wave equations which yielded a set of time-dependent modal amplitude equations and the two-variable perturbation method which yield a set of time-dependent equations which approximated the behavior of the first set of equations. Both methods produced results which were relatively easy to apply and used the Runge-Kutta algorithm which required little computation time. An alternative approach to solve this problem would be a finite difference approach. However, difficulties can be foreseen in the development of the finite difference equations modelling the problem along with the complications occurring due to the boundary conditions of the problem. Thus, the benefits of the methods discussed in this thesis can be appreciated.

From the numerical and graphical presentation of results in Chapter 5, the following observations can be made. First, the effect of the gas-dynamic nonlinearities seems to be small in both methods of analysis for velocity sensitive combustion. This point can be observed from a quantitative comparison of the tabular results or by observing the effects of this condition on the stability boundaries. Second, the effect of the

correction variable modelling the physical boundaries of the chamber seems to have a significant effect in both methods of analysis for velocity sensitive combustion. By including the effect of this correction variable, a significant increase occurs in the interaction index which is the criteria for the stability of the system. However, this effect seems to be more significant for the standing wave case than the traveling wave cases. The effects of initial conditions for the time dependent equations, the numerical value for the burning rate and step size of integration, seem to have very little significance in the measure of the stability limits of velocity sensitive combustion. However, the order term ϵ has a strong effect upon the stability of the problem. This is to be expected since the order term is the measure of the effect of nonlinearities occurring in the system. The increase in this value corresponds to a decrease in the stability limit which is physically reasonable.

In this study, the effect of time delay of the combustion process was neglected. However, time delay has been found in other studies to be an important phenomena in correctly modelling the actual problems of velocity sensitive combustion. It is recommended that this effect can be incorporated by including the corresponding terms with $j = 1$ in the acoustic wave equations (3.20). A corresponding set of perturbations can then be derived to account for time delay and both these equations and equations (3.20) can be numerically evaluated by modifying the existing Runge-Kutta programs presented in the Appendices. It is also recommended that an experimental program be developed to measure the effects of velocity sensitive combustion in an annular combustion chamber. Once achieving this goal, one could correlate the measurement results to the analytical results that have been presented to ascertain the validity of this analysis.

Since instability of combustion is sensitive to small changes in engine geometry and operating conditions, a particular engine must be subjected to a large number of firings before its designers can say confidently that it is free from instability. With a large engine such testing can account for a substantial part of development costs. Herein lies the importance of devising reliable theories of instability and inexpensive tests of a propellant's acoustical characteristics. Until instability of combustion is understood well enough so that it can be eliminated while an engine is in the design stage, rocket engines must continue to be intensively tested for stability--particularly when the lives of astronauts will eventually depend on safe, reliable operation of the engine [17].

REFERENCES

REFERENCES

1. Crocco, L., and Cheng, S. I., Theory of Combustion Instability in Liquid Propellant Rocket Motors, AGARD Monograph No. 8, Butterworths Scientific Pub., Ltd., London, 1956.
2. Scala, S. M., "Transverse Wave and Entropy Wave Combustion Instability in Liquid Propellant Rockets," Princeton University Aeronautical Engineering Report No. 380, April 1959, (Ph.D. Thesis).
3. Reardon, F. H., "An Investigation of Transverse Mode Combustion Instability in Liquid Propellant Rocket Motors," Princeton University Aeronautical Engineering Report No. 550, June 1961, (Ph.D. Thesis).
4. Culick, F. E. C., "Stability of High Frequency Pressure Oscillations in Gas and Liquid Rocket Combustion Chambers," M. I. T. Aerophysics Laboratory Report No. 480, June 1961.
5. Zinn, B. T., "A Theoretical Study of Nonlinear Transverse Combustion Instability in Liquid Propellant Rocket Motors," Princeton University AMS Technical Report No. 732, May 1966, (Ph.D. Thesis).
6. Maslen, S. H., and Moore, F. K., "On Strong Transverse Waves Without Shocks in a Circular Cylinder," Journal of Aeronautical Sciences, Vol. 23, No. 6, 1956, pp. 583-593.
7. Priem, R. J., and Guentert, D. C., "Combustion Instability Limits Determined by a Nonlinear Theory and a One-Dimensional Model," NASA TN D-1409, October 1962.
8. Sirignano, W. A., "A Theoretical Study of Nonlinear Combustion Instability: Longitudinal Mode," Princeton University AMS Technical Report No. 677, March 1964, (Ph.D. Thesis).
9. Mitchell, C. E., "Axial Mode Shock Wave Combustion Instability in Liquid Propellant Rocket Engines," Princeton University AMS Technical Report No. 798, (NASA CR 72259), July 1967, (Ph.D. Thesis).
10. Burnstein, S. Z., and Chinitz, W. "Nonlinear Combustion Instability in Liquid Propellant Rocket Motors," Jet Propulsion Laboratory Quarterly Reports prepared under Contract 951946.
11. Powell, E., "Nonlinear Combustion Instability in Liquid Propellant Rocket Engines," Georgia Institute of Technology, September 1970, (Ph.D. Thesis).

12. Morse, P. M., and Ingard, K. U., Theoretical Acoustics, McGraw Hill Book Company, New York, 1968.
13. Kinsler, L. E., and Frey, A. R., Fundamentals of Acoustics, John Wiley and Sons, Inc., New York, 1962.
14. Nayfeh, A. H., Perturbation Methods, Pure and Applied Mathematics, A Wiley-Interscience Series of Texts, Monographs and Tracts, 1972.
15. Conte, S. D., and deBoor, C., Elementary Numerical Analysis, an Algorithmic Approach, McGraw Hill Book Company, New York, 1972.
16. Hornbeck, R. W., Numerical Methods, Quantum Publishers, Inc., New York, 1975.
17. Sotter, J. G., and Flandro, G. A., "Resonant Combustion in Rockets," Scientific American, December 1968, pp. 95-103.

APPENDICES

APPENDIX A

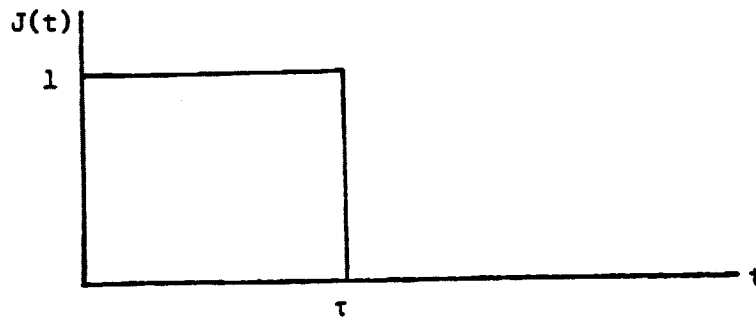
GENERAL TIME DELAY FUNCTION

GENERAL TIME DELAY FUNCTION

The development and nature of the time-delay function is of the same form of the convolution integral for impulse response in vibration theory. The general form of the time delay function is

$$\omega(t) = \int_0^t J(t - \xi) \frac{d\omega_0}{d\xi} d\xi . \quad (\text{A.1})$$

A simple illustration of the time delay function is in the case of a finite step function $J(t)$.



(some specific time constant)

Figure A1. Step Function $J(t)$

From the figure, the step function $J(t)$ is defined as

$$J(t) = \begin{cases} 1 & t < \tau \\ 0 & t > \tau \end{cases} . \quad (\text{A.2})$$

Therefore, substituting some time delay $(t - \xi)$ for time t , the result is

$$J(t - \xi) = \begin{cases} 1 & t - \xi < \tau \\ 0 & t - \xi > \tau \end{cases}$$

or

$$J(t - \xi) = \begin{cases} 1 & t - \tau < \xi \\ 0 & t - \tau > \tau \end{cases} \quad (\text{A.3})$$

Graphically representing equation (A.2) results in Figure A2.

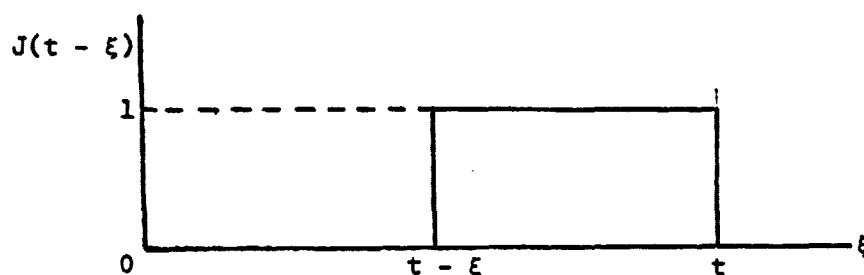


Figure A2. Step Time Delay Function $J(t - \xi)$

Substituting into the general time-delay integral the particular step function in terms of the non-dimensional variable ξ

$$\omega(t) = \int_0^{t - \tau} 0 \frac{d\omega_0}{d\xi} d\xi + \int_{t - \tau}^t 1 \frac{d\omega_0}{d\xi} d\xi \quad (\text{A.4})$$

Therefore, simplifying equation (A.3)

$$\omega(t) = \omega_0(t) - \omega_0(t - \tau) \quad (\text{A.5})$$

where $\omega_0(t)$ is a generalized function of time and $\omega_0(t - \tau)$ is functional time delay.

APPENDIX B

RUNGE-KUTTA PROGRAM OF THE MODAL
AMPLITUDE WAVE EQUATIONS


```

30 FORMAT (1X, 'INITIAL CONDITIONS', //, 1X, 4X, 'F1', F10.4, /
1, 1X, 4X, 'DF1/DT', F10.4, //, 1X, 4X, 'F2', F10.4, //, 1X, 4X, 'DF2
2/DT', F10.4, //, 1X, 4X, 'G1', F10.4, //, 1X, 4X, 'DG1/DT', F10.4, /
3, 1X, 4X, 'G2', F10.4, //, 1X, 4X, 'DG2/DT', F10.4, //)
WRITE (6, 40)
40 FORMAT (1X, 3X, 'TIME', 9X, 'F1', 10X, 'F2', 10X, 'G1', 9X, 'G2',
1, 15X, 'ACP1', 10X, 'ACP2', 9X, 'ACP3', 9X, 'ACP4', //)

```

C
C
C

RUNGE-KUTTA ALGORITHM

DC 100 J = 1, NMAX

C

```

P1=H*E1(T, F1, F2, G1, G2, F1P, F2P, G1P, G2P)
Q1=H*E2(T, F1, F2, G1, G2, F1P, F2P, G1P, G2P)
R1=H*E3(T, F1, F2, G1, G2, F1P, F2P, G1P, G2P)
S1=H*E4(T, F1, F2, G1, G2, F1P, F2P, G1P, G2P)
T1=H*E5(T, F1, F2, G1, G2, F1P, F2P, G1P, G2P)
U1=H*E6(T, F1, F2, G1, G2, F1P, F2P, G1P, G2P)
V1=H*E7(T, F1, F2, G1, G2, F1P, F2P, G1P, G2P)
W1=H*E8(T, F1, F2, G1, G2, F1P, F2P, G1P, G2P)

```

C

```

P2=H*E1(T+H/2, F1+P1/2, F2+Q1/2, G1+R1/2, G2+S1/2, F1P
1+T1/2, F2P+U1/2, G1P+V1/2, G2P+W1/2)
Q2=H*E2(T+H/2, F1+P1/2, F2+Q1/2, G1+R1/2, G2+S1/2, F1P
1+T1/2, F2P+U1/2, G1P+V1/2, G2P+W1/2)
R2=H*E3(T+H/2, F1+P1/2, F2+Q1/2, G1+R1/2, G2+S1/2, F1P
1+T1/2, F2P+U1/2, G1P+V1/2, G2P+W1/2)
S2=H*E4(T+H/2, F1+P1/2, F2+Q1/2, G1+R1/2, G2+S1/2, F1P
1+T1/2, F2P+U1/2, G1P+V1/2, G2P+W1/2)
T2=H*E5(T+H/2, F1+P1/2, F2+Q1/2, G1+R1/2, G2+S1/2, F1P
1+T1/2, F2P+U1/2, G1P+V1/2, G2P+W1/2)
U2=H*E6(T+H/2, F1+P1/2, F2+Q1/2, G1+R1/2, G2+S1/2, F1P
1+T1/2, F2P+U1/2, G1P+V1/2, G2P+W1/2)
V2=H*E7(T+H/2, F1+P1/2, F2+Q1/2, G1+R1/2, G2+S1/2, F1P
1+T1/2, F2P+U1/2, G1P+V1/2, G2P+W1/2)
W2=H*E8(T+H/2, F1+P1/2, F2+Q1/2, G1+R1/2, G2+S1/2, F1P
1+T1/2, F2P+U1/2, G1P+V1/2, G2P+W1/2)

```

C

```

P3=H*E1(T+H/2, F1+P2/2, F2+Q2/2, G1+R2/2, G2+S2/2, F1P
1+T2/2, F2P+U2/2, G1P+V2/2, G2P+W2/2)
Q3=H*E2(T+H/2, F1+P2/2, F2+Q2/2, G1+R2/2, G2+S2/2, F1P
1+T2/2, F2P+U2/2, G1P+V2/2, G2P+W2/2)
R3=H*E3(T+H/2, F1+P2/2, F2+Q2/2, G1+R2/2, G2+S2/2, F1P
1+T2/2, F2P+U2/2, G1P+V2/2, G2P+W2/2)
S3=H*E4(T+H/2, F1+P2/2, F2+Q2/2, G1+R2/2, G2+S2/2, F1P
1+T2/2, F2P+U2/2, G1P+V2/2, G2P+W2/2)
T3=H*E5(T+H/2, F1+P2/2, F2+Q2/2, G1+R2/2, G2+S2/2, F1P
1+T2/2, F2P+U2/2, G1P+V2/2, G2P+W2/2)
U3=H*E6(T+H/2, F1+P2/2, F2+Q2/2, G1+R2/2, G2+S2/2, F1P
1+T2/2, F2P+U2/2, G1P+V2/2, G2P+W2/2)
V3=H*E7(T+H/2, F1+P2/2, F2+Q2/2, G1+R2/2, G2+S2/2, F1P

```

$1+T2/2., F2P+U2/2., G1P+V2/2., G2P+W2/2.)$
 $W3=H+E5(T+H/2., F1+P2/2., F2+Q2/2., G1+R2/2., G2+S2/2., F1P$
 $1+T2/2., F2P+U2/2., G1P+V2/2., G2P+W2/2.)$

C

$P4=H+E1(T+H, F1+P3, F2+Q3, G1+R3, G2+S3, F1P+T3, F2P+U3, G1P$
 $1+V3, G2P+W3)$
 $G4=H+E2(T+H, F1+P3, F2+Q3, G1+R3, G2+S3, F1P+T3, F2P+U3, G1P$
 $1+V3, G2P+W3)$
 $R4=H+E3(T+H, F1+P3, F2+Q3, G1+R3, G2+S3, F1P+T3, F2P+U3, G1P$
 $1+V3, G2P+W3)$
 $S4=H+E4(T+H, F1+P3, F2+Q3, G1+R3, G2+S3, F1P+T3, F2P+U3, G1P$
 $1+V3, G2P+W3)$
 $T4=H+E5(T+H, F1+P3, F2+Q3, G1+R3, G2+S3, F1P+T3, F2P+U3, G1P$
 $1+V3, G2P+W3)$
 $U4=H+E6(T+H, F1+P3, F2+Q3, G1+R3, G2+S3, F1P+T3, F2P+U3, G1P$
 $1+V3, G2P+W3)$
 $V4=H+E7(T+H, F1+P3, F2+Q3, G1+R3, G2+S3, F1P+T3, F2P+U3, G1P$
 $1+V3, G2P+W3)$
 $W4=H+E8(T+H, F1+P3, F2+Q3, G1+R3, G2+S3, F1P+T3, F2P+U3, G1P$
 $1+V3, G2P+W3)$

C

$F1=F1+((P1+2.*P2+2.*P3+P4)/6.)$
 $F2=F2+((Q1+2.*Q2+2.*Q3+Q4)/6.)$
 $G1=G1+((R1+2.*R2+2.*R3+R4)/6.)$
 $G2=G2+((S1+2.*S2+2.*S3+S4)/6.)$
 $F1P=F1P+((T1+2.*T2+2.*T3+T4)/6.)$
 $F2P=F2P+((U1+2.*U2+2.*U3+U4)/6.)$
 $G1P=G1P+((V1+2.*V2+2.*V3+V4)/6.)$
 $G2P=G2P+((W1+2.*W2+2.*W3+W4)/6.)$

C

$ACP1=-F1P+EPS*(-F1+F2-G1+G2+0.5*(G1P+G2P+F1P+F2P))$
 $ACP2=-F2P+EPS*(-0.25*(G1+G1-F1+F1)+0.25*(F1P+F1P-G1P$
 $1+G1P))$
 $ACP3=-G1P+EPS*(-F1+G2+F2+G1+0.5*(F1P+G2P-G1P+F2P))$
 $ACP4=-G2P+EPS*(0.5*F1+G1+0.5*(F1P+G1P))$

C

$T=T+H$
 $L=L+1$
 $IF (L .EQ. 3) GO TO 110$
 $GO TO 100$
 $110 WRITE (6,50) T, F1, F2, G1, G2, ACP1, ACP2, ACP3, ACP4$
 $50 FORMAT (1X, F3.4, 3X, F10.5, 2X, F10.5, 3X, F10.5, 2X, F10.5, 5X$
 $1, F10.5, 2X, F10.5, 3X, F10.5, 2X, F10.5)$
 $L=1$
 $100 CONTINUE$
 $CALL EXIT$
 END

APPENDIX C

**RUNGE-KUTTA PROGRAM OF THE
PERTURBATION EQUATIONS**

C GARY H COONALD NON-LINEAR COMBUSTION EQUATIONS DERIVED
 C FROM THE
 C TWO-VARIABLE PERTURBATION METHOD

C GOVERNING EQUATIONS-CASE - NO TIME DELAY (J=0)
 C

$$E1(T, A1, B1, A2, B2, A3, B3, A4, B4) = (-0.5 * SIG3 * A1 - 0.5 * K * B1 \\ 1 - 0.5 * I * (A1 * A3 + B1 * B3 + A2 * A4 + B2 * B4) - 0.5 * N * WBAR * (B1 * A3 - A1 \\ 2 * B3 + A2 * A4 - A2 * B4)) * EPS$$

$$E2(T, A1, B1, A2, B2, A3, B3, A4, B4) = (-0.5 * SIG3 * B1 + 0.5 * K * A1 \\ 1 - 0.5 * I * (A1 * B3 + A3 * A4 + B2 * A2 + B4) - 0.5 * N * WBAR * (A1 * A3 + B1 \\ 2 * B3 + A2 * A4 + B2 * B4)) * EPS$$

$$E3(T, A1, B1, A2, B2, A3, B3, A4, B4) = (-0.5 * SIG3 * A2 - 0.5 * K * B2 \\ 1 - 0.5 * I * (A1 * A4 + B1 * B4 - A2 * A3 - B2 * B3) - 0.5 * N * WBAR * (A4 * B1 - A1 \\ 2 * B4 + A2 * B3 - A3 * B2)) * EPS$$

$$E4(T, A1, B1, A2, B2, A3, B3, A4, B4) = (-0.5 * SIG3 * B2 + 0.5 * K * A2 \\ 1 - 0.5 * I * (A4 * A1 + B1 * A3 + B2 * A2 + B3) - 0.5 * N * WBAR * (A1 * A4 + B1 \\ 2 * B4 - A2 * A3 - B2 * B3)) * EPS$$

$$E5(T, A1, B1, A2, B2, A3, B3, A4, B4) = (-0.5 * SIG3 * A3 - 4. * K * B3 \\ 1 - 0.125 * I * (A2 * A2 - B2 * B2 + B1 * B1 - A1 * A1 - 0.125 * WBAR * N * (A1 * B1 \\ 2 - A2 * B2)) * EPS$$

$$E6(T, A1, B1, A2, B2, A3, B3, A4, B4) = (-0.5 * SIG3 * B3 + 4. * K * A3 \\ 1 - 0.25 * I * (A2 * B2 + A1 * B1) - 0.0625 * WBAR * N * (A2 * A2 - B2 * B2 - A1 * A1 \\ 2 + B1 * B1)) * EPS$$

$$E7(T, A1, B1, A2, B2, A3, B3, A4, B4) = (-0.5 * SIG3 * A4 - 4. * K * B4 \\ 1 - 0.25 * I * (A1 * B2 + A1 * A2) - 0.125 * WBAR * N * (A1 * B2 + A2 * B1)) * EPS$$

$$E8(T, A1, B1, A2, B2, A3, B3, A4, B4) = (-0.5 * SIG3 * B4 + 4. * K * A4 \\ 1 - 0.25 * I * (B2 * A1 + A2 * B1) + 0.125 * WBAR * N * (A1 * A2 - B1 * B2)) * EPS$$

C
 C DIMENSION F1(500), F2(500), G1(500), G2(500)
 C REAL K, N, I
 C L=1
 C T=0.

C
 C READ INITIAL CONDITIONS AND CONSTANTS

C
 C EPS=ORDER TERM (EPSILON)
 C WBAR=STEADY STATE BURNING RATE
 C N=INTERACTION INDEX
 C K=CORRECTION VARIABLE (BAFFLES, WALL LININGS, NOZZLES
 C ,ETC.)
 C I=GAS DYNAMIC INDEX
 C A1, B1, A2, B2, A3, B3, A4, B4=MODAL AMPLITUDES COEFFICIENTS

C
 C READ (5,1) WBAR, N, K, NMAX, EPS, I
 C 10 FORMAT (3F10.4, I3, 2F10.4)
 C READ (5,1) A1, B1, A2, B2, A3, B3, A4, B4
 C 12 FORMAT (9F10.4)

C
 C READ STEP SIZE

REPRODUCIBILITY OF THE
 ORIGINAL PAGE IS POOR

```

READ (5,16) H
14 FORMAT (F10.5)
   SIGD=HBAR/EPS
   WRITE (6,20) SIGD,HBAR,N,K,H,EPS,I
20 FORMAT (1X,4X,'SIGMA BAR',F10.4,'/1X,4X,'STEADY STATE
1 3LIVING RATE=(HBAR)',F10.4,'/1X,4X,'INTERACTION INDEX
2-(N)',F10.4,'/1X,4X,'CORRECTION VARIABLE-(K)',F10.4,'/
3,1X,4X,'STEP SIZE-(H)',F10.4,'/1X,4X,'EPSILON-(EPS)',
4,F10.4,'/1X,4X,'GAS DYNAMIC INDEX-(I)',F10.4,'//)
   WRITE (6,30) A1,B1,A2,B2,A3,B3,A4,B4
30 FORMAT (1X,'INITIAL CONDITIONS',//,1X,4X,'A1',F10.4,3X
1,'B1',F10.4,'/1X,4X,'A2',F10.4,3X,'B2',F10.4,'/1X,4X
2,'A3',F10.4,3X,'B3',F10.4,'/1X,4X,'A4',F10.4,3X,'B4'
3,F10.4,'//)
   WRITE (6,40)
40 FORMAT (1X,7X,'TIME',7X,'A1',7X,'B1',12X,'A2',11X,'B2'
1,11X,'A3',11X,'B3',10X,'A4',10X,'B4',/)

```

C
C
C

RUNGE KUTTA ALGORITHM

C

```

DO 100 J = 1,NMAX

```

```

P1=H*E1(T,A1,B1,A2,B2,A3,B3,A4,B4)
Q1=H*E2(T,A1,B1,A2,B2,A3,B3,A4,B4)
R1=H*E3(T,A1,B1,A2,B2,A3,B3,A4,B4)
S1=H*E4(T,A1,B1,A2,B2,A3,B3,A4,B4)
T1=H*E5(T,A1,B1,A2,B2,A3,B3,A4,B4)
U1=H*E5(T,A1,B1,A2,B2,A3,B3,A4,B4)
V1=H*E7(T,A1,B1,A2,B2,A3,B3,A4,B4)
W1=H*E8(T,A1,B1,A2,B2,A3,B3,A4,B4)

```

C

```

P2=H*E1(T,H/2.,A1+P1/2.,B1+Q1/2.,A2+R1/2.,B2+S1/2.,A3
1+T1/2.,B3+U1/2.,A4+V1/2.,B4+W1/2.)
Q2=H*E2(T,H/2.,A1+P1/2.,B1+Q1/2.,A2+R1/2.,B2+S1/2.,A3
1+T1/2.,B3+U1/2.,A4+V1/2.,B4+W1/2.)
R2=H*E3(T,H/2.,A1+P1/2.,B1+Q1/2.,A2+R1/2.,B2+S1/2.,A3
1+T1/2.,B3+U1/2.,A4+V1/2.,B4+W1/2.)
S2=H*E4(T,H/2.,A1+P1/2.,B1+Q1/2.,A2+R1/2.,B2+S1/2.,A3
1+T1/2.,B3+U1/2.,A4+V1/2.,B4+W1/2.)
T2=H*E5(T,H/2.,A1+P1/2.,B1+Q1/2.,A2+R1/2.,B2+S1/2.,A3
1+T1/2.,B3+U1/2.,A4+V1/2.,B4+W1/2.)
U2=H*E5(T,H/2.,A1+P1/2.,B1+Q1/2.,A2+R1/2.,B2+S1/2.,A3
1+T1/2.,B3+U1/2.,A4+V1/2.,B4+W1/2.)
V2=H*E7(T,H/2.,A1+P1/2.,B1+Q1/2.,A2+R1/2.,B2+S1/2.,A3
1+T1/2.,B3+U1/2.,A4+V1/2.,B4+W1/2.)
W2=H*E8(T,H/2.,A1+P1/2.,B1+Q1/2.,A2+R1/2.,B2+S1/2.,A3
1+T1/2.,B3+U1/2.,A4+V1/2.,B4+W1/2.)

```

C

```

P3=H*E1(T,H/2.,A1+P2/2.,B1+Q2/2.,A2+R2/2.,B2+S2/2.,A3
1+T2/2.,B3+U2/2.,A4+V2/2.,B4+W2/2.)
Q3=H*E2(T,H/2.,A1+P2/2.,B1+Q2/2.,A2+R2/2.,B2+S2/2.,A3

```

1+T2/2.,.33+U2/2.,.A4+V2/2.,.B4+W2/2.)
 43=H+E3(T+H/2.,.A1+P2/2.,.B1+Q2/2.,.A2+R2/2.,.B2+S2/2.,.A3
 1+T2/2.,.33+U2/2.,.A4+V2/2.,.B4+W2/2.)
 53=H+E4(T+H/2.,.A1+P2/2.,.B1+Q2/2.,.A2+R2/2.,.B2+S2/2.,.A3
 1+T2/2.,.33+U2/2.,.A4+V2/2.,.B4+W2/2.)
 T3=H+E5(T+H/2.,.A1+P2/2.,.B1+Q2/2.,.A2+R2/2.,.B2+S2/2.,.A3
 1+T2/2.,.33+U2/2.,.A4+V2/2.,.B4+W2/2.)
 U3=H+E6(T+H/2.,.A1+P2/2.,.B1+Q2/2.,.A2+R2/2.,.B2+S2/2.,.A3
 1+T2/2.,.33+U2/2.,.A4+V2/2.,.B4+W2/2.)
 V3=H+E7(T+H/2.,.A1+P2/2.,.B1+Q2/2.,.A2+R2/2.,.B2+S2/2.,.A3
 1+T2/2.,.33+U2/2.,.A4+V2/2.,.B4+W2/2.)
 W3=H+E8(T+H/2.,.A1+P2/2.,.B1+Q2/2.,.A2+R2/2.,.B2+S2/2.,.A3
 1+T2/2.,.33+U2/2.,.A4+V2/2.,.B4+W2/2.)

C

P4=H+E1(T+H, A1+P3, B1+Q3, A2+R3, B2+S3, A3+T3, B3+U3, A4+V3
 1+B4+W3)
 Q4=H+E2(T+H, A1+P3, B1+Q3, A2+R3, B2+S3, A3+T3, B3+U3, A4+V3
 1+B4+W3)
 R4=H+E3(T+H, A1+P3, B1+Q3, A2+R3, B2+S3, A3+T3, B3+U3, A4+V3
 1+B4+W3)
 S4=H+E4(T+H, A1+P3, B1+Q3, A2+R3, B2+S3, A3+T3, B3+U3, A4+V3
 1+B4+W3)
 T4=H+E5(T+H, A1+P3, B1+Q3, A2+R3, B2+S3, A3+T3, B3+U3, A4+V3
 1+B4+W3)
 U4=H+E6(T+H, A1+P3, B1+Q3, A2+R3, B2+S3, A3+T3, B3+U3, A4+V3
 1+B4+W3)
 V4=H+E7(T+H, A1+P3, B1+Q3, A2+R3, B2+S3, A3+T3, B3+U3, A4+V3
 1+B4+W3)
 W4=H+E8(T+H, A1+P3, B1+Q3, A2+R3, B2+S3, A3+T3, B3+U3, A4+V3
 1+B4+W3)

C

A1=A1+((P1+2.,.Q2+2.,.P3+P4)/6.)
 B1=B1+((Q1+2.,.Q2+2.,.Q3+Q4)/6.)
 A2=A2+((P1+2.,.Q2+2.,.P3+P4)/6.)
 B2=B2+((Q1+2.,.Q2+2.,.Q3+Q4)/6.)
 A3=A3+((T1+2.,.T2+2.,.T3+T4)/6.)
 B3=B3+((U1+2.,.U2+2.,.U3+U4)/6.)
 A4=A4+((V1+2.,.V2+2.,.V3+V4)/6.)
 B4=B4+((W1+2.,.W2+2.,.W3+W4)/6.)

C

T=T+4

C

F1(J)=A1+COS(T)+B1+SIN(T)
 G1(J)=A2+COS(T)+B2+SIN(T)
 F2(J)=A3+COS(2.*T)+B3+SIN(2.*T)
 G2(J)=A4+COS(2.*T)+B4+SIN(2.*T)

C

L=L+1

IF (L .EQ. 3) GO TO 110

GO TO 100

110 WRITE (6,50) T, A1, B1, A2, B2, A3, B3, A4, B4

```
50 FORMAT (1X,F8.4,3X,F10.5,2X,F10.5,3X,F10.5,2X,F10.5,3X  
1,F10.5,2X,F10.5,3X,F10.5,2X,F10.5)
```

```
L=1
```

```
100 CONTINUE
```

```
L=L+1
```

```
T=0
```

```
WRITE (6,41)
```

```
41 FORMAT (1X,///,1X,3X,'TIME',)X,'F1',10X,'F2',11X,'G1'  
1,12X,'G2',/)
```

```
DO 210 J = 1,NMAX
```

```
T=T+H
```

```
L=L+1
```

```
IF (L .EQ. 3) GO TO 210
```

```
GO TO 230
```

```
210 WRITE (6,500) T,F1(J),F2(J),G1(J),G2(J)
```

```
500 FORMAT (1X,F8.4,3X,F10.5,2X,F10.5,3X,F10.5,2X,F10.5)
```

```
L=1
```

```
230 CONTINUE
```

```
CALL EXIT
```

```
END
```

REPRODUCED FROM
ORIGINAL PAGE IS POOR

APPENDIX D

PROGRAM FOR EXACT SOLUTION OF
STANDING WAVE CASE

```

C GARY H MCDONALD
C ANALYTIC SOLUTION-STANDING WAVE CASE
  DIMENSION F1(500),F2(500)
  PI=3.1415926
  H=0.1
  XL=0.0
  NMAX=500
  EPS=.1
  WBAR=C.1
  L=1

C
C READ IN GAS DYNAMIC INDEX AND INTERACTION INDEX
C
  READ (5,5) I,XN
  5 FORMAT (I5,F10.5)

C
C INITIAL CONDITIONS
C
  READ (5,10) C1,C3,PHI1,PHI3
  10 FORMAT (4F10.4)

C
  WRITE (6,15) I
  15 FORMAT (1X,'GAS DYNAMIC INDEX',I5)
  WRITE (6,15) XN
  16 FORMAT (1X,'INTERACTION INDEX',F7.2,///)
  WRITE (6,20) C1,C3,PHI1,PHI3
  20 FORMAT (1X,'INITIAL CONDITIONS',//,1X,4X,'C1',F10.4,/,
  1,1X,4X,'C3',F10.4,/,1X,4X,'PHI1',F10.4,/,1X,4X,'PHI3',
  2,F10.4,/)
  WRITE (6,30)
  30 FORMAT (1X,2X,'TIME',14X,'A1',13X,'A3',13X,'B1',12X
  1,'B3',15X,'C1',12X,'C3',11X,'PHI1',10X,'PHI3',/)

C
  DO 100 J = 1,NMAX
  XL=XJ+EPS
  IF (XN .EQ. 0..AND. I .EQ. 1) GO TO 60
  IF (XN .EQ. 40..AND. I .EQ. 0) GO TO 50

C
C NO GAS DYNAMICS
C
  50 CONTINUE
  RU=1.0
  S=(.35355*XN*EPS*(-1.))**J
  T=1.-EXP(-0.5*WBAR*XJ)
  U=S*T
  V=1./COS(U)
  W=EXP(-0.5*WBAR*XJ)
  C1=W*V
  Z=(SIN(U)/COS(U))
  C3=(W/2.3284)*Z
  PHI1=PHI1

```

```

PHI3=2.*PHI1-((2.*RJ+1.)/2.)*PI
GO TO 200

C
C
C
40 COMBUSTION

60 CONTINUE
R0=2.
CS=(EPS*(-1.)*J)/(2.*WBAR)
CT=1.-EXP(-0.5*WBAR*XJ)
CL=CS*CT
CV=2./(EXP(CU)+1./EXP(CU))
CW=EXP(-0.5*WBAR*XJ)
C1=CW*CV
C2=(EXP(CU)-1./EXP(CU))/(EXP(CU)+1./EXP(CU))
C3=(CW/2.)*C2
PHI1=PHI1
PHI3=2.*PHI1-RJ*PI

200 CONTINUE
A1=C1*COS(PHI1)
B1=C1*SIN(PHI1)
A3=C3*COS(PHI3)
B3=C3*SIN(PHI3)
F1(J)=A1*COS(XJ)+B1*SIN(XJ)
F2(J)=A3*COS(2.*XJ)+B3*SIN(2.*XJ)
IF (L .EQ. 2) GO TO 500
L=L+1
GO TO 100

500 TIME=XJ
WRITE (6,5000) TIME,A1,A3,B1,B3,C1,C3,PHI1,PHI3
5000 FORMAT (1X,F7.4,3X,F10.5,5X,F10.5,4X,F10.5,4X,F10.5,5X
1,F10.5,5X,F10.5,4X,F10.5,4X,F10.5)
L=1
100 CONTINUE

C
C
X0=0.
L=1
WRITE (6,6000)
6000 FORMAT (1X,///,1X,3X,'TIME',12X,'F1',15X,'F2',/)

C
DO 3000 = 1,NMAX
X0=XJ+H
IF (L .EQ. 2) GO TO 700
L=L+1
GO TO 300

700 TIME=XJ
WRITE (6,7000) TIME,F1(J),F2(J)
7000 FORMAT (1X,F7.4,8X,F10.5,7X,F10.5,/)
L=1
300 CONTINUE

C

```

REPRODUCIBILITY OF THE
ORIGINAL PAGE IS POOR

CALL EXIT
END

APPENDIX E
PROGRAM OF EXACT SOLUTION
OF TRAVELING WAVE CASE

```

C GARY H MCDONALD
C ANALYTIC SOLUTION-TRAVELLING WAVE CASE
  DIMENSION F1(500),F2(500),G1(500),G2(500)
  PI=3.1415926
  H=0.1
  X0=0.0
  NMAX=500
  EPS=0.1
  WBAR=0.1
  L=1

C
C READ IN GAS DYNAMIC INDEX AND INTERACTION INDEX
C
  READ (5,5) I,XN
  5 FORMAT (I5,F10.5)

C
C INITIAL CONDITIONS
C
  READ (5,10) A1,A2,A3,A4
  10 FORMAT (4F10.4)
  WRITE (6,15) I
  15 FORMAT (1X,'GAS DYNAMIC INDEX',I5)
  WRITE (5,16) XN
  16 FORMAT (1X,'INTERACTION INDEX',F7.2,///)
  WRITE (5,20) A1,A2,A3,A4
  20 FORMAT (1X,'INITIAL CONDITIONS',//,1X,4X,'A1',F10.4,/,
  1,1X,4X,'A2',F10.4,/,1X,4X,'A3',F10.4,/,1X,4X,'A4',
  2,F10.4,/)
  WRITE (5,30)
  30 FORMAT (1X,4X,'TIME',14X,'A1',15X,'A2',15X,'A3',17X
  1,'A4',/)
  DO 100 J = 1,NMAX
  XJ=XJ+EPS
  IF (XN .EQ. 0..AND. I .EQ. 1) GO TO 60
  IF (XN .EQ. 20..AND. I .EQ. 0) GO TO 50

C
C NO GAS DYNAMICS
C
  50 CONTINUE
  S=0.70711*EPS*XN
  T=1.-EXP(-0.5*WBAR*XJ)
  U=S*T
  V=1./COS(U)
  W=EXP(-0.5*WBAR*XJ)
  A2=W*V
  Z=SIN(U)/COS(U)
  A4=(W/2.82842)*Z
  GO TO 200

C
C NO COMBUSTION
C

```

```

50 CONTINUE
   CS=EPS/WBAR
   CT=1.-EXP(-0.5*WBAR*XJ)
   CU=CS*CT
   CV=2./(EXP(CU)+1./EXP(CU))
   CW=EXP(-0.5*WBAR*XJ)
   A1=CW*CV
   CZ=(EXP(CU)-1./EXP(CU))/(EXP(CU)+1./EXP(CU))
   A3=(CW/2.)*CZ
   GO TO 200
200 B1=-A2
    B2=A1
    B3=-A4
    B4=A3
    F1(J)=A1*COS(XJ)+B1*SIN(XJ)
    G1(J)=A2*COS(XJ)+B2*SIN(XJ)
    F2(J)=A3*COS(2.*XJ)+B3*SIN(2.*XJ)
    G2(J)=A4*COS(2.*XJ)+B4*SIN(2.*XJ)
    IF (L .EQ. 2) GO TO 300
    L=L+1
    GO TO 100
500 TIME=XJ
    WRITE (6,5000) TIME,A1,A2,A3,A4
5000 FORMAT (1X,F7.4,7X,(4(F12.6,5X)))
    L=1
100 CONTINUE
C
C
    XL=0.0
    L=1
    WRITE (6,6000)
6000 FORMAT (1X,///,1X,3X,'TIME',12X,'F1',15X,'F2',16X,'G1',
1,14X,'G2',/)
C
    DO 300 J = 1,NMAX
    XJ=XJ+H
    IF (L .EQ. 2) GO TO 700
    L=L+1
    GO TO 300
700 TIME=XJ
    WRITE (6,7000) TIME,F1(J),F2(J),G1(J),G2(J)
7000 FORMAT (1X,F7.4,9X,F10.5,7X,F10.5,8X,F10.5,7X,F10.5)
    L=1
300 CONTINUE
    CALL EXIT
    END

```

APPENDIX F

PRESENTATION OF ACOUSTIC
PRESSURE CALCULATIONS

ACOUSTIC PRESSURE DERIVATION

To calculate expressions for acoustic pressure, recall equation (2.48) which stated

$$p = \rho = e^{-\left(\epsilon \frac{\partial \phi}{\partial t} + \frac{1}{2} \epsilon^2 \left(\bar{u}^2 + 2\bar{u} \frac{\partial \phi}{\partial z} + \vec{\nabla} \phi \cdot \vec{\nabla} \phi\right)\right)}. \quad (\text{F.1})$$

This equation represents the unsteady state deviations of acoustic pressure. When expanding equation (F.1) into a Taylor series expansion, the resulting equation becomes

$$p = \rho = 1 - \epsilon \frac{\partial \phi}{\partial t} + \epsilon^2 \left[-\frac{1}{2}(\bar{u}^2 + \vec{\nabla} \phi \cdot \vec{\nabla} \phi) - \bar{u} \frac{\partial \phi}{\partial z} + \frac{1}{2} \left(\frac{\partial \phi}{\partial t}\right)^2 \right] + \dots \quad (\text{F.2})$$

Recall that the steady state solution was represented in equation (2.35) by

$$\bar{p} = e^{-\left(\frac{1}{2} \epsilon^2 \left(\frac{\partial \phi}{\partial z}\right)^2\right)}.$$

When expanding (F.3) into its Taylor series expansion, the result becomes

$$\bar{p} = 1 - \frac{1}{2} \epsilon^2 \left(\frac{d\bar{\phi}}{dz}\right)^2 + \dots \quad (\text{F.4})$$

where \bar{p} is the steady state acoustic pressure. Therefore, the difference in general acoustic pressure and steady state pressure can be expressed by subtracting equation (F.4) from (F.2). For this investigation, a restriction on the velocity potential ϕ was that it was a function of θ and t only. In doing this, the pressure difference equation becomes

$$p - \bar{p} = -\epsilon \frac{\partial \phi}{\partial t} + \frac{\epsilon^2}{2} \left[-\left(\frac{\partial \phi}{\partial \theta}\right)^2 + \left(\frac{\partial \phi}{\partial t}\right)^2 \right] . \quad (F.5)$$

Using the same Fourier series expansion for the velocity potential ϕ as expressed in equation (3.18), the acoustic pressure difference equation (F.5) can be expressed in terms of the product of modal amplitudes and trigonometric function in the transverse θ direction. Substituting the appropriate forms of equation (3.18) into equation (F.5) and simplifying, the resulting pressure difference equation become

$$\begin{aligned} \frac{p - \bar{p}}{\epsilon} = & \left[-\frac{df_1}{dt} + \epsilon \left[-(f_1 f_2 + g_1 g_2) + \frac{1}{2} \left(\frac{dg_1}{dt} \frac{dg_2}{dt} + \frac{df_1}{dt} \frac{df_2}{dt} \right) \right] \right] \cos \theta \\ & + \left[-\frac{df_2}{dt} + \epsilon \left[k(g_1^2 - f_1^2) + k \left(\left(\frac{df_1}{dt} \right)^2 - \left(\frac{dg_1}{dt} \right)^2 \right) \right] \right] \cos 2\theta \\ & + \left[-\frac{dg_1}{dt} + \epsilon \left[-(f_1 g_2 - f_2 g_1) + \frac{1}{2} \left[\frac{df_1}{dt} \frac{dg_2}{dt} - \frac{dg_1}{dt} \frac{df_2}{dt} \right] \right] \right] \sin \theta \\ & + \left[-\frac{dg_2}{dt} + \epsilon \left[\frac{1}{2} f_1 g_1 + \frac{1}{2} \left(\frac{df_1}{dt} \right) \left(\frac{dg_1}{dt} \right) \right] \right] \sin 2\theta . \end{aligned} \quad (F.6)$$

Since the coefficients in equation (F.6) are functions of time only, these coefficients have been included in the calculations of the program in Appendix B. Thus, for any given angle θ , values for the modal amplitude at any given time range can be calculated therefore determining the acoustic pressure difference of that desired location.